

**EPR-based structural and functional  
characterization of the C-terminal domain of  
the osmoregulated glycine betaine  
transporter BetP from *Corynebacterium  
glutamicum***

**Inaugural-Dissertation**

**zur**

**Erlangung des Doktorgrades**

der Mathematisch-Naturwissenschaftlichen Fakultät

der Universität zu Köln

vorgelegt von

**Sascha Carsten Thomas Nicklisch**  
aus Köln

Köln, Oktober 2008

**Berichterstatter:**

Prof. Dr. Reinhard Krämer

Prof. Dr. Günter Schwarz

Tag der Disputation: 01.12.2008

“Der Mensch hat dreierlei Wege, klug zu handeln: erstens durch Nachdenken, das ist der edelste; zweitens durch Nachahmen, das ist der leichteste und drittens durch Erfahrung, das ist der bitterste.”

(Konfuzius)

## Abstract

As a Gram-positive soil bacterium, *Corynebacterium glutamicum* regularly encounters various kinds of stresses that threaten the cell's survival. Beside an alternating pH and temperature, the cells are faced with changes in the osmolarity of the external medium. Recently, it was shown that the secondary glycine betaine uptake system BetP of this bacterium is able to autonomously sense a hyperosmotic stress induced cytoplasmic accumulation of potassium as specific stimulus (osmo-/chemosensor). Subsequently, the carrier is able to regulate its activity in response to the extent of the osmotic stress it is exposed to (osmoregulator). Further studies revealed that changes in the structure and/or orientation of the cytoplasmically exposed C-terminal domain of the carrier seem to be critically involved in stimulus sensing and/or signal transduction. Since the molecular mechanisms related to these processes are barely understood to date, in the present work Site-Directed Spin Labelling-Electron Paramagnetic Resonance (SDSL-EPR) spectroscopy was applied for the first time to probe the molecular dynamics during BetP function. Focus was on the structure and structural changes of the C-terminal domain or adjacent protein and/or lipid domains. Strategically engineered BetP mutants with single cysteine substitutions at the beginning (545), in the centre (572) and close to the end (589) of the C-terminal domain were tested for sustained transport activity as well as for optimal labelling and reconstitution into *E. coli* lipids to obtain enough highly purified material for EPR analysis. Absorption of about 90% of spin labelled BetP by Bio-Beads was observed when the standard reconstitution procedure was used. We concluded that at least the C-domain is apparently involved in this process. A new procedure for the reconstitution of the carrier into *E. coli* liposomes was established with about 6-7times higher protein recovery compared to the standard Bio-Bead method. SDSL-EPR revealed that the structure/conformation of the whole C-terminal domain seem to be influenced by the incorporation into *E. coli* lipids. The activation of BetP mutants by hyperosmotic stress showed at least at the terminal part of the C-domain a certain mobility effect, indicative of a structural/conformational change. However, the extent of this mobility effect was strongly dependent on the nature (osmotic and/or ionic strength) of the used osmolyte. The preliminary distance measurements of single and double spin labelled BetP variants confirmed an oligomeric state (e.g. trimer) of BetP in detergent as well as reconstituted into liposomes. In addition, a slight effect of a proline substitution in a deregulated triple mutant (BetP-S545C/Y550P/S589C) on the structure of the C-terminal domain was observed.

The data provided in this work are combined in a current model outlining possible C-terminal structures and dynamic motions upon BetP activation.

## Kurzzusammenfassung

Als Gram-positives Bodenbakterium ist *Corynebacterium glutamicum* regelmäßig diversen Stresssituationen ausgesetzt, die das Überleben der Zelle beeinträchtigen können. Neben wechselnden pH- und Temperatur-Werten, werden die Zellen auch mit Osmolaritätsschwankungen des umgebenden Mediums konfrontiert. Es konnte gezeigt werden, dass das sekundäre Glycinbetain Aufnahmesystem BetP aus diesem Bakterium in der Lage ist, den unter hyperosmotischen Bedingungen intrazellulär erhöhten Kaliumgehalt als spezifischen Stimulus autonom zu detektieren (Osmo-/Chemosensor) und seine Aktivität daraufhin an das Ausmaß des Stresses anzupassen (Osmoregulator). Weiterführende Untersuchungen zeigten, dass Änderungen in der Struktur und/oder der relativen Orientierung der C-terminalen Domäne des *carrier* einen starken Einfluss auf die Stimulusdetektion und/oder die nachgeschaltete Signaltransduktion haben. Da die molekularen Mechanismen solcher sensorischen Eigenschaften von Transportproteinen bislang nur unzureichend untersucht und verstanden sind, wurde in der vorliegenden Arbeit eine Kombination aus ortsspezifischer Spinmarkierung (*site-directed spin labelling*, SDSL) und Elektronenspinresonanzspektroskopie (ESR) angewendet, um die molekulare Dynamik während des Aktivierungsprozesses von BetP zu untersuchen. Im Fokus lagen dabei zum einen die tertiäre Struktur des Transporters als auch die Aufklärung von strukturellen Änderungen der C-Domäne sowie deren mögliche Interaktion mit angrenzenden Protein- und/oder Lipid-Bereichen im aktivierten Protein. Strategisch eingeführte Cystein-Reste zu Beginn (545), in der Mitte (572) und nahe dem Ende (589) der C-Domäne wurden auf ihre jeweilige Aktivitätsregulation hin überprüft. Darüber hinaus wurden die Markierungs- und Rekonstitutionsschritte für jede Mutante optimiert, um eine hohe Ausbeute an spinmarkiertem, gereinigtem Material für die EPR-basierten Analysen zu erhalten. Es konnte eine hochgradige Absorption von BetP durch den direkten Kontakt zu den Bio-Beads (bis zu 90%) während des herkömmlichen Rekonstitutions-Assay identifiziert werden. Daraufhin wurde eine neue Rekonstitutionsmethode für den verlustfreien Einbau von spinmarkiertem BetP Protein in *E. coli*-Liposomen etabliert, deren Effizienz um etwa 60% höher lag als mit der herkömmlichen Methode. Die SDSL-ESR-Studien zeigten zum einen, dass der Einbau von solubilisiertem BetP in *E. coli*-Liposomen einen ausgeprägten Einfluss auf die Konformation und/oder räumliche Orientierung der C-Domäne hat. Eine hyperosmotisch induzierte Aktivierung des Transportproteins zeigte zudem eine erhöhte spinlabel-Mobilität am Ende der C-Domäne auf, die auf strukturelle Änderungen während des Aktivierungsprozesses hinwies. Das Ausmaß der Mobilisierung war dabei maßgeblich von der Art (Ionenstärke, Osmolalität) des benutzten Osmolytes abhängig. Die vorläufigen Ergebnisse der Abstandsmessungen

## Kurzzusammenfassung

---

von Einzel- und Doppelcystein-Mutanten bestätigten einen oligomeren Zustand (z.B. Trimer) von solubilisiertem und in *E. coli*-Liposomen eingebautem BetP. Darüber hinaus konnte gezeigt werden, dass der zusätzliche Einbau eines Prolins in einer deregulierten Dreifachmutante BetP-S545C/Y550P/S589C einen Einfluss auf die Struktur der C-terminalen Domäne im nicht aktiven Zustand des Proteins hat.

Die in der vorliegenden Arbeit gewonnenen Daten konnten in einem aktuellen Topologie-Modell kombiniert werden, das die möglichen Konformationen und die Dynamik der C-terminalen Domäne während des Aktivierungsprozesses von BetP zusammenfasst.

## Contents

<b>1. INTRODUCTION.....</b>	<b>1</b>
1.1. <i>Corynebacterium glutamicum</i> .....	1
1.2. Osmosis and osmotic properties of a cell .....	3
1.3. Measurement of osmotic pressure.....	4
1.4. Hypoosmotic stress in microorganisms .....	5
1.5. Hyperosmotic stress and response in microorganisms .....	6
1.6. Osmosensing and osmoregulation .....	9
1.7. Osmoregulated uptake systems .....	9
1.8. Solute uptake systems in <i>C. glutamicum</i> .....	11
1.9. Glycine betaine transporter BetP from <i>C. glutamicum</i> .....	13
1.10. EPR (Electron Paramagnetic Resonance) .....	19
1.11. Objectives of this thesis .....	21
<b>2. MATERIALS AND METHODS.....</b>	<b>23</b>
2.1. Bacterial strains and plasmids .....	24
2.2. Growth media and cultivation conditions .....	24
2.3. Molecular biological approaches.....	26
2.4. General analytical approaches .....	28
2.5. Biochemical approaches.....	32
2.6. EPR measurements.....	39
<b>3. RESULTS .....</b>	<b>41</b>
3.1. Substitution mutants and strategic labelling .....	43
3.2. Activity regulation of BetP variants in <i>E. coli</i> lipids .....	45
3.3. Optimization of the reconstitution process .....	48
3.4. Mobility profiles of C-terminal BetP variants .....	52
3.5. Distance measurements with BetP variants .....	65
<b>4. DISCUSSION.....</b>	<b>74</b>
4.1. Activity regulation of BetP variants in <i>E. coli</i> lipids .....	75
4.2. Optimization of the reconstitution process .....	77
4.3. Mobility profiles of C-terminal BetP variants .....	79
4.4. Distance measurements with BetP variants .....	88
4.5. Future aspects .....	95
<b>5. SUMMARY .....</b>	<b>97</b>
<b>6. REFERENCES .....</b>	<b>99</b>
<b>7. APPENDIX.....</b>	<b>113</b>

---

# Abbreviations

ABC	ATP-binding cassette
AHT	Anhydrotetracycline
Amp <sup>R</sup>	Resistance towards ampicillin
AP	Antarctic phosphatase
BCCT family	Betaine-choline-carnitine-transporter family
BCIP	5-bromo-4-chloro-3-indoyl phosphate
bp	Base pairs
BSA	Bovine serum albumin
CAPS	<i>N</i> -cyclohexyl-3-aminopropanesulfonic acid
CrOx	Chromium-(III)-oxalate ( $\text{Cr}(\text{C}_2\text{O}_4)^{3-}$ )
cysless	= cysteine-less (mutant protein lacking any native cysteine)
DDM	<i>n</i> -dodecyl- $\beta$ -D-maltopyranoside
DEER	Double electron-electron resonance
DMSO	Dimethylsulfoxide
DNA	Desoxyribonucleic acid
dNTP	Desoxynukleosidtriphosphate
DPG	Diphosphatidylglycerol
DOPC	1,2-Dioleoyl- <i>sn</i> -Glycero-3-Phosphocholine
DOPG	1,2-Dioleoyl- <i>sn</i> -Glycerol-3-Phosphoglycerol
DTB	Desthiobiotin
DTT	Dithiothreitol
DW	(cell) Dry weight
EDTA	Ethylendiaminetetraacetic acid
EPR	Electron paramagnetic resonance
ESE	Electron spin echo
ESR	Elektronenspinresonanz
et al.	<i>et alii</i> (latin = "and others")
FRET	Fluorescence resonance energy transfer
g	Gravitational acceleration ( $9.81 \text{ m/s}^2$ )
GB	Glycine betaine
H <sub>2</sub> O <sub>dd</sub>	Double-distilled water, "bidest. water"
HABA	4-Hydroxy-azobenzene-2-carboxyl acid
HFS	Hyperfine splitting
kb	Kilo base pairs
kDa	Kilo Dalton
K <sub>M</sub>	Michaelis-Menten constant
KP <sub>i</sub>	Potassium phosphate buffer
LB medium	Luria Bertani medium



## Abbreviations

---

LPR	Lipid-protein ratio
MSC	Mechanosensitive channel
MFS	Major facilitator superfamily
MTSSL	(1-oxy-2,2,5,5-tetramethylpyrroline-3-methyl)-methanethiosulfonate
NBT	Nitro-blue tetrazolium chloride
NaP <sub>i</sub>	Sodium phosphate buffer
NiEDDA	Ni(II) ethylenediaminediacetate
OD <sub>600</sub>	Optical density at 600nm
PAGE	Polyacrylamide gel electrophoresis
PCR	Polymerase chain reaction
PE	Phosphatidylethanolamin
PEG	Polyethyleneglycol
PG	Phosphatidylglycerol
PVDF	Polyvinylidene difluoride
RT	Room temperature
SDS	Sodium dodecyl sulphate
SDSL	Site-directed spin labelling
SHFS	Superhyperfine splitting
SSS	Sodium/Solute Symporter
tetA	Tetracycline resistance gene
TCA	Trichloroacetic acid
TEMED	N,N,N',N'-tetramethyl-ethylendiamine
TM	Transmembrane
TRIS	2-amino-hydroxymethylpropane-1,3-diol
o/n culture	Overnight culture
RPM	Rounds per minute
V <sub>max</sub>	Maximal uptake rate

# 1. Introduction

Beside fluctuations in temperature, pH or nutrient depletion, most microorganisms have to deal with alternating osmolalities (water scarcity or surplus) – so called osmotic stress - in their natural habitat (Gross *et al.*, 1996, Desmond *et al.*, 2002). A stress emerges, when a changing environmental factor influence the growth or even survival of an affected organism. To overcome or bypass these deleterious circumstances, various survival strategies have been employed by bacteria (Hecker *et al.*, 1996, Hecker *et al.*, 2001). For this purpose, microorganisms have to sense outside stimuli and subsequently respond to sudden environmental changes with appropriately regulated gene expression and protein activity to ensure survival and cell proliferation.

## 1.1. *Corynebacterium glutamicum*

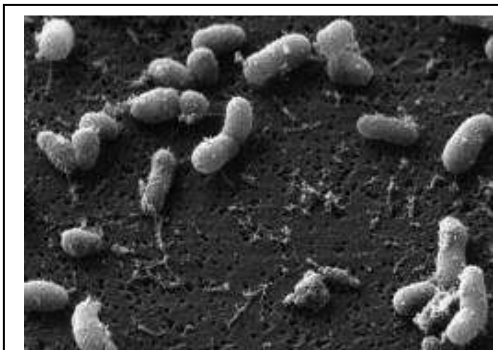
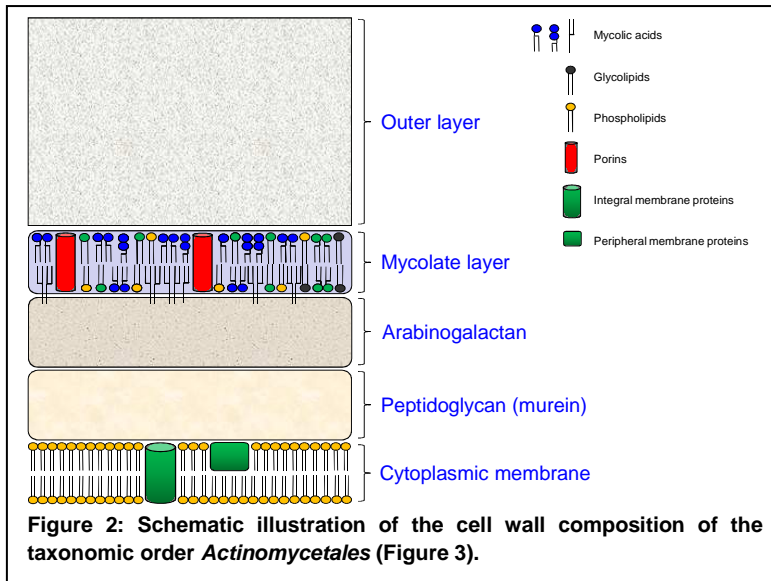


Figure 1: Scanning electron micrograph of *C. glutamicum* ATCC13032 WT (N. Möker, 2002).

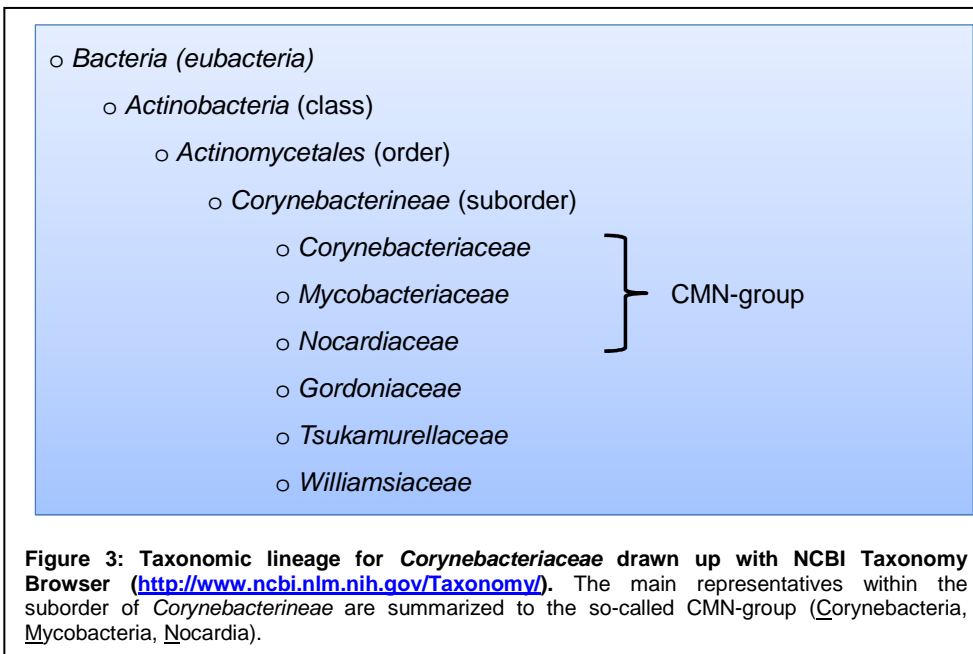
As an immobile, topsoil (= mineral horizon A; Allaby, 1994) bacterium *Corynebacterium glutamicum* is regularly exposed to an ever-changing environment. It was first described 1957 as glutamate-producing strain *Micrococcus glutamicus* (Kinoshita *et al.*, 1957, Udaka, 1960). *C. glutamicum* is a Gram-positive, non-pathogenic, facultative-anaerobic and non-sporulating bacterium that possesses a club-

(greek „coryne“= club) or rod-shaped cell morphology referred to as coryneform bacteria (Figure 1). With a G/C content of 46-74mol-% Corynebacteria belong to the big group of high-G/C-containing bacteria forming the class Actinobacteria (Figure 3; Funke *et al.*, 1995; Abe *et al.*, 1967). Among these, the heterogeneous order of Actinomycetales - which includes the Mycobacteria, Nocardia and the Corynebacteria - is characterized by a unique cell wall structure (Stackebrandt *et al.*, 1997; Daffé *et al.*, 1998; Daffé, 2005). This so-called mycolic acid layer (mycolate layer) is bearing on the top of the normal peptidoglycan (murein) and arabinogalactan layer (Figure 2). In addition to the plasma membrane it provides a second permeability barrier, containing channel-forming proteins, the porins, which facilitate the diffusion of hydrophilic substances (Nikaido, 1994, 2003; Lichtinger *et al.*, 1998; Puech *et al.*, 2001). Due to its close phylogenetic relationship to pathogenic bacteria like *Mycobacterium tuberculosis*, *Mycobacterium leprae* or *Corynebacterium diphtheria*, as common germs for severe illnesses and diseases, *C. glutamicum* is still in the focus of medical investigations as a non-pathogenic model

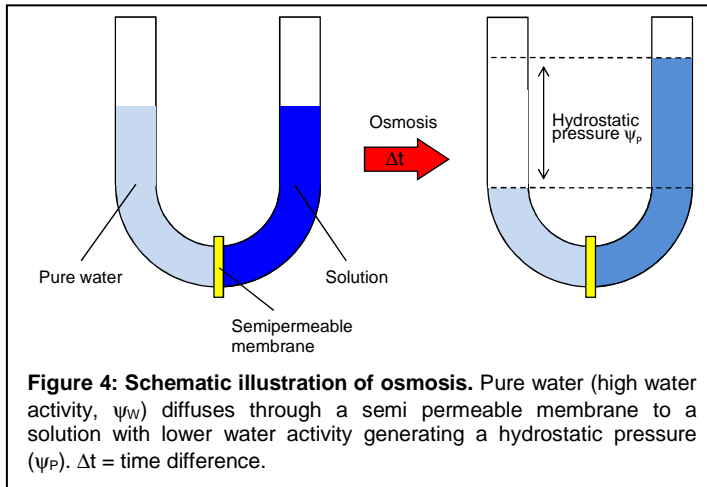


organism. Today, particular attention is paid on the bacterium due to its utmost importance for large-scale production of amino acids. Among these are L-glutamate and L-lysine with current production rates of 1.500.000 tons/year and 550.000 tons/year, respectively (Kataoka *et al.*, 2006, Hermann, 2003).

However, during fermentation cells are subjected to various kinds of stress. One of the stresses concerned is a hyperosmotic environment due to the accumulation of high substrate or product concentrations in the external medium (Kawahara *et al.*, 1997; Varela *et al.*, 2004). Thus, the investigation of the physical response of cells to encounter these unfavourable situations is of great importance for the economic sense of industrial production.



## 1.2. Osmosis and osmotic properties of a cell



Osmotic (greek “osmos” = penetration, push, drive) stress is a common challenge encountered by eukaryotic and prokaryotic cells. The semipermeability of the cytoplasmic membrane is responsible for the influence of the external osmolarity on the bacterial cell, because it retains

macromolecules, ions and polar substances but allows free diffusion of water in both directions, known as the fundamental principle of osmosis (Figure 4; Bovell, 1963).

The chemical potential of water – also referred to as water activity  $\psi_w$  – is a sum of both, the solute potential  $\psi_s$  (osmotic potential) and the pressure potential ( $\psi_p$ , turgor pressure) of a given solution:

$$(1) \psi_w = \psi_s + \psi_p \quad (\text{water activity})$$

The water activity  $\psi_w$  quantifies the tendency of water to move from one area to another due to osmosis: The lower the overall water activity, the higher the potential to attract water and *vice versa*. The turgor pressure  $\psi_p$  is a mechanical, outward-directed pressure exerted from the plasma membrane on the cell wall of plants and bacteria and can be positive (tension) or negative (suction power). In most bacteria the cell turgor is essential for growth and cell division and reaches values up to 15-25atm in Gram-positive bacteria, whereas in Gram-negative organisms it ranges from 1-5atm (Koch, 1983; Poolman and Glaasker, 1998). The solute potential ( $\psi_s$ , osmotic potential), however, is always negative and can be described by Van’t Hoff’s equation for diluted solutions (<100mM):

$$(2) \psi_s = - (R * T * c) \quad (\text{solute potential})$$

With R as the ideal gas constant, T as the absolute temperature in °K and c as the total solute concentration.

Hence,  $\psi_s$  is directly proportional to the absolute temperature and the concentration of dissolved particles (colligative property) in a given solution and decreases with a rising amount of solutes. In reference to equation (1), water flows through a cytoplasmic

membrane towards a lower chemical potential until both, the solute potential  $\psi_S$  and the turgor pressure  $\psi_P$  are equal (Cosgrove, 2000):

$$(3) \psi_W = \psi_S + \psi_P = 0, \text{ if } \psi_S = \psi_P \quad (\text{full turgescence})$$

Due to the fact, that the cytoplasm is an aqueous solution supplied with salts, sugars, amino acids and other chemicals compounds, the water activity  $\psi_W$  of living cells under physiological conditions is more negative than that of the surrounding medium, leading to an inward directed water flux that maintains the crucial cell turgor. Fluctuations in the external osmolarity, on the other hand, may reduce the cell's water activity and hence increase its turgor pressure (hypoosmotic stress) or on the contrary decrease the cell's  $\psi_P$  (hyperosmotic stress). According to equation (1) and the colligative property of  $\psi_S$  (2), the overall water activity of a cell is mainly determined and can be adjusted by the internal solute pool (osmoregulation). Bacteria and plants thereby have to be able to tightly regulate their internal solute concentrations to ensure viable cell functions and reproduction (Kempf and Bremer, 1998; Chater and Nikaido, 1999).

### 1.3. Measurement of osmotic pressure

As a prerequisite for studies on bacterial osmoregulation and osmosensing it is important to be able to measure the osmotic pressure imposed by growth media and supplements. For this purpose, the water activity can be linked to the osmotic pressure  $\Pi$  by the relation:

$$(4) \Pi = - (R * T / V_W) * \ln \psi_W \quad (\text{osmotic pressure})$$

Here,  $V_W$  is the partial molar volume of water and measured in  $[\text{m}^3 * \text{mol}^{-1}] = [\text{J} * \text{m}^{-3}] = [\text{N} * \text{m}^{-2}]$ , so in pressure units.

From equation (4) the osmolarity of a given solution can be derived as the sum of the molar concentrations of all osmotically effective particles ( $\Sigma c$ ):

$$(5) \text{Osmolarity } [\text{mol/L}] = \Sigma c \sim \Pi / R * T$$

The osmolarity can be calculated but not measured. That's why in practical approaches the osmotic pressure per weight of solvent, the osmolality, is used:

$$(6) \text{Osmolality } [\text{osmol/kg}] = \Pi / R * T$$

The osmolality in turn can be measured, but not calculated because the different properties of a particular solute (e.g. charge, size, form) are included into the total water potential as single-potentials and affect it to different extents. So, the osmolality is merely an approximation for the osmolarity of a given solution, however simply quantifiable for investigations on microbial adaptation to osmotic stress situations.

### 1.4. Hypoosmotic stress in microorganisms

A hypoosmotic (greek “hypo“= below, under) stress occurs for living cells when the external osmolality is decreased, e.g. the water activity of the external medium is higher in relation to the cytoplasm of the cell. This causes an instant influx of water and an increase in cell turgor. Although the cell walls of Gram-negative bacteria can sustain pressures up to 100atm, the permanent increase of  $\psi_P$  would inevitably lead to cell burst (Csonka, 1989; Carpita *et al.*, 1985). To overcome this unfavourable situation, microorganisms have to dispose internal solutes to even out the differences in chemical potential and thus leading to a decrease in turgor.

For this purpose, specific transporters and mechanosensitive channels (Mscs) as release valves are rapidly activated to reduce the driving force for water entry (Anishkin and Kung, 2005; Hamill and Martinac, 2001; Csonka and Epstein, 1996). Mscs are ubiquitous among prokaryotes, unspecific and have different pore sizes as well as different sensitivities towards the applied mechanical stress that activates them (Berrier *et al.*, 1992). They all have in common, that their activity is directly controlled via changes in the lateral tension of the membrane as a response to changes in the external osmolality (downshift). Upon a change from high to low osmolalities, the open probability of these channels increases by several orders of magnitude as a function of the coupling mechanism between protein conformation and membrane stretch (pressure sensitivity). Thereby, the respective channels work cooperatively: upon hypoosmotic stress the channel with the lowest conductance opens first, sequentially followed by the channels with higher conductance to provide a graduation of efflux response (Martinac 2001; Bezanilla and Perozo, 2002). In this context, the best studied efflux channels so far are the two species MscL (MechanoSensitive Channel of Large conductance) and MscS (Small) from *E. coli*, with conductances of 3nS and 1nS, respectively (Levina *et al.*, 1999; Sukharev *et al.*, 1993, 1999). In addition, a third and yet barely studied MscM (Mini) channel (~0.1nS) opens as first response under hypoosmotic conditions and - with rising pressures - additionally the MscS channel (Berrier *et al.*, 1996). At turgor pressures causing a tension sufficient to rupture the membrane, also the MscL channel opens. Whereas single deletion mutants lacking the gene for MscS (*yggB*) or MscL (*mscL*) remain fully functional after applying a hypoosmotic shock, the respective double mutants die, indicating the physiological

importance of both channels and implying that MscM alone is not able to protect *E. coli* during an osmotic downshift (Sukharev *et al.*, 1994; Levina *et al.*, 1999; Booth and Louis, 1999).

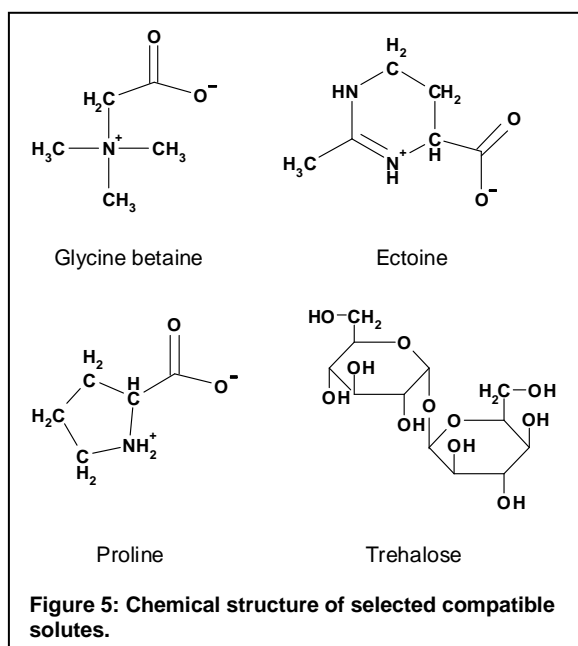
Homologues of MscL and MscS could also be identified in *Mycobacterium tuberculosis* (Chang *et al.*, 1998) and in *Corynebacterium glutamicum* (Nottebrock *et al.*, 2003). In case of *C. glutamicum*, the MscL- and MscS-channel seem to be responsible for the specific efflux of glycine betaine, proline and – to a less extent – of some cations (Ruffert *et al.*, 1997, 1999). However, the respective double deletion strain lacking the genes for both channels still showed a hypoosmotically induced glycine betaine efflux, arguing for at least one additional MS channel (Nottebrock *et al.*, 2003).

### **1.5. Hyperosmotic stress and response in microorganisms**

During a hyperosmotic (greek “hyper“ = above, excess) stress the osmolality of the external medium is increased and water flows out of the cell, thereby changing the cell's hydration, volume and/or turgor pressure. The consecutive water efflux inevitably leads to plasmolysis and growth slowdown or even a stop of growth. As a response, cells have developed a variety of mechanisms to restore cell turgor and balance water stress. According to Wood (1999) this response can be at least divided in three overlapping phases: (1) an instant but passive dehydration of the cytoplasm (seconds-minutes), (2) an active process of rehydrating the cytoplasm by accumulation of ions or osmolytes (up to an hour) and (3) a remodelling of the cell by changes of gene expression profiles (up to one or more hours).

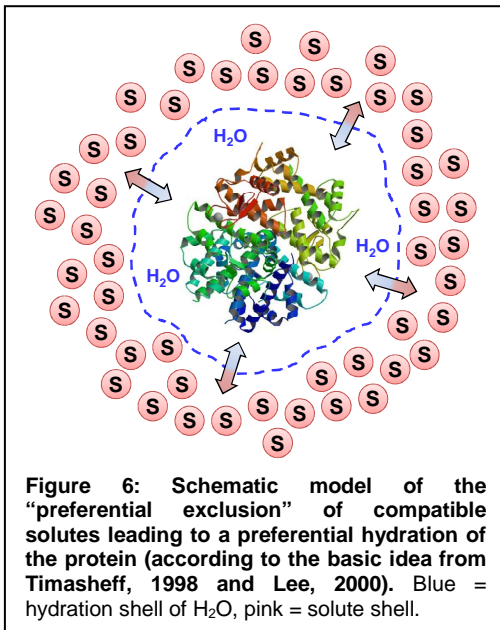
As an initial step during the rehydration phase, many bacteria transiently and rapidly accumulate potassium (Dinnbier *et al.*, 1988; Whatmore and Reed, 1990; Whatmore *et al.*, 1990). Potassium is a widespread ion in nature and the dominant cation in the cytoplasm of microorganisms with amounts of 100-600mM (Ballal *et al.*, 2007; McLaggan *et al.*, 1994). The increase in internal potassium can be achieved by both, passively via hyperosmotic-induced water efflux out of the cells and actively via specific potassium uptake systems. In *E. coli* active accumulation is mediated by the low affinity and low capacity Kup system as well as the high efficient transporters Kdp and TrK as the main transport systems for potassium (Bakker, 1993; Schlösser *et al.*, 1995). Recently, two potassium uptake systems were identified in *C. glutamicum*: a Kup system with similarities to the cation/proton symporter Kup from *E. coli* and a potassium channel (CgIK) with striking similarity to MthK from *Methanobacterium thermoautotrophicum* (Becker, 2007). Preliminary results with knock-out deletion strains indicated, that CgIK is the major constituent for potassium uptake in *C. glutamicum* (Becker, 2007; personal

communication, M. Becker). However, both systems could not yet be further characterized biochemically or kinetically. Also, there is no evidence for a specific activation of potassium uptake systems in *C. glutamicum* upon hyperosmotic stress. To maintain electroneutrality and to prevent alkalisation in *E. coli* and *C. glutamicum* cells, the potassium accumulation is accompanied by the synthesis of glutamate as a counterion, whereas in *B. subtilis* the nature of the counter ion still remains elusive (Caylay *et al.*, 1991; McLaggan *et al.*, 1994; Morbach and Krämer, 2002; Whatmore and Reed, 1990). In addition, the internal nucleic acid counterion putrescine or other protons are exchanged by potassium and exported (Csonka, 1989; Munro *et al.*, 1972).



In contrast to (extreme) halophiles with their common “salt-in” strategy, moderate osmotolerant bacteria use a “organic-solute-in” strategy in a second phase of the hyperosmotic response to prevent chaotropic effects during the adaptation phase (Oren 2006, 2008). In this regard, the internal charge accumulation (potassium, glutamate) leads to aggregation of cellular macromolecules and thus may interfere with the metabolism (Wood, 1999). To counteract this effect, the ions are exchanged against neutral, so-called compatible solutes either by uptake or biosynthesis (Csonka, 1989; Galinski and Trüper, 1994). These osmoprotectants are characterized by being compatible with normal physiological functions of the cell while accumulated to very high intracellular levels up to several moles per litre (Braun, 1997; Arakawa and Timasheff, 1985; Timasheff, 1991). In addition, they are neutral or zwitterionic at physiological pH and soluble up to molar concentrations (Csonka, 1989). Depending on their molecular structure, these compounds can be subdivided into (i) amino acids and derivatives (e.g. glutamate, proline, ectoine, and glycine betaine), (ii) polyols (e.g. glycerol, glycosylglycerol), (iii) sugars (e.g. trehalose, sucrose) and (iv) others (e.g. carnitine, choline-O-sulphate). Among these, glycine betaine, ectoine, proline and trehalose are the most abundant and thus most effective osmoprotectants in the domain Bacteria (Oren, 2008; Figure 5).



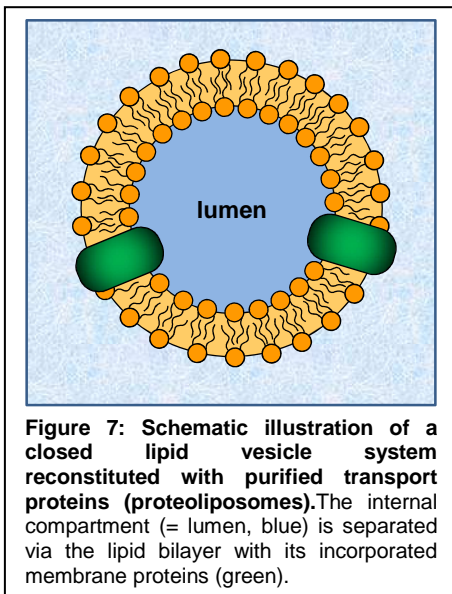


Beside their function as osmoprotectants, these organic solutes have the intrinsic property to stabilize the native conformation of proteins. This attribute can be explained by the model of "preferential exclusion" proposed by Arakawa and Timasheff (1985). The model indicates that compatible solutes are preferentially excluded from the hydration shell of a protein, leading to stronger interactions of the water molecules with the protein surface (preferential hydration, Figure 6). The stabilizing effect of the organic solutes thereby derives from the different affinities towards the native and denatured status of the

protein: in a denatured protein the lipophilic peptide backbone is exposed, leading to thermodynamically unfavourable interactions with the predominantly hydrophilic compatible solutes which in turn promote the native protein conformation. One mechanism for preferential exclusion is the "sterical exclusion" that occurs, when the radius of the compatible solute is considerably bigger than that of the water molecule leading to a tight solvation shell around the protein (Arakawa and Timasheff, 1985). A second mechanism deals with the increased surface tension of the respective solvation shell due to the inhomogeneous distribution of the solvents within the cytoplasm (according to Gibbs isotherm). The denaturation of a protein thereby leads to an increased free surface energy - which is the product of surface tension multiplied by the overall surface - leading to an unfavourable energy imbalance compared to the native state. This energy imbalance is reduced, when the protein (and its hydration shell) adopts a small volume or overall surface, so to say the native conformation (Timasheff, 1998).

Since the uptake of compatible solutes is more favourable in terms of energy and carbon cost as compared to biosynthesis, the activation of specific uptake systems for compatible solutes is in general the first response (short-term response) to hyperosmotic conditions. For the sake of long-term adaptation, enzymes for *de novo* synthesis of compatible solutes and for transporters get additionally regulated at the level of gene expression. However, if compatible solutes are not present in the environment, the bacterium is forced to exclusively synthesize its osmoprotectants. *C. glutamicum* thereby uses several pathways to synthesize glutamine (Frings *et al.*, 1993; Rönsch *et al.*, 2003), proline (Ankri *et al.*, 1996; Ley, 2001) and trehalose (Wolf *et al.*, 2003) after an osmotic upshift.

## 1.6. Osmosensing and osmoregulation



Most bacteria possess uptake systems in their membrane which mediate the immediate accumulation of compatible solutes upon an osmotic upshift of the external medium. These systems have to be tightly-regulated on the level of protein activity as well as at the level of gene expression to ensure a proper adaptation to varying hyperosmotic stress (osmoregulation). Thus, as a basic prerequisite for an efficient osmoregulation, cells have to exhibit sensitive receptor systems which either directly or indirectly perceive the encountered stress (osmosensors). The detected stimulus has then to be

converted and transmitted to a cell intrinsic osmoregulatory network that finally regulates the catalytic activity of its transport systems and/or biosynthesis pathways depending on the extent of the emerged stress. According to this, the elucidation of bacterial osmosensory and osmoregulatory mechanisms relies on the identification and characterization of osmosensory transporters, their encoding genes as well as the solutes and ions that serve as substrates and cosubstrates, respectively. For this purpose, current investigations focus on the measurement of the respective transport activity under (hyper-) osmotic conditions *in vivo* with intact cells and *in vitro* with inverted membrane vesicles (IMV) or artificial lipid vesicles reconstituted with purified transporters (proteoliposomes, Figure 7). Referring to the latter, this artificial membrane system provides the major opportunity to manipulate a set of conditions (e.g. the internal and external buffer, lipid and protein composition/ratio, liposome size, etc.) that facilitates the discrimination of activating stimuli (e.g. turgor pressure, membrane strain, internal and external osmolarity/ionic strength/ion concentration, macromolecular crowding) or substrate and cosubstrate specificity (Wood, 2007; Papahadjopoulos, 1978; Olsen *et al.*, 1979).

## 1.7. Osmoregulated uptake systems

Since the import of solutes against their electrochemical gradient requires metabolic energy, primary (ATP-Binding Cassette, ABC) and secondary (ion-linked) transporters are commonly used as uptake systems for osmoprotectants (Bremer and Krämer, 2000; Wood, 1999; Wood *et al.*, 2001). Among these, ProP of *Escherichia coli* and BetP of *Corynebacterium glutamicum* are the best studied secondary uptake systems in which the solute transport is coupled to the electrochemical gradient of a cosubstrate. One of the

best studied ABC transporter in terms of activity regulation upon hyperosmotic stress is OpuA from *Lactococcus lactis* in which the transport is directly coupled to ATP hydrolysis as the driving force. These prototypical osmosensory transporters are characterized by detecting changes in osmotic pressures and respond by mediating the uptake of compatible solutes without the assistance of other proteins. In this context, great efforts are currently made on revealing the detailed molecular mechanism of osmotic stress detection and signal transduction within these autonomously working carrier proteins.

The ABC transporter OpuA from *L. lactis* facilitates the unidirectional transport of glycine betaine at the expense of two molecules ATP (Van der Heide *et al.*, 2000; Patzlaff *et al.*, 2003). The protein consists of 573 amino acid residues forming eight  $\alpha$ -helical transmembrane domains and a binding protein domain oriented to the periplasm. Its initial uptake rates increase with a rising medium osmolality (osmoregulator), whereas the osmolality threshold for the transporter activation increases with increasing amount of anionic lipids in the membrane fraction of proteoliposomes (Van der Heide *et al.*, 2001). In addition, the rapid activation of OpuA seems to be indifferent to the nature of the triggering ion, although divalent ions are more effective than monovalent ions. To this respect and due to the fact that the ionic strength of a solution varies as the square of ion charge (equation (7); Wood, 2007), OpuA was proposed to be a ionic strength sensor (Biemans-Oldehinkel *et al.*, 2006; Van der Heide *et al.*, 2001).

$$(7) I = 1 / 2 * \sum(m_i * z_i^2) \quad \text{(ionic strength of a solution)}$$

With  $i$  = amount of ions,  $m_i$  = ion molalities (moles/kg solvent) and  $z_i$  = ion charges.

Accordingly, the proposed model for the osmosensing mechanism of OpuA is based on electrostatics: under physiological conditions intracellular tandem CBS (Cystathionine- $\beta$ -Synthase) domains of OpuA are interacting with the surrounding membrane surface. Upon hyperosmotic shock, the internal ionic strength rises and the competing ions release the CBS domains from the membrane thereby activating the transporter (electrostatic switch). In addition, the C-terminal stretch of anionic residues serves as a modulator reducing the ionic strength threshold for activation via electrostatic repulsion with the predominantly anionic membrane surface (Biemans-Oldehinkel *et al.*, 2006).

In *E. coli* a member of the Major Facilitator Superfamily (MFS), ProP, mainly catalyzes the uptake of proline, glycine betaine and ectoine in symport with  $H^+$  (Culham *et al.*, 1993; Cairney *et al.*, 1985a). It is a 500-residue integral membrane protein with 12 transmembrane helices as well as N- and C-terminal hydrophilic domains, both facing the

cytoplasm. The C-terminal domain contains specific heptad repeats: a peptide that can form characteristic, homodimeric, antiparallel,  $\alpha$ -helical coiled-coil structures stabilised by electrostatic interactions and putatively leading to a ProP dimerisation *in vivo* (Hillar *et al.*, 2005; Culham *et al.*, 1993). It was assumed, that the sensory function of ProP is at least partially located in this C-domain (Culham *et al.*, 2000). In this regard, the C-terminal coiled coil structure seemed to tune the osmotic activation threshold (modulator function), because a higher osmotic pressure was required to activate ProP derivatives with disrupted coiled-coils (Tsatskis *et al.*, 2005). Although ProP is fully functional in the absence of any other protein, its maximal activity is reduced to 20% in strains lacking a certain accessory protein, called ProQ. ProQ is a soluble cytoplasmic protein of 232 amino acids that is proposed to fine tune the osmotic response of ProP in terms of activity (Wood, 1999; Kunte *et al.*, 1999). In contrast to OpuA, ProP seems to respond to osmotically induced changes in cytoplasmic ions (predominantly potassium) and also non-ionic solutes and macromolecules (Culham *et al.*, 2003). Recent considerations suggest that ProP senses the osmotic pressure by its hydration state: as the osmotic pressure increases, water molecules are subtracted from the protein leading to a dehydration-induced structural change that activates ProP (Wood, 2006). Due to the fact that both OpuA and ProP are able to mediate the accumulation of compatible solutes in cells and in artificial lipid vesicles (proteoliposomes), they unify the properties of a transporter, an osmosensor and an osmoregulator.

Analogous investigations were carried out on the osmoregulated carrier BetP in *C. glutamicum*. However, as a prerequisite for a detailed analysis of a single uptake system *in vivo*, accessory osmoregulated transporters had to be identified and characterized to discriminate specific and general contributions of each in terms of compatible solute uptake.

### **1.8. Solute uptake systems in *C. glutamicum***

*Corynebacterium glutamicum* possesses five secondary carriers for the uptake of compatible solutes (Peter *et al.*, 1998a; Steger *et al.*, 2004; Figure 8). Among these, the constitutively expressed ectoine/betaine/proline transporter EctP is only regulated at the level of activity after an osmotic upshift whereas the high affinity proline uptake system PutP is independent from the external osmolality and supposed to take up proline in symport with sodium for the anabolic cell metabolism (Weinand *et al.*, 2007). The activity of the proline/ectoine permease ProP, the betaine/ectoine carrier LcoP and the betaine transporter BetP is regulated by the external osmolality at the level of activity and expression. Together with the carnitine transporter CaiT (Eichler *et al.*, 1994) from *E. coli*, and the two betaine uptake systems BetL (Sleator *et al.*, 1999) from *Listeria*

*monocytogenes* and OpuD (Kappes *et al.*, 1996) from *Bacillus subtilis*, the three secondary carriers BetP, LcoP and EctP belong to the BCCT (Betaine-, Carnitine-, Choline-Transporter) family which is involved in the uptake of quaternary ammonium compounds (Saier, 2000). ProP from *C. glutamicum* belongs to the MFS (Major Facilitator Superfamily) transporters like ProP from *E. coli* (Culham *et al.*, 1993), whereas PutP is assigned to the SSS (Sodium:Solute Symporter) family like the proline carrier OpuE from *B. subtilis* (Von Blohn *et al.*, 1997).

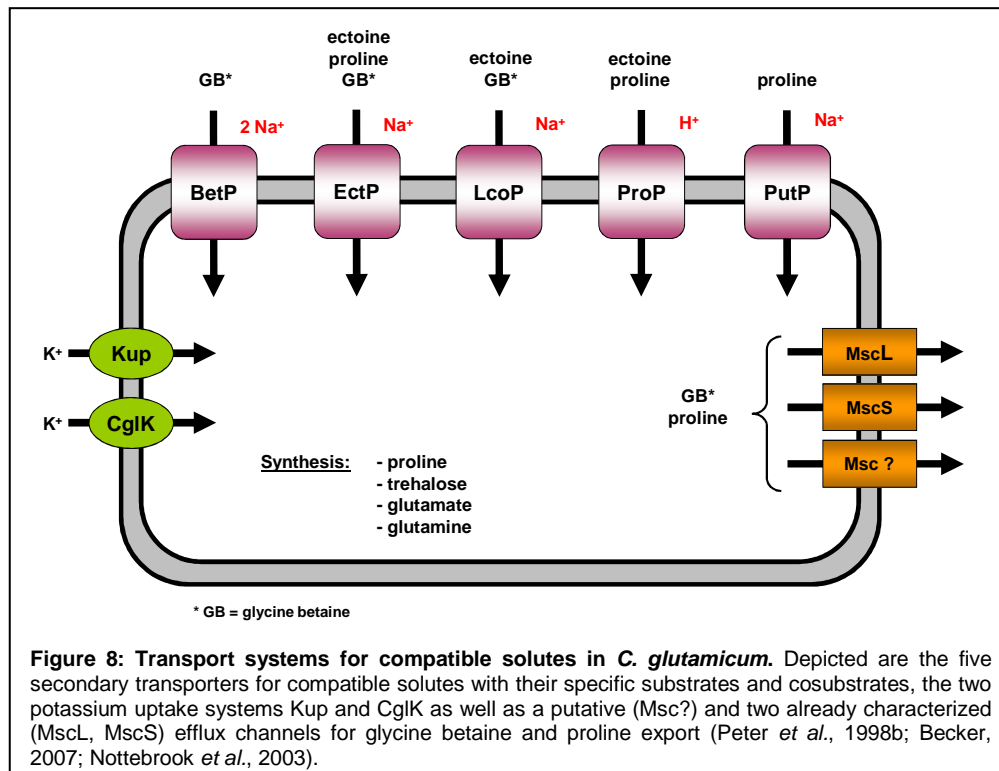


**Figure 8: Transport systems for compatible solutes in *C. glutamicum*.** Depicted are the five secondary transporters for compatible solutes with their specific substrates and cosubstrates, the two potassium uptake systems Kup and CgIK as well as a putative (Msc?) and two already characterized (MscL, MscS) efflux channels for glycine betaine and proline export (Peter *et al.*, 1998b; Becker, 2007; Nottebrook *et al.*, 2003).

The four osmoregulated secondary transporters in *C. glutamicum* (BetP, EctP, LcoP, and ProP) catalyze the symport of their respective compatible solute with Na<sup>+</sup>-ions or protons, each exhibiting different substrate specificities and -affinities (Table 1). The overlapping substrate spectra thus allow an effective adaptation to osmotic changes of the environment if a particular solute is not available.

To this regard, RNA dot blot experiments and appropriate complementation studies showed, that the hyperosmotic stress-induced expression of the genes *betP*, *proP* and *lcoP* is supposed to be mediated via an osmosensitive two-component signal transduction system composed of the sensor kinase MtrB and its cognate response regulator MtrA (Möker *et al.*, 2004).

**Table 1: Osmoregulated uptake systems in *C. glutamicum* and respective kinetic parameters.** According to the kinetic characterization by Farwick *et al.* (1995), Peter *et al.* (1998b) and Steger *et al.* (2004).

Carrier	Family	Substrate	CS	$K_M$ (CS) [mM]	$K_M$ (S) [ $\mu$ M]	$V_{max}$ [ $\mu$ mol/min $\cdot$ g DW]	Regulation level (upon osmoshock)
BetP	BCCT	GB	Na <sup>+</sup>	4.1	8.6	110	activity & expression
EctP	BCCT	ectoine	Na <sup>+</sup>	9.1	63	27	activity
		GB			333	34	
		proline			1200	34	
LcoP	BCCT	GB	Na <sup>+</sup>	36	154	8.5	activity & expression
		ectoine			539	8.6	
ProP	MFS	proline	H <sup>+</sup>	n.d.	48	71	activity & expression
		ectoine			132	129	
PutP	SSS	proline	Na <sup>+</sup>	n.d.	7.6	20	not osmoregulated

**Note:** BCCT=Betaine-Choline-Carnitine-Transporter; MFS=Major Facilitator Superfamily; SSS=Sodium:Solute Symporter; GB = glycine betaine; S = substrate; CS = cosubstrate; DW = dry weight (of cells).

## 1.9. Glycine betaine transporter BetP from *C. glutamicum*

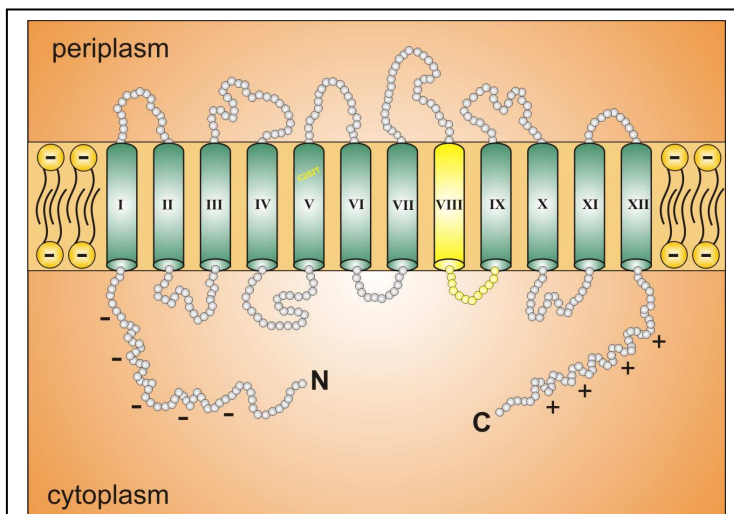


**Figure 9: Predicted topology model of the secondary glycine betaine carrier BetP-C252T from *Corynebacterium glutamicum* (TMHMM 2.0, "<http://www.cbs.dtu.dk/services/TMHMM/>").** The transmembrane segments are displayed as green cylinders. Marked in yellow is a conservative region of the proteins in the BCCT family that is possibly involved in substrate binding (Vinothkumar *et al.*, 2006). The predominant charges of each cytoplasmic extension at physiological pH are depicted as “-” (negative) and “+” (positive). The suffix “-C252T” represents the substitution of the sole native cysteine at amino acid position 252 for a threonine to obtain a cysless (*cysteine-less*) BetP variant.

As mentioned above, one of the best-studied carriers involved in osmoregulation of *C. glutamicum* is the secondary glycine betaine transporter BetP that catalyzes the symport of its sole substrate with two sodium ions (Farwick *et al.*, 1995; Peter *et al.*, 1996). BetP is a 595-residue integral membrane protein that comprises 12 transmembrane segments as well as a highly negatively charged hydrophilic N-terminal domain of approximately 62

amino acids and a highly positively charged hydrophilic C-terminal domain of 55 amino acids. Both of these terminal domains are cytoplasmically exposed and important for osmostress-dependent activity regulation (Figure 9; Peter *et al.*, 1997; Rübenhagen *et al.*, 2000). Driven by the electrochemical sodium potential  $\Delta\mu_{Na^+}$ , BetP is able to build up extremely high glycine betaine gradients of  $4 \times 10^6$  (inside:outside). The carrier exhibits a moderate affinity of  $8.6\mu$ M for its substrate glycine betaine and a high  $K_M$  (= lower affinity)

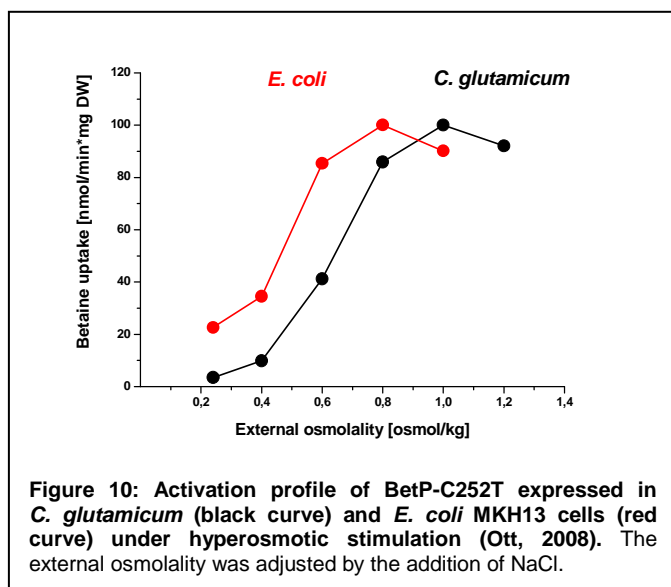
of 4.1mM for its cosubstrate sodium (Farwick *et al.*, 1995; Table 1). With  $V_{\max}$  values of 110 [ $\mu\text{mol}/\text{min}\cdot\text{g}$  cell dry weight], BetP is together with the acetate and glucose transporters one of the fastest uptake systems in *C. glutamicum* (Ebbighausen *et al.*, 1991; Marx *et al.*, 1996).

### **1.9.1. BetP - osmosensing and activity regulation**

In the absence of any osmotic stress BetP is almost inactive. Once the external osmolality rises and the activation threshold is reached (0.3-0.4osmol/kg), BetP in *C. glutamicum* cells gets activated in less than one second (activated state) with its activation optimum at 1.2osmol/kg (Peter *et al.*, 1996; Peter *et al.*, 1998b). As soon as the hyperosmotic stress has been compensated by the appropriate uptake of compatible solutes, BetP activity is reduced (activity adaptation) to prevent excessive solute accumulation (Morbach and Krämer, 2000). In this adaptation phase, the net uptake of glycine betaine is reduced to 66% of the overall transport rate due to both, a reduced import activity and a specific counter-exchange activity of the transporter (Botzenhardt *et al.*, 2004). The heterologous expression of BetP in *E. coli* cells as well as the functional reconstitution of purified BetP protein in proteoliposomes led to the conclusion that this transporter operates autonomously (e.g. independent of accessory proteins or macromolecules) and thus harbours altogether three functions: (i) the catalytic activity of glycine betaine transport, (ii) sensing of hyperosmotic stress, and (iii) osmoregulation, i.e. adjustment of the transport rate to the actual extent of osmotic stress (Rübenhagen *et al.*, 2000; Morbach and Krämer, 2004b).

The search for the activating stimulus took advantage of proteoliposomes that cannot build up a turgor pressure due to the lack of a cell wall-like structure that may sustain a certain hydrostatic pressure. Reconstituted BetP was shown to become fully activated while retaining the characteristic regulation pattern found in cells after an osmotic upshift. Thus, the (high) turgor pressure in the Gram-positive *Corynebacterium glutamicum* could be ruled out as an activating stimulus. Other possible stimuli, like membrane tension, internal or external osmolarity as well as ionic strength, showed no significant influence on BetP activation (Rübenhagen *et al.*, 2001). The effect of molecular crowding (Minton, 2005; Wood, 2007), e.g. the enrichment of cytoplasmic molecules due to cell dehydration, could not be investigated up to now. Nevertheless, using the hydration state of a protein as an indicator for hyperosmotic stress is still a challenging suggestion and was already proposed by Wood (2006) for the activation of ProP from *E. coli*. It could be figured out, that an increase in the luminal  $\text{K}^+$  concentration alone, i.e. at the side where the hydrophilic domains are located, is sufficient to activate BetP (Rübenhagen *et al.*, 2001). In addition, cations with similar physical properties as  $\text{K}^+$ , such as  $\text{Rb}^+$  and  $\text{Cs}^+$ , also

induced the activation of BetP, whereas bigger ions ( $\text{NH}_4^+$ ) or macromolecules (choline) did not. These results necessitated a reclassification of the so far entitled BetP-osmosensor to a chemosensor or - in particular - a potassium sensor (Rübenhagen *et al.*, 2001).



Unexpectedly, when heterologously expressed in *E. coli* cells, the activation profile of BetP upon hyperosmotic stress still remained similar, while the optimum of the transport activity was shifted to lower values of 0.6-0.8 osmol/kg, e.g. a lower external osmolality was required to reach optimal activation of the transporter (Figure 10; Peter *et al.*, 1996). Further investigations in the proteoliposomal system

proved a strong influence of the membrane phospholipid composition on the activation profile of BetP: the higher the fraction of negatively charged phospholipids, the higher was the threshold concentration of  $\text{K}^+$  necessary for activation (Krämer and Morbach, 2004b). In particular, the regulation pattern of the reconstituted transporter resembles that of native BetP in *C. glutamicum* cells, when the liposomes comprised more phosphatidylglycerol (Schiller *et al.*, 2006). Although, the internal potassium concentration was shown to be a specific stimulus for BetP activation, the sensitivity towards  $\text{K}^+$  seemed to be at least partly dependent on the net (negative) charge of the surrounding phospholipid headgroups in the corresponding membrane system (Table 2).

**Table 2:** Phospholipid headgroup composition of the inner and outer membrane extracts from *E. coli* K12 and *C. glutamicum* ATCC13032 according to Morein *et al.* (1996) and Hoischen and Krämer (1990).

Phospholipid	net charge	<i>E. coli</i> (grown at 37°C)	<i>C. glutamicum</i> (grown at 30°C)
		IOM	IOM
[% of total phospholipids]			
PE	neutral (0)	79 ± 3	~ 0
PG	negative (-1)	17 ± 3	87 ± 1.9
DPG	neutral (0)	4 ± 2	1 ± 0.4

**Note:** PE=phosphatidylethanolamine; PG= phosphatidylglycerol; DPG=diphosphatidylglycerol; IOM=inner and outer membrane fraction.



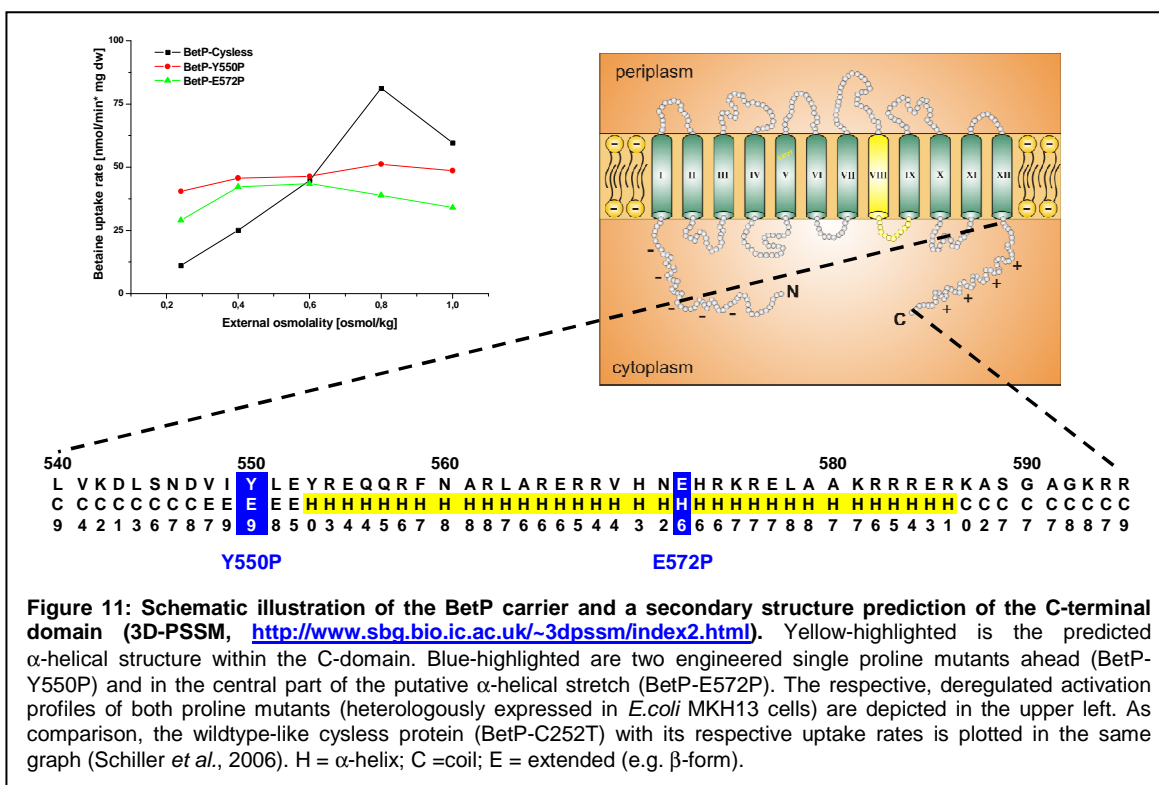
### 1.9.2. BetP – Putative sensory domains and binding sites

The potassium-specific activation of BetP requires a binding site for the ion. Except for a sequence homology to a potassium binding site of pyruvate kinases in loop 2 (Jurica *et al.*, 1998; Schiller *et al.*, 2004a), the primary sequence of the transporter does not include a motif known to be involved in K<sup>+</sup> recognition. Due to the fact, that the half-maximal activation of BetP is reached at an internal potassium concentration of 220mM (Rübenhagen *et al.*, 2000), the putative sensory domain of the protein is supposed to need high amounts of the stimulating ion to detect and transmit the signal for activation.

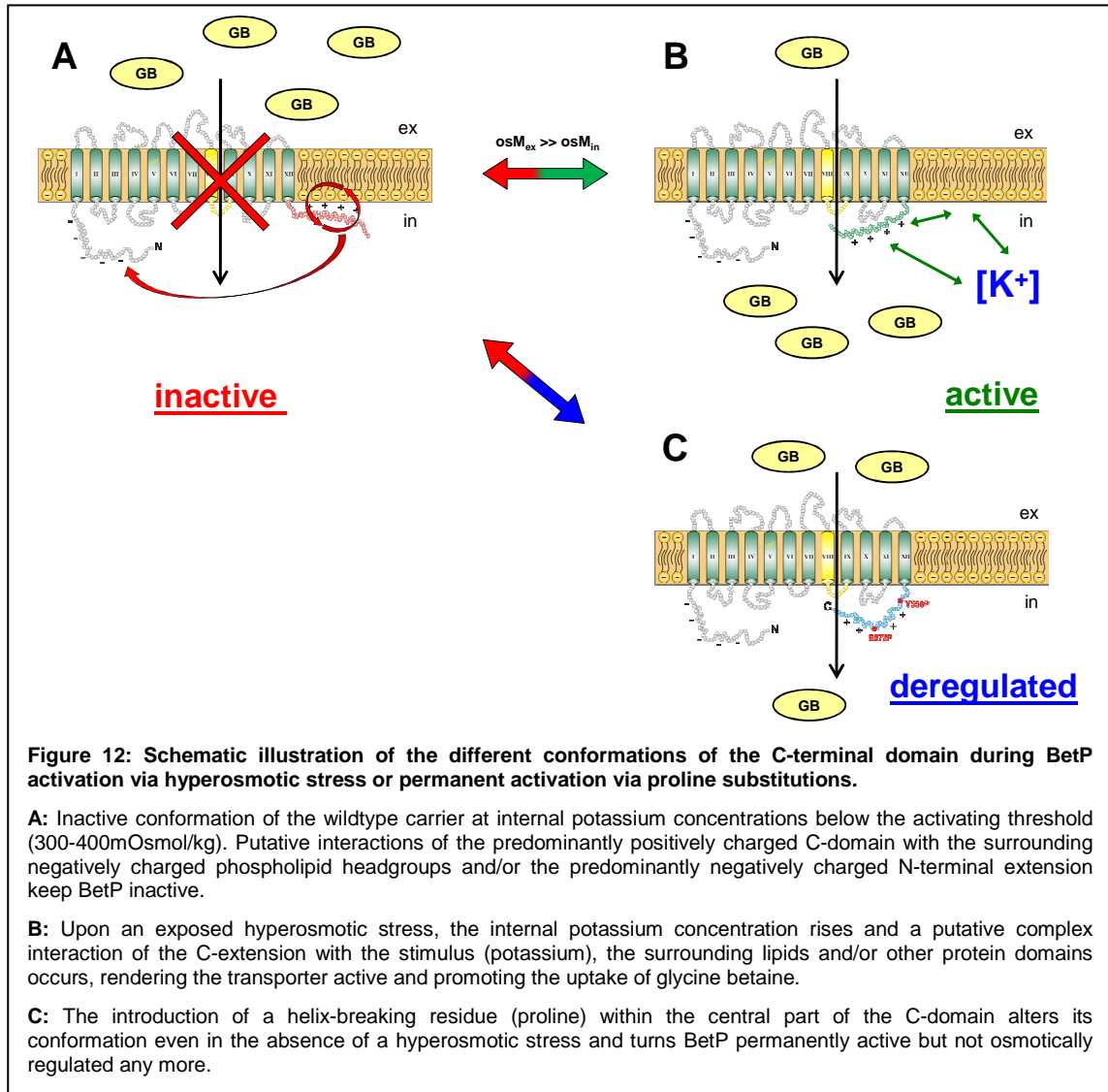
In search of the defined localization of the sensor region within the protein, former investigations in intact *C. glutamicum* cells demonstrated that both hydrophilic domains of BetP strongly influence the activation profile. Truncation of the N-terminal domain of BetP led to a decrease in osmosensitivity, e.g. a higher osmotic stress was necessary to activate an N-terminally truncated BetP (Peter *et al.*, 1998a). However, the truncation of the C-terminal domain by 25 and 45 amino acids led to deregulation of the carrier protein. As a consequence, these BetP mutants were permanently active in betaine transport, independent of the applied hyperosmotic stress. On the other hand, truncation of only 12 terminal amino acids led to partial deregulation, e.g. the activity optimum of this  $\Delta$ 12 mutant was shifted to lower osmolalities, but the protein was still able to sense K<sup>+</sup> (Peter *et al.*, 1998a; Schiller *et al.*, 2004b). These preliminary experiments revealed, that the C-terminal domain (i) was crucial for sensing the stimulus (K<sup>+</sup>) and furthermore (ii) acted as an inhibitory element for BetP activation, because terminal deletions with more than 25 amino acids led to a permanent activation even in the absence of osmotic stress.

By series of constructs, it was intended to narrow down the putative sensory region within the last 25 amino acids of the C-terminal extension. For this purpose, a set of C-terminal mutants were generated via site-directed mutagenesis and analyzed with regard to an involvement in signal perception and/or activity regulation of BetP. It turned out, that a specific glutamate residue at position 572 seemed to be critically involved in potassium sensing: substitutions with glutamine (E572Q), aspartate (E572D), lysine (E572K) and proline (E572P) led to a deregulated activation profile of the respective BetP variant, either heterologously expressed in *E. coli* or reconstituted in proteoliposomes made from *E. coli* lipids (Schiller, 2004; Schiller *et al.*, 2004b). However, in *C. glutamicum* cells all mutants - except the proline variant E572P - regained their ability to detect osmostress (Schiller *et al.*, 2006). As a result, it was stated that (i) the higher amount of negatively charged PG (phosphatidylglycerol) in the membrane of *C. glutamicum* stabilizes the inactive conformation of the sensory domain (Table 2) and (ii) the correct conformation and/or orientation of the C-terminal domain is important for correct stimulus sensing.

The latter conclusion was drawn based on the fact that - according to former *in silico* and CD-spectroscopy analysis – the central part of the C-terminal domain (amino acid positions 553-586) was thought to form the secondary structure of an  $\alpha$ -helix (Figure 11; Burger, 2002). The introduction of proline as a common “helix-breaker” was supposed to alter the conformational properties of the helix. This in turn might impair crucial protein-potassium-membrane interactions and render BetP permanently active (Figure 11, insert upper left). Advanced efforts have been spent on a proline-scan within the C-terminal domain of BetP that confirmed this hypothesis. In addition, it could be shown that not only a retained integrity of the central part of the  $\alpha$ -helix, but also the primary structure of this protein domain seemed to be essential to ensure a proper osmoregulated activity response of BetP (Ott, 2008).



To summarize the results of former and current investigations spent on BetP, Figure 12 displays a preliminary model for the osmotically induced activation of the glycine betaine transporter. It focuses on the presumably different conformations of the C-terminal extension during the activation process as a prerequisite for correct stimulus sensing and signal transduction.



To prove whether the C-terminal conformation and/or relative orientation is altered during the activation process, a specific measuring method was required to allow both, the investigation of the functional BetP protein within a native-like surrounding (e.g. incorporated in proteoliposomes) and – if possible – a time-resolved monitoring of the putative structural changes within the C-terminal domain during an applied hyperosmotic upshift. For this purpose, the Electron Paramagnetic spin Resonance (EPR) spectroscopy was introduced as a promising tool for screening intra- and intermolecular dynamics within macromolecules.

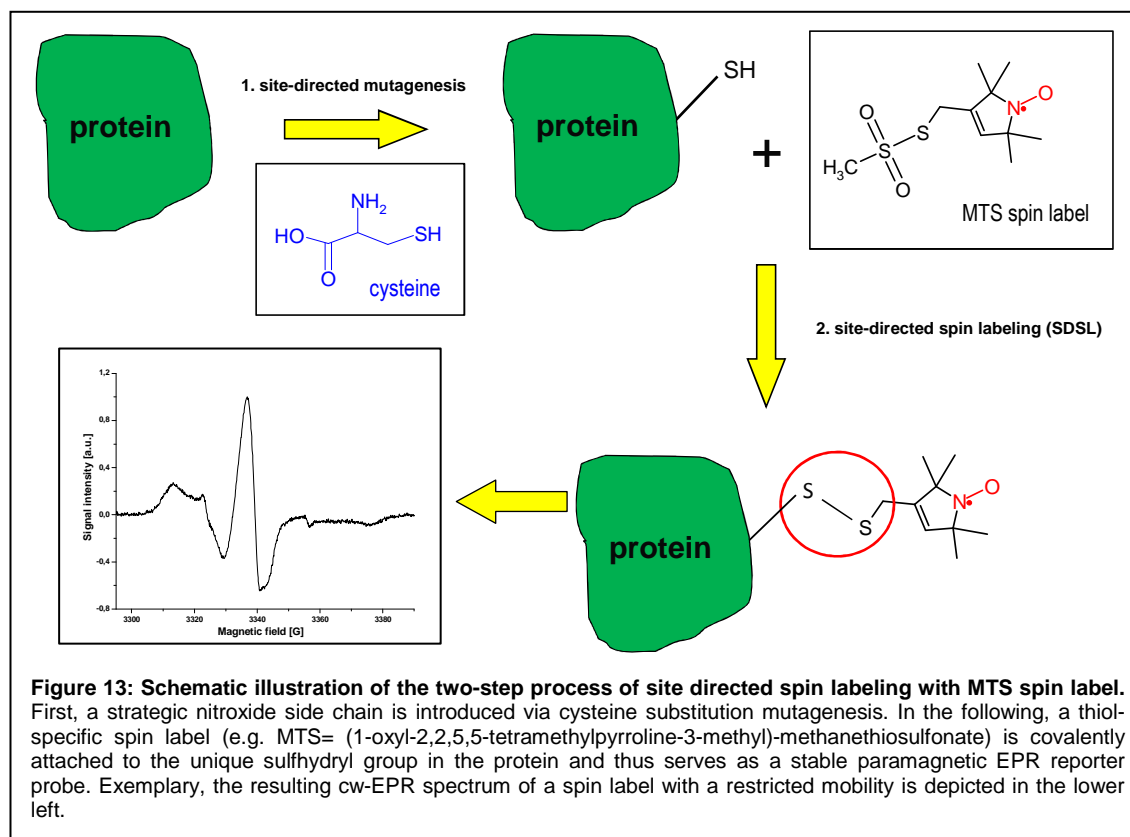
## 1.10. EPR (Electron Paramagnetic Resonance)

To understand the function as well as intra- and intermolecular interactions of a given biomacromolecule, precise knowledge of structure and dynamics is mandatory. Nowadays, protein structures and complexes are mainly determined by two-dimensional NMR (Nuclear Magnetic Resonance) spectroscopy and X-Ray crystallography (Banaszak, 2000). Although both, X-ray crystallography and multidimensional NMR are powerful methods for obtaining the three-dimensional structure of proteins, these techniques are not suitable to determine the structure of protein transient states and the functional dynamics of membrane proteins. The limitations in NMR spectroscopy depend on being to a large extent confined to soluble proteins. Furthermore, it has a relatively low spectral resolution that can be improved via  $^{13}\text{C}$  and  $^{15}\text{N}$  labelling and it needs high amounts of highly concentrated protein samples. Although X-ray crystallography has no size or species limitations for the protein under study, it suffers from a technically very challenging preparation of high-quality crystals of proteins. Furthermore, these crystals only represent a “static snapshot” of one single protein conformation and thus do not allow studying the functional dynamics of proteins.

In contrast, the combination of Site-Directed Spin Labelling and Electron Paramagnetic Resonance (SDSL-EPR) spectroscopy has become a powerful method for probing the structure and structural changes within proteins. The strength of the method applies to those proteins which are not amenable to the atomic-resolution techniques like multidimensional NMR spectroscopy or X-ray crystallography. In addition, the application of SDSL-EPR is not limited by the size of the protein and also large proteins or protein complexes can be studied (Hubbell and Altenbach, 1994).

### 1.10.1. SDSL-EPR properties and benefits

The EPR method was developed in 1944 by E. K. Zavoisky and is based on resonant absorption of electromagnetic radiation by substances with unpaired – so called paramagnetic – electrons (free radicals, transition metal ions or semiconductors). Since the natural occurrence of paramagnetic species in macromolecules is limited, the strategic introduction of a versatile probe containing a stabilized radical centre became a powerful tool in structure-function studies of proteins and biological systems (Figure 13; Burr and Koshland, 1964; Berliner, 1976). Here, natural amino acids at desired sites are replaced by cysteine residues via site-directed mutagenesis, which are then modified by nitroxide spin labels, typically MethaneThioSulfonate Spin Labels (MTSSL, Figure 13).



EPR spectroscopy of site-directed spin labelled biomolecules has become a powerful method for probing the structure and conformational dynamics of water-soluble and membrane proteins of arbitrary molecular weight under conditions relevant to function (Klug *et al.*, 1998; Hubbell *et al.*, 2000; Hubbell *et al.*, 1998; Hubbell *et al.*, 1996; Steinhoff, 2002). The method is applicable to any protein that retains its function after spin labelling. The resulting EPR spectra (Figure 13, insert lower left) comprise a wealth of information on the spin label surrounding in the protein: (i) a restricted or a higher spin label mobility hints to a buried or exposed site of the spin label within the protein structure, respectively, (ii) time-resolved analysis of spin label interactions with secondary and/or tertiary structure elements allows the determination of protein dynamics and conformational changes during protein function on sub-ns to ms and even seconds time scale (Rink *et al.*, 2000; Mchaourab *et al.*, 1996; Steinhoff *et al.*, 1994; Hubbell *et al.*, 2000), (iii) accessibility measurements with paramagnetic, hydrophilic (oxygen) or hydrophobic (CrOx, NiEDDA) quenchers provide insight into the relative orientation of the spin label towards the water phase, the lipid phase or the protein environment (Hubbell *et al.*, 1998; Altenbach, 1989; Farahbakhsh *et al.*, 1995), and (iv) detailed structural information can be achieved by introducing a second paramagnetic site and determining inter- and intramolecular distances from about 5 to 80 Å by measuring magnetic spin-spin interactions (Eaton *et al.*, 1993; Jeschke, 2002; Borovykh *et al.*, 2006; Steinhoff *et al.*, 1991). Thus, the combination of local and global information from SDSL-EPR can provide sufficient information to model

the structure of a protein. EPR data analysis of a series of spin labelled variants of a given protein thus provides the protein topography and the orientations of individual segments of the protein. A complete analysis allows modelling of protein structures with a spatial resolution at the level of the backbone fold. Furthermore, the method is sensitive to molecular dynamics, protein equilibrium fluctuations and conformational changes of functional relevance (Steinhoff and Hubbell, 1996; Hustedt and Beth, 1999; Mchaourab *et al.*, 1997).

### **1.11. Objectives of this thesis**

The aim of the present work is an analysis of structural and conformational changes within a particular domain (C-terminal domain) during the activation process of the secondary transporter BetP from *Corynebacterium glutamicum*. BetP is an osmoregulated glycine betaine uptake system that can autonomously sense its activating stimulus – the internal  $K^+$  concentration - (chemosensor) and respond to an increased medium osmolality (trigger) with a graduated rise in transport activity (osmoregulator) (Rübenhagen *et al.*, 2000; Morbach and Krämer, 2004b). Despite the knowledge of the regulatory behaviour of BetP related to stimuli, membrane composition and the importance of terminal domains in osmosensing and osmoregulation (Rübenhagen *et al.*, 2001; Schiller *et al.*, 2004b), the molecular mechanisms of these processes are still unknown. Recent studies suggested that the C-terminal domain and in particular its conformation and relative orientation is crucial for a correct stimulus sensing and/or signal transduction in BetP (Schiller *et al.*, 2004b; Schiller *et al.*, 2006). The current model for the activation process includes a complex C-domain/N-domain/phospholipid interaction in the inactive state of the transporter. However, upon the hyperosmotically-induced activation of BetP, a “switch”-like movement of the C-domain towards the surrounding protein or lipid environment was assumed to occur (Figure 12). In addition, it was suggested that BetP forms an oligomeric state (i.e. trimers in detergent and in *E. coli* lipids) and that this quaternary structure may be relevant for osmosensing and/or osmoregulation as well (Ziegler *et al.*, 2004, Ressler *et al.*, submitted).

In the present work site-directed spin labelling electron paramagnetic resonance spectroscopy (SDSL-EPR) was applied for the first time to probe structure and conformational dynamics during BetP function. We were interested in the structure and structural changes of the C-terminal domain or of protein domains in the close vicinity to the C-domain. For this purpose, we constructed three different BetP mutants with strategically located single cysteine residues at the beginning (S545C), in the centre (E572C) and close to the end (S589C) of the C-domain and monitored structural changes via continuous wave and pulsed EPR spectroscopy. The covalent attachment of EPR-

specific spin probes to these cysteines intended to allow the monitoring of both, (i) changes in the local environment of the spin label (accessibility and mobility profiles) before, during and after the activation process as well as (ii) absolute distances between two spin labels (spin-spin interactions) in non-activated or permanently active BetP variants. The combination of local and global information derived from these investigations should provide a preliminary model for intra- and intermolecular dynamics within the suggested homo-trimer of the activated secondary transporter.

Transport measurements with the selected purified and spin labelled BetP variants reconstituted in *E. coli* lipids should confirm the already characterized regulation profiles of each heterologously expressed (*E. coli* DH5 $\alpha$ ) mutant protein and attest the general applicability of the EPR method with regard to a functional BetP transporter (Nicklisch, 2005).

## 2. Materials and methods

If not mentioned separately, all used chemicals and reagents were purchased from the following manufacturers:

- Anatrace Inc. (Maumee, Ohio, USA)
- Avanti Polar Lipids Inc. (Alabaster, USA)
- BioRad Laboratories GmbH (Munich, Germany)
- Carl Roth GmbH + Co. KG (Karlsruhe, Germany)
- Difco Laboratories Inc. (Detroit, USA)
- Eppendorf AG (Hamburg, Germany)
- Fermentas GmbH (St. Leon-Roth, Germany)
- GE Healthcare Europe GmbH (Munich, Germany)
- IBA GmbH (Göttingen, Germany)
- Merck KGaA (Darmstadt, Germany)
- Millipore GmbH (Eschborn, Germany)
- NEB GmbH (Frankfurt am Main, Germany)
- Qiagen GmbH (Hilden, Germany)
- Roche Diagnostics GmbH (Mannheim, Germany)
- SERVA Electrophoresis GmbH (Heidelberg, Germany)
- Sigma-Aldrich Chemie GmbH (Munich, Germany)
- Spectrum Europe B.V. (Breda, The Netherlands)
- Toronto Research Chemicals Inc. (North York, Canada)
- Whatman GmbH (Dassel, Germany)

Note:

- Schleicher & Schüll GmbH, Schleicher & Schüll Microscience GmbH and Schleicher & Schüll Bioscience GmbH were acquired by Whatman GmbH (November 2004)
- Amersham Pharmacia Biosciences was acquired by GE Healthcare GmbH (April 2004)



## 2.1. Bacterial strains and plasmids

Table 3 and Table 4 contain the summary of the bacterial strains and plasmids with their respective genetic properties used in this work.

Table 3: *E. coli* strains used in this work with their respective genotypes.

<i>E. coli</i> strains	Genotype	Reference
DH5 $\alpha$ mcr	<i>endA1 supE44 thi-1<math>\lambda</math> recA1 gyrA96 relA1 DeoR <math>\Delta</math>(lacZYA-argF) U169 <math>\Phi</math>80dlacZ <math>\Delta</math>M15 mcrA <math>\Delta</math>(mrr hsdRMS mcrBC)</i>	Grant <i>et al.</i> , 1990
MKH13	<i>araD39 (argF-lac) U169 relA51 rps150 flbB5301 deoC ptsF25 <math>\Delta</math>(putPA)101 V(proP)2 <math>\Delta</math>(proU)</i>	Haardt <i>et al.</i> , 1995

Table 4: Plasmids used in this work with the respective antibiotic resistance and the performed codon exchanges.

Plasmid	Resistance	Properties	Reference
pASK-IBA5	Amp <sup>R</sup>	expression vector	Skerra, 1994
pASK-IBA5- <i>betP</i>	Amp <sup>R</sup>	pASK-IBA5 containing <i>betP</i> cloned in BsaI/HindIII cutting site; N-terminal <i>Strep</i> -Tag II	Rübenhagen <i>et al.</i> , 2000
pAcl1	Amp <sup>R</sup>	pASK-IBA5- <i>betP</i> with codon exchange = C252T (cysteine-free protein)	Rübenhagen <i>et al.</i> , 2001
pAcl1 S61C	Amp <sup>R</sup>	pAcl1 with codon exchange S61C	Rübenhagen, dissertation 2001
pAcl1 S545C	Amp <sup>R</sup>	pAcl1 with codon exchange S545C	Rübenhagen, dissertation 2001
pAcl1 E572C	Amp <sup>R</sup>	pAcl1 with codon exchange E572C	Schiller <i>et al.</i> , 2006
pAcl1 S589C	Amp <sup>R</sup>	pAcl1 with codon exchange S589C	Nicklisch, diploma thesis 2005
pAcl1 S545C/S589C	Amp <sup>R</sup>	pAcl1 with codon exchange S545C and S589C	Nicklisch, diploma thesis 2005
pAcl1 S545C/Y550P/S589C	Amp <sup>R</sup>	pAcl1 with codon exchange S545C, Y550P and S589C	Nicklisch, diploma thesis 2005

Note: Amp<sup>R</sup> = resistance towards ampicillin and derivatives (e.g. carbenicillin)

## 2.2. Growth media and cultivation conditions

### 2.2.1. Growth media for *E. coli* cells

The cultivation of *E. coli* cells was performed in rich medium LB (Lysogeny Broth, "Luria broth") with 10g/L Bacto-tryptone (Difco, Detroit, USA), 5g/L yeast extract and 10g/L NaCl (Sambrook *et al.*, 1989). For agar plates 15g/L Bacto-Agar (Difco, Detroit, USA) was added before autoclaving. If appropriate, the medium was supplemented with the antibiotic carbenicillin to a final concentration of 50 $\mu$ g/ml.

For the production of transformation-competent *E. coli* cells the SOB medium (2% Bacto-tryptone, 0.5% yeast extract, 10mM NaCl, 2.5mM KCl, 10mM MgSO<sub>4</sub>, 10mM MgCl<sub>2</sub>) was used according to Hanahan (1985). This nutritionally rich and isotonic medium supports cell survival during the preparation and transformation process due to the provision of a source for nitrogen and growth factors (yeast extract) as well as essential ions for a variety of enzymatic reactions and DNA replication (e.g. NaCl, KCl, MgSO<sub>4</sub>). Subsequent to the transformation with foreign plasmid DNA, the stressed *E. coli* cells were regenerated in SOB medium supplemented with 20mM glucose (= SOC medium) to provide a readily available carbon and energy source for mending the cell perforations made to facilitate the entering of DNA.

### 2.2.2. Expression and cultivation conditions

All *E. coli* strains used in this work were cultivated in shaking flasks with lateral baffles under aerobic conditions at 37°C. The growth of the bacterial cultures was followed by determining the Optical Density (OD) of the medium at 600nm (Optical thickness of the used micro cuvettes=10mm; Spectrophotometer Novaspec II, GE Healthcare Europe GmbH, Germany). For *E. coli* cells an OD<sub>600</sub> of 1 corresponds to a bacterial suspension of approximately 10<sup>9</sup> cells per ml. For heterologous overexpression, the respective *betP* gene was cloned into the vector pASK-IBA5 (IBA GmbH, Göttingen), in which *Strep-betP* is under the control of the *tetA* promotor. Afterwards, *E.coli* DH5α cells were transformed with the resulting plasmid DNA. These cells were then cultivated over night in 5ml LB medium supplemented with carbenicillin (50µg/ml) at 37°C. Subsequently, the cells were transferred into fresh LB medium with an optical density (OD<sub>600</sub>) of 0.1 and cultivated at 37°C. When the cultures reached an optical density of OD<sub>600</sub>=1, *betP* expression was induced by the addition of 200µg AnHydroTetracycline (AHT) per litre culture and cells were harvested after 3-4h growth.

To increase the yields of cell mass, the respective cells were also cultivated in a 10L Braun glass vessel fermenter (Sartorius AG, Göttingen). For this purpose, the starter cultures of *E. coli* DH5α cells were prepared as described above. Hence, the main culture was grown at 37°C with an air flow rate of 10l/min and a stirring rate of 1200RPM. To prevent excessive foaming, 1ml of PolyPropylene Glycol (PPG; Sigma, Munich, Germany) was added prior to the induction. When the cultures reached an optical density of OD<sub>600</sub>=1, *betP* expression was induced by the addition of 100µg AnHydroTetracycline (AHT) per litre culture and cells were harvested after 3-4h growth. The concentration of the inductor (AHT) had to be halved, because cultures treated with 200µg AHT per litre medium stopped growing or even died after 1-2h of induction (“scale-up” problem).

## 2.3. Molecular biological approaches

### 2.3.1. Preparation of competent *E. coli* cells and transformation

The method of Inoue *et al.* (1990) was used to prepare competent *E. coli* DH5 $\alpha$  cells and to transform these cells with (recombinant) plasmid DNA. For this purpose, 5ml LB medium were inoculated with *E. coli* cells and cultivated for 8h at 37°C. 1ml of this culture was used to inoculate 250ml SOB medium and cells were then cultivated for further 16h at 37°C until an optical density of OD<sub>600</sub>=0.6 was reached. Subsequently, the culture was chilled on ice for 10min. Cells were harvested by centrifugation (2000g, 4°C, 10min). The cell pellet was suspended in 80ml ice-cold TB buffer (10mM Pipes, pH 6.7; 250mM KCl; 55mM MnCl<sub>2</sub>; 15mM CaCl<sub>2</sub>) and thereupon collected by a second centrifugation step (2000g, 4°C, 10min). Cells were then suspended in 20ml ice-cold TB buffer before DMSO was added stepwise, until a final concentration of 7% (v/v) was reached, and incubated for 10min on ice. Aliquots of 100 $\mu$ L were transferred into pre-cooled reaction tubes, immediately frozen in liquid nitrogen and stored at -80°C. For transformation, a 100  $\mu$ L aliquot of competent *E. coli* cells was thawed on ice and 5-10 $\mu$ l ligation product or about 1 $\mu$ l plasmid DNA was added. Then, the cells were incubated for 30min on ice. After heat shock at 42°C for 45s, cells were immediately mixed with 400 $\mu$ L SOC medium and cultivated for 1h at 37°C. The cell suspension was plated on LB agar plates containing 50 $\mu$ g/ml carbenicillin, and cultivated for 16h at 37°C.

To prepare competent *E. coli* MKH13 cells the method of Chung *et al.* (1989) was used. In short, 5ml LB medium were inoculated with *E. coli* MKH13 cells and cultivated for 16h at 37°C. Then 150 $\mu$ l of this culture was used to inoculate 15ml LB medium and cells were cultivated for another 16h at 37°C until an optical density of OD<sub>600</sub>=0.4 was reached. For each transformation, a 1ml aliquot was transferred into a reaction tube. After centrifugation (2000g, 4°C, 5min), cells were suspended in 100 $\mu$ l TSS buffer (LB medium, 10% PEG, 5% DMSO, 50mM MgCl<sub>2</sub>) and 1 $\mu$ l of plasmid DNA was added to the final solution. Then, the cells were incubated for 30min on ice. Subsequently the cells were mixed with 400 $\mu$ l SOC medium and cultivated for 1h at 37°C. The cell suspension was plated on LB agar containing 50 $\mu$ g/ml carbenicillin, and cultivated for 16h at 37°C.

### 2.3.2. DNA techniques

#### 2.3.2.1. Isolation of plasmid DNA from *E. coli*

The isolation of plasmid DNA from *E. coli* cells was performed following a modified method of alkaline lysis (Birnboim and Doly, 1979). For this purpose, 2ml of an overnight culture of *E. coli* cells with an appropriate amount of antibiotic was used. For the isolation

of plasmid DNA from this culture, the NucleoSpin<sup>®</sup> Plasmid DNA Purification kit (Macherey-Nagel, Düren, Germany) was used as recommended by the manufacturer. In contrast to the original protocol, the cells of the overnight culture were centrifuged at 11.000g for 2min and the final elution of plasmid DNA was carried out with 50µl of autoclaved H<sub>2</sub>O<sub>dd</sub>.

### **2.3.2.2. Gel electrophoresis and extraction of DNA from agarose gels**

Gel electrophoresis of DNA was performed using 0.8 to 2% (w/v) agarose gels in 1xTAE buffer (40mM Tris; 2mM EDTA, pH 8.0; 20mM acetic acid) as described by Sambrook *et al.* (1989). For this purpose, DNA samples were mixed with 5xLoading Dye (Fermentas, St. Leon-Roth, Germany). After electrophoresis, the DNA was stained with ethidium bromide. For the detection of stained DNA, the Image Master VDS system (Amersham Biosciences, Freiburg, Germany) was used.

### **2.3.2.3. Polymerase chain reaction (PCR)**

The *in vitro* amplification of specific DNA fragments was performed by the polymerase chain reaction (PCR, Mullis *et al.*, 1986) using the Taq PCR Master Mix (Qiagen, Hilden, Germany) as recommended by the manufacturer. For this purpose, two primers were used, flanking the DNA region, which should be amplified. Primers were diluted to a concentration of 10pmol/µl with autoclaved H<sub>2</sub>O<sub>dd</sub>. The annealing temperature was chosen with respect to the respective base sequence of the forward and reverse primer. For each guanine and cytosine 4°C, for each adenine and thymine 2°C are required to separate the hydrogen bonds. Total DNA, plasmid DNA, or a cell suspension, which was diluted in H<sub>2</sub>O<sub>dd</sub> and incubated for 10min at 95°C, were used as templates. The PCR reaction was performed using the thermocycler Mastercycler<sup>®</sup> personal or Mastercycler<sup>®</sup> gradient (Eppendorf AG, Hamburg, Germany). A 20µl PCR reaction mixture was prepared as follows:

- 10µl Master-Mix (Qiagen, Hilden)
- 1µl primer forward [10µM]
- 1µl primer reverse [10µM]
- 1µl template
- H<sub>2</sub>O<sub>dd</sub> ad 20µl

The amplification reaction was initiated by denaturing the template for 4min at 95°C. The following steps were performed in 30 cycles: Denaturing the DNA for 30 seconds at 95°C, hybridization of the primers for 30 seconds at the specific annealing temperature, and polymerisation for 1 min per kb at 72°C. After final incubation for 10min at 72°C, the samples were kept at 4°C or -20°C. To separate the PCR product from the starting

material (template, primers, reagents) and for subsequent cloning experiments, the PCR product could be purified either with the NucleoSpin<sup>®</sup> Extract Kit (Macherey-Nagel, Düren, Germany) as recommended by the manufacturer, or by agarose gel electrophoresis as described in section 2.3.2.2.

### **2.3.2.4. DNA sequencing**

After mutagenesis or cloning, the respective plasmid constructs were sequenced to check if only the desired mutations were introduced and no accessory mutations occurred during the PCR reaction. The underlying sequencing method is based on the dideoxy sequencing or chain termination method developed by Sanger *et al.* (1977) with modifications done by Zimmermann *et al.* (1990). In short, chain termination occurs due to the use of dideoxynucleotides (ddNTPs), which are labelled with different fluorescent dyes. These modified nucleotides, when integrated into a sequence, prevent the addition of further nucleotides and thus the DNA chain is terminated ("chain termination"). The resulting sequencing products are separated by capillary electrophoresis and subsequently detected with automatic sequencing equipment. Thus, chain terminations closest to the primer generate the smallest DNA molecules (which migrate faster through the capillary), and chain terminations farther away from the primer generate larger DNA molecules (which are slower and therefore will be detected later). Detecting the terminal fluorescent dye of each fragment with a one-base-offset finally identifies the whole DNA sequence.

For this purpose, PCR products (10-50ng/μl) or plasmid DNA (30-100ng/μl) and the respective forward or reverse sequencing primers (10pmol/μl) were transferred to a reaction tube and send to an external sequencing laboratory (GATC Biotech AG, Konstanz, Germany).

## **2.4. General analytical approaches**

### **2.4.1. Determination of protein concentrations**

It has to be noted that although the molecular mass of the used standard protein Bovine Serum Albumin (BSA, 66.4kDa) in the assays is similar to the BetP (64.2kDa), the amino acid composition is different. This systematic error (e. g. a different amount of basic amino acid residues (His, Lys, Arg): BetP=47, BSA=102) may thus lead to an underestimation of the real protein content in the samples and have to be taken into account for the quantitative analyses (Peter *et al.*, 1996; Racusen, 1973; Brown, 1975; Reed *et al.*, 1980, Hirayama *et al.*, 1990).

### 2.4.1.1. Bradford analyses

For the determination of the protein concentrations of soluble protein preparations or whole cell extracts, the method of Bradford (1976) was used. This method bases on binding of the dye Coomassie (Coomassie Brilliant Blue G-250) to arginine and hydrophobic residues in a protein which induces an absorbance shift in the dye from 470nm (unbound) to 595nm (bound). Accordingly, the increase in absorbance at 595nm is proportional to the protein amount in the respective sample.

The used Roti<sup>®</sup>Quant kit (Carl Roth GmbH + Co. KG, Karlsruhe, Germany) provided a linear measuring range of the assay with BSA (Bovine Serum Albumin) that stretches from 5 up to 2000µg/ml (Roti<sup>®</sup>-Quant Universal Operating Manual). For each measurement, 1 to 10µg of protein was diluted in 100µl H<sub>2</sub>O<sub>dd</sub> and supplemented with 900µl 1xRoti<sup>®</sup>Quant reagent. Solutions of BSA (NEB, Frankfurt/Main, Germany) with known concentrations were used as standard. The optical density of the samples was measured at 595nm and the respective concentration of the BetP protein in solution was determined by the use of a BSA calibration curve.

### 2.4.1.2. Amido Black analyses

For determination of the concentration of membrane proteins after the affinity purification or reconstitution, the Amido Black method (Schaffner and Weissmann, 1973) was used. This method was selected, because it is less susceptible to interference by the presence of detergents or lipids in the sample solution and has a higher sensitivity (down to 0.75µg/ml protein, Schaffner and Weissmann, 1973) compared to e.g. the Bradford assay (2.4.1.1). The Amido Black dye stoichiometrically binds to basic amino acids (Arg, Lys, His) in a protein and can be quantified by measuring the optical density at 630nm and comparing it to the respective absorption of a standard protein (e.g. BSA) with known concentration.

For this purpose, 5-20µl of highly concentrated BetP elution fractions (confirmed by UV detection of the major elution peak) was diluted in H<sub>2</sub>O<sub>dd</sub> to a final volume of 225µl. Solutions of BSA were used as a standard. Subsequently 30µL solution 1 (1M Tris, 2% SDS, pH(HCl) = 7.4) and 50µL solution 2 (90 % trichloroacetic acid) were added to the sample, mixed and incubated for 2min at room temperature (RT). A nitrocellulose filter (HA membrane filters, pore diameter 0.45µm, Millipore, Eschborn, Germany) was temporary equilibrated with H<sub>2</sub>O<sub>dd</sub> and then placed on the Millipore filter system. The samples of interest were applied as distinct spots on the filter and washed with 200µl solution 3 (6% trichloroacetic acid). After rinsing the filter with another 2ml of solution 3, the samples were dyed for 10min in Amido Black dye solution (0.25% (w/v) Amido Black, 45% (v/v) methanol, 10% (v/v) acetic acid). Then, the filter was washed in H<sub>2</sub>O<sub>dd</sub>,

decolorized 2-3 times using solution 4 (90% (v/v) methanol, 2% (v/v) acetic acid), rinsed again with water, and dried at RT for 5-10min. Each protein spot was then transferred into 1ml of solution 5 (25mM NaOH, 50 $\mu$ M EDTA, 50% (v/v) ethanol) and incubated at RT for 10min under constant shaking. The optical density of the obtained solutions was measured at 630nm and the concentration of each sample was determined by the use of a BSA calibration curve. For an optimal coherency and a correct correlation between absorption colorimetry and used protein concentration, the spots of the standard proteins were always applied to the same filter as the spots of the protein sample of unknown concentration.

### **2.4.2. SDS-Polyacrylamide Gel Electrophoresis (PAGE)**

For the electrophoretic analyses of proteins under denaturing conditions, cell extract, isolated proteins, or proteoliposomes were diluted in loading dye (4% SDS, 20% glycerol (w/v), 50mM Tris, 2%  $\beta$ -mercaptoethanol (v/v), 10mM EDTA, 0.01% serva blue G, pH(HCl)=6.8) and subjected to SDS-PAGE using 12% SDS polyacrylamide gels (Laemmli *et al.*, 1970).

A 12% separation gel was composed of:

- 6ml separation gel buffer (1.5M Tris, 0.4% SDS, pH(HCl)=8.8)
- 8.4ml H<sub>2</sub>O<sub>dd</sub>
- 9.6ml acryl amide : bisacrylamide (30 : 0.8)
- 240 $\mu$ l ammonium persulfate (100mg/ml)
- 10 $\mu$ l TEMED

A 5% stacking gel was composed of:

- 2.5ml stacking gel buffer (0.5 M Tris, 0.4% SDS, pH(HCl)=6.76)
- 5.9ml H<sub>2</sub>O<sub>dd</sub>
- 1.6ml acryl amide : bisacrylamide (30 : 0.8)
- 100 $\mu$ l ammonium persulfate (100mg/ml)
- 10 $\mu$ l TEMED

10xelectrophoresis buffer: 250mM Tris, 1.92M glycine, 35mM SDS, pH(HCl)=8.2 to 8.3.

Gel electrophoresis was performed in MINI Vertical Dual Plate Electrophoresis Units (Carl Roth GmbH, Karlsruhe, Germany) at 50-60V for 30-45min in the stacking gel phase and subsequently at 140-160V for 45-60min in the separation gel phase. The visualization of proteins within the SDS gels was performed by means of Coomassie Brilliant Blue

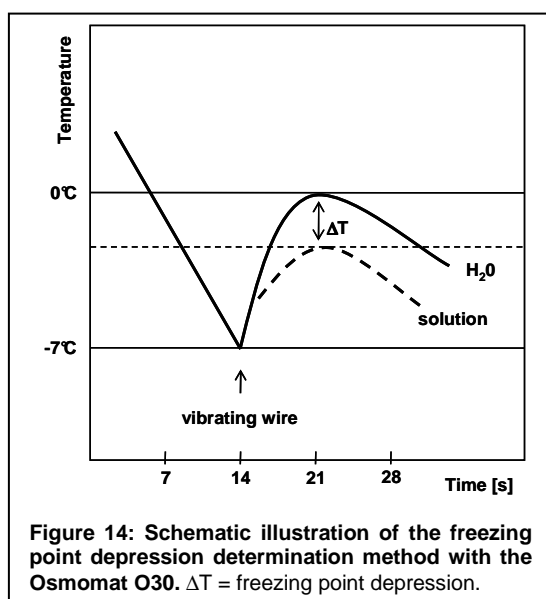
staining developed by Sambrook *et al.* (1989). For this purpose, the SDS-gels were incubated in staining solution (0.2% Coomassie Brilliant Blue G-250, 45% (v/v) methanol, 10% acetic acid) for 1 to 16 h, followed by decolorizing of the gels using 10% acetic acid.

### 2.4.3. Immunoblot analyses

The detection of specific proteins after gel electrophoresis was carried out by means of immunoblotting. For this purpose, the proteins were transferred from the SDS gels to an Immobilon™-P PolyVinylidene DiFluoride (PVDF) membrane (Millipore, Roth, Karlsruhe, Germany) by semi-dry blotting (Kyhse-Anderson, 1984). The membrane was first moistened in methanol and then temporarily equilibrated in transfer buffer (10mM CAPS, 10% (v/v) methanol, pH(NaOH)=11) before use. Subsequently, the membrane was placed on top of six filters (Whatman GmbH, Dassel, Germany), which were equilibrated in the same buffer. The SDS-gel was applied on top of the membrane and covered with another six filters, which were also equilibrated in transfer buffer. The protein transfer was performed with a semi-dry blotter (GE Healthcare, Munich, Germany) for 45min at 0.8mA/cm<sup>2</sup> membrane area. After incubation for 60min in blocking buffer (50mM Tris, 0.15M NaCl, 3% (w/v) BSA, pH(HCl)=7.5) at RT, the membrane was incubated for further 60min in blocking buffer supplemented with the first antibody (Strep-tag II antibody (MAB), IBA GmbH, Göttingen, Germany), using a 1 : 1000 dilution. After 3 washing steps with washing buffer (50mM Tris, 0.15M NaCl, 0.3% (w/v) BSA, pH(HCl)=7.5) for 20min each, the second antibody (Anti-Mouse IgG alkaline phosphatase, Sigma-Aldrich, Munich, Germany), was diluted 1 : 10000 in blocking buffer, and the membrane was incubated in this solution for 60min at RT. After three additional washing steps (20min each), the signal was detected by the addition of the alkaline phosphatase substrate BCIP (5-Bromo-4-Chloro-3-Indolyl Phosphate) and NBT (Nitro-Blue Tetrazolium Chloride) in reaction buffer (100mM Tris, 100mM NaCl, 5mM MgCl<sub>2</sub>, pH(HCl)=9.5) to a final concentration of 0.02% and 0.03%, respectively (Roth, Karlsruhe, Germany). The alkaline phosphatase hydrolyses BCIP to form an intermediate that dimerises to a "Dehydroindigo" precipitate exhibiting a dark-blue indigo dye. At the same time NBT (oxidant) is reduced to the dark-blue NBT-diformazan by the two reducing equivalents generated by the dimerisation. Due to the fact that the reaction proceeds at a steady rate, the signal intensity was increased with a longer incubation of the membrane with the reagents (5 to 60min in the dark), before the reaction was stopped by the addition of H<sub>2</sub>O<sub>dd</sub>.



## 2.4.4. Determination of the osmolality



For the determination of the osmolality of buffers and media, an osmometer (Osmomat O30, Gonotec, Berlin, Germany) was used as recommended by the manufacturer.

This device uses the technique of freezing point depression to determine the osmotic strength of a given solution. Thereby, the sample is thermoelectrically cooled down to  $-7^{\circ}\text{C}$  (cooling without freezing) and subsequently frozen by means of a vibrating wire (Figure 14). The formation of ice (-crystals) then produces warmth that leads to

a specific increase in temperature. For pure  $\text{H}_2\text{O}_{\text{dd}}$  this temperature rise is saturated at  $0^{\circ}\text{C}$  (= freezing point of pure water). Depending on the amount of solutes in the respective sample this freezing point is proportionally depressed and thus allows determining the concentration of dissolved particles in a given solution.

Prior to each determination series, pure  $\text{H}_2\text{O}_{\text{dd}}$  served as blank value and  $9.46\text{g NaCl/kg H}_2\text{O}_{\text{dd}}$  ( $0.3\text{osmol/kg}$ ) as standard solution to calibrate the device. For each measurement a total sample volume of  $50\mu\text{l}$  was used.

## 2.5. Biochemical approaches

### 2.5.1. Membrane preparation

For the isolation of BetP derivatives, *E. coli* DH5 $\alpha$  *mcr* cells transformed with pASK-IBA5-*strep-betP* (BetP fused to a Strep-tag at its N-terminus) were cultivated at  $37^{\circ}\text{C}$  in LB medium and supplemented with carbenicillin ( $50\mu\text{g/ml}$ ). Induction was carried out in exponentially growing cells ( $\text{OD}_{600}=0.9$ ) upon the addition of  $200\mu\text{g}$  anhydrotetracycline/litre cell culture. The cells were harvested 3-4h after induction, washed ( $100\text{mM KP}_i$ ,  $\text{pH}=7.5$ ) and stored at  $-20^{\circ}\text{C}$  for long time or at  $4^{\circ}\text{C}$  in the case the membrane preparation was scheduled for the next day. To prepare membranes, the cells were thawed on ice and suspended in lysis buffer ( $100\text{mM KP}_i$ ,  $\text{pH}=7.5$ ;  $1\text{mM EDTA}$ ;  $2\mu\text{g/ml}$  buffer DNase (Sigma-Aldrich, Munich, Germany); 1 tablet EDTA-free Complete protease inhibitor (Roche, Mannheim, Germany) per  $100\text{ml}$  buffer). Subsequently, cells were disrupted by three passes through a high-pressure cell in a French<sup>®</sup> Press (Thermo Electron Corporation, Needham Heights, USA) with an effective internal cell pressure of  $10.000\text{ PSI}$ . Afterwards, the crude extract was centrifuged for 30min at  $12.000\text{g}$  and  $4^{\circ}\text{C}$

to separate the cell debris. The supernatant was then ultracentrifuged for 45min at 210.000g at 4°C to collect the desired membrane fraction. Membranes were washed once in lysis buffer and collected via ultracentrifugation (45min, 210.000g, 4°C). Aliquots of 1ml were transferred into reaction tubes, frozen in liquid nitrogen and stored at -80 °C until further usage.

### **2.5.2. Purification of Strep-BetP by Strep-tag II / StrepTactin affinity chromatography**

The isolation and purification of Strep-BetP from the *E. coli* membranes was carried out by *Strep*<sup>®</sup> *tag II* affinity chromatography (IBA, Göttingen, Germany) via FPLC (fast protein liquid chromatography, GE Healthcare, Munich, Germany). For this purpose, the respective membranes were first dissolved in solubilisation buffer (50mM KP<sub>i</sub>, pH=7.5; 8.6% glycerol; 1mM EDTA). The membrane solubilisation was performed via the drop wise addition of 2% (w/v) DDM (n-dodecyl-β-D-maltopyranoside, Anatrace, Ohio, USA) and incubation for 30-60min at 4°C under constantly stirring. Membranous remains were separated by centrifugation for 20min at 87.000g and 4°C in a Beckman TLX ultracentrifuge (Beckman, Munich, Germany) and the supernatant diluted 1:4 with low-salt purification buffer lacking DDM (50mM KP<sub>i</sub>, pH 7.5; 200mM NaCl; 8.6% glycerol; 1mM EDTA) was collected. The diluted supernatant fraction containing solubilised Strep-BetP was then purified by *Strep-tag*<sup>®</sup> II/StrepTactin affinity chromatography (IBA, Göttingen, Germany), using a 5-ml column of *Strep-Tactin*<sup>®</sup> MacroPrep<sup>®</sup> resin. The column was pre-equilibrated with 10 column volumes low-salt purification buffer (50mM KP<sub>i</sub>, pH 7.5; 200mM NaCl; 8.6% glycerol; 1mM EDTA, 0.1% DDM) before the soluble membrane proteins were applied to the column. Subsequently to the application of the supernatant fraction, two washing steps with 10 column volumes high-salt (50mM KP<sub>i</sub>, pH=7.5; 500mM NaCl; 1mM EDTA; 8.6% glycerol, 0.1% DDM) and 10 column volumes low-salt purification buffer were carried out. In the case when spin labelled BetP variants were used, an intermediate step during the purification was added (2.5.3). Non-labelled Strep-BetP variants were eluted with 35ml purification buffer supplemented with 5mM DesThioBiotin (DTB). The elutions were fractionated in 2ml reaction tubes, frozen in liquid nitrogen and stored at -80°C until further usage. The flow rate during all washing and elution steps was adjusted to 0.5ml/min and the whole chromatography was performed at 4°C.

### **2.5.3. Site-directed spin labelling (SDSL) with thiol specific reporter molecules**

To probe the structural and dynamic aspects of the BetP protein using the EPR (Electron Paramagnetic Resonance, section 1.10) method, it is crucial to incorporate a specific reporter molecule at strategic amino acid positions within the carrier structure. Nitroxide spin labels are the most popular organic radicals used as markers in EPR spectroscopy. This is because nitroxide probes have a high stability and a well-known shape of EPR spectra. Among these spin labels, thiol-specific alkyl-thiosulfonates are the most important ones, because they possess a very high specificity and a rapid reactivity concerning the covalent attachment to native or engineered cysteine residues by a disulfide bond formation.

For this purpose both, spin labelling and the pre-treatment with the reducing agent DiThioThreitol (DTT; Sigma-Aldrich, Munich, Germany) were performed at 4°C directly on the Strep Tactin column after binding of Strep-BetP and the subsequent washing steps that remove unspecific bound protein (2.5.2). All washing steps prior to the labelling procedure were carried out with degassed (15-20min sonification) low-salt purification buffer (50mM KP<sub>i</sub>, pH 7.5; 200mM NaCl; 8.6% glycerol; 1mM EDTA, 0,1% DDM) to prevent the spontaneous oxidation of cysteines to cystines (cysteine dimers). Accordingly, the thiol groups of the target cysteines were first reduced with two column volumes of freshly prepared 10mM DTT dissolved in low-salt purification buffer, incubated for 3h and then washed in excess (5-10 column volumes) with the same degassed buffer. Subsequently, the reaction with the nitroxide spin label ((1-oxyl-2,2,5,5-tetramethylpyrroline-3-methyl) methanethiosulfonate, MTS; Toronto Research Chemicals, North York, Canada) was carried out on the column with a molar spin label-to-protein ratio of 10:1 for 16h at 4°C. Unbound spin label was removed by washing with 10 column volumes of low-salt buffer and subsequently the labelled BetP-protein was eluted from the column using the purification buffer supplemented with 5mM desthiobiotin (Sigma-Aldrich, Munich, Germany).

### **2.5.4. Preparation of macroporous polystyrene beads (Bio-Beads SM2)**

To remove the detergent during both types of reconstitution applied in this work (2.5.6 and 2.5.7) a hydrophobic, insoluble adsorbent (Bio-Beads SM2, BioRad, Munich, Germany) was used. Bio-Beads were prepared as described by Holloway *at al.* (1973). In short, 30g of Bio-Beads were added to 200ml methanol and incubated for 15-30min at RT under gently stirring. The swelled beads were collected on a sintered glass funnel and washed

with further 500ml methanol. Immediately after this, the beads were washed with 2-3l of  $H_2O_{dd}$  avoiding desiccation and stored in  $H_2O_{dd}$  until further usage.

### 2.5.5. Liposome preparation

For the preparation of liposomes, *E. coli* phospholipids (Polar Lipid Extract, 20mg/ml in chloroform, Avanti Polar Lipids, Alabaster, USA), or synthetic phosphatidylglycerols (DOPC, 1,2-Dioleoyl-*sn*-Glycero-3-Phosphocholine; DOPG, 1,2-Dioleoyl-*sn*-Glycero-3-Phosphoglycerol; Avanti Polar Lipids, Alabaster, USA) were used. For this purpose, the solvent was evaporated to dryness in a rotary evaporator (30°C; temperature should be at least above phase transition temperature of the lipids). Traces of solvent were removed overnight (16h) by freeze-drying (lyophilisation). Subsequently, the lyophilized lipids were dissolved in 100mM  $KP_i$ , 2mM  $\beta$ -mercaptoethanol, pH=7.5, to a final concentration of 20mg of phospholipids/ml suspension, frozen in liquid nitrogen and stored at -80°C. For all experiments dealing with labelling of cysteine residues, the lyophilized lipids were suspended in 100mM  $KP_i$  (pH=7.5) buffer lacking  $\beta$ -mercaptoethanol, because this antioxidant reduces disulfide bonds. To avoid lipid oxidation during preparation and long-term storage, the aliquots were kept under a nitrogen atmosphere. Prior to use, liposomes were formed by extrusion (Avanti Mini-Extruder, Avanti Polar Lipids, Alabaster, USA) 15 times through polycarbonate filters (pore diameter 400nm, Whatman, Dassel, Germany).

### 2.5.6. Reconstitution of Strep-BetP derivatives into *E. coli* liposomes (Bio-Beads)

If not mentioned otherwise, the purified betaine carrier was reconstituted into lipids as described by Rigaud *et al.* (1995). In short, *E. coli* lipids prepared from *E. coli* polar lipid extract were diluted to a concentration of 5mg/ml in extrusion buffer and extruded (Avanti Mini-Extruder, Avanti, Alabaster, USA) 15 times through polycarbonate filters (pore diameter 400nm, Whatman, Dassel, Germany). The resulting liposomes were solubilised by stepwise addition of 20% (v/v, in  $H_2O_{dd}$ ) Triton X-100. The insertion of detergent was monitored by measurement of the turbidity at 540nm. Upon saturation with detergent, the liposomes were incubated for 20min at RT and subsequently mixed with Strep-BetP in elution buffer at a lipid-to-protein ratio of 30:1 (w/w). The mixture was incubated for 30-60min at RT under gentle stirring. To remove detergent, SM2 Bio-Beads (BioRad, Munich, Germany), pre-washed with  $H_2O_{dd}$ , were added at a Bio-Bead (wet weight, filter-dried) to Triton X-100 ratio of 5 and a Bio-Beads to DDM ratio of 10 (w/w). The mixture was kept under gentle stirring at room temperature for 1h, and the same amount of fresh Bio-Beads was added. After 1h of gentle stirring, the double amount of fresh Bio-Beads was added, and the mixture was stirred at 4°C. After 16h, the single amount of Bio-Beads was added

and the mixture was gently stirred for an additional hour at 4°C. Finally, the Bio-Beads were separated from mixture and the solution was centrifuged for 20min at 337.000g and 4°C in a Beckman TLX ultracentrifuge (Beckman, Munich, Germany) to collect the formed proteoliposomes. After centrifugation, the proteoliposomes were extruded 15 times through polycarbonate filters (pore diameter 400nm) in 100mM KPi (pH=7.5) and washed two times by centrifugation (20min, 337.000g, 4°C) and suspension in the same buffer. The resulting suspension was adjusted to 60µg lipid/µl solution, frozen in liquid nitrogen, and stored at -80°C.

### **2.5.7. Reconstitution of Strep-BetP derivatives into *E. coli* liposomes (Bio-Beads/dialysis)**

The solubilisation and preforming of *E. coli* liposomes was done as described in section 2.5.6. Then, solubilised BetP-SL protein was added at a lipid-to-protein ratio of 20:1 (w/w) and incubated for 30min at room temperature under constant stirring to promote protein incorporation. To remove excess detergent, a combination of dialysis and hydrophobic adsorption on SM2 Bio-Beads (Biorad, Munich, Germany) was used. In short, the dialysis bag (50kDa cut-off, Cellulose Ester, Spectra-Por/Float-A-Lyzer, Spectrum Europe B.V., The Netherlands) was loaded with the mixed lipid-protein-detergent micelles and dialysed (1:50) against 100mM KPi (pH 7.5) supplemented with 1mM EDTA. Additionally, Bio-Beads were added to the external buffer with a Bio-Bead (wet weight, filter-dried) to Triton X-100 ratio of 5 and a Bio-Bead to DDM ratio of 10 (w/w) per batch. The batch procedure was segmented in three parts: adding fresh Bio-Beads and incubation for 1h at room temperature, adding the double amount of fresh Bio-Beads and incubating over night at 4°C and on the next day adding fresh Bio-Beads and incubating again for 1h at 4°C. Finally, the formed proteoliposomes were collected by ultracentrifugation (20min, 337.000g, 4°C), washed 3 times in 100mM KPi (pH 7.5) and concentrated to yield a total BetP concentration of 50-100µM (100µM ~ 6.42mg/ml). Proteoliposomes were frozen in liquid N<sub>2</sub> and stored at -80°C until use.

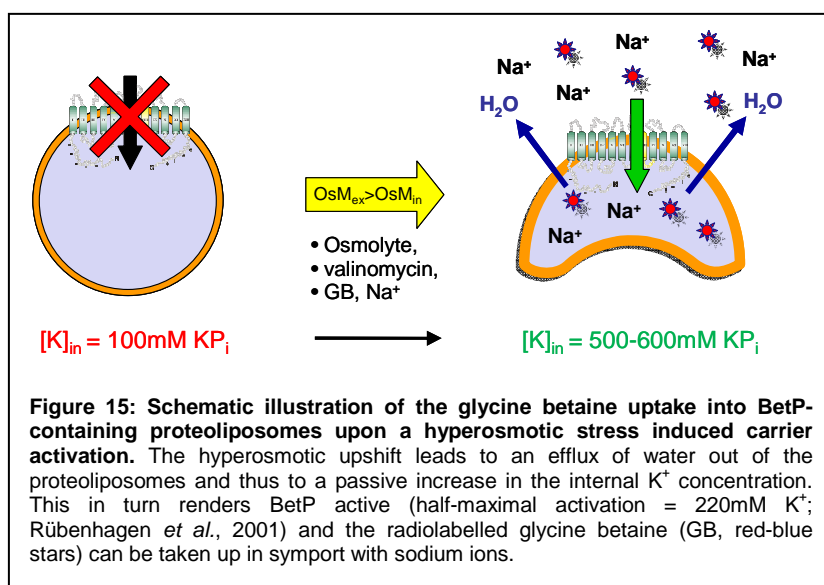
### **2.5.8. Variation of the lipid composition in proteoliposomes**

One big drawback of the new Bio-Bead/dialysis reconstitution method (2.5.7) was the fact, that not only the detergent molecules of dodecylmaltoside ( $M_r = 511\text{Da}$ ; aggregation number = 110-140; Le Maire *et al.*, 2000) and Triton X-100 ( $M_r = 625\text{Da}$ ; aggregation number = 75-165; Le Maire *et al.*, 2000) could pass the dialysis bag (mean cut-off = 50kDa) and get absorbed by the externally applied Bio-Beads but also the lipid molecules with a mean molecular mass of about 700-1000Da. Accordingly, the Lipid-to-Protein Ratio (LPR) after the dialysis had to be readjusted, to guarantee proper sealed proteoliposomes

and a functional protein incorporation. In addition, the introduction of negatively charged lipids (DOPG) should mimic the native lipid composition of the *C. glutamicum* membrane and thus allow the detailed analysis of the lipid effects on the regulation properties of BetP (Table 2, Introduction).

For this purpose, proteoliposomes made from *E. coli* phospholipids were fused with liposomes or emulsions composed of synthetic phospholipids. Hence, proteoliposomes were prepared as described in sections 2.5.6 and 2.5.7 with a starting lipid-to-protein ratio of 20:1 (w/w). These proteoliposomes were then mixed with an appropriate amount of synthetic lipids (e.g. DOPC, 1,2-Dioleoyl-*sn*-Glycero-3-Phosphocholine, Avanti Polar Lipids, Alabaster, USA) and extruded (15 times). Before freezing the samples in liquid nitrogen and storing at  $-80^{\circ}\text{C}$ , the samples were subjected to a freeze-thaw cycles for three times (Kasahara and Hinkle, 1977; Pick, 1981) in order to assure a proper integration of the fused lipids.

### 2.5.9. Transport measurements (glycine betaine uptake in proteoliposomes)



To test whether the introduction of a spin label at a distinct cysteine position within the carrier is not detrimental for the functional activity of BetP, proteoliposomes of the respective BetP-SL variants were prepared as described in sections 2.5.6 and

2.5.7 and their glycine betaine uptake rates were determined via radiochemical transport measurements (Figure 15). For this purpose, proteoliposomes were gently thawed at room temperature and extruded 15 times through a polycarbonate filter (400nm pore size, Whatman, Newton, USA). The homogenized proteoliposomes were collected by ultracentrifugation (20min,  $337.000\text{g}$ ,  $4^{\circ}\text{C}$ ). The final sample was suspended in the extrusion buffer ( $100\text{mM KP}_i$ ,  $\text{pH}=7.5$ ) to a lipid concentration of  $60\text{mg lipid/ml}$  suspension. During the transport measurements, an appropriate amount of proteoliposomes with  $2\text{--}2.5\mu\text{g}$  BetP was diluted 200-fold in  $50\text{mM NaP}_i$  ( $\text{pH}=7.5$ ;  $\sim 100\text{mosmol/kg}$ ) containing  $15\mu\text{M } [^{14}\text{C}]$  glycine betaine and  $0.5\mu\text{M}$  valinomycin to create an outwardly directed  $\text{K}^+$

diffusion potential. To establish hyperosmotic conditions, proline (up to 800-900mM) was added to the external buffer (100mM  $KP_i$ , pH=7.5). The uptake measurements were started with the addition of the liposomes and samples were taken and filtered rapidly through 0.45 $\mu$ m GS nitrocellulose filters (Millipore, Eschborn, Germany) on a multiple filtration unit (Hoefer, GE Healthcare, Munich, Germany) after 5 and 10s. The filters were immediately washed with 100mM LiCl, and the radioactivity ( $\beta^-$  decay) was determined by liquid scintillation counting (Beckman, Munich, Germany).

### **2.5.10. Determination of proteoliposomal leakage**

An indispensable prerequisite for high quality EPR studies on BetP-containing proteoliposomes in terms of salt-induced activation was a preceding verification of the liposomal integrity, because only structural changes related to the external hyperosmotic upshift-induced activation of BetP were of interest. In addition, also a proper rightside-out orientation of the BetP protein after the reconstitution procedure was important for the correct interpretation of the EPR results (3.4.4). Although, all freshly prepared EPR samples were initially checked to those effects, diverse extrusion, centrifugation and concentration processes during the adjustment of the different hyperosmotic conditions could impair the properties of the liposomes. To separate putatively disrupted lipid vesicles prior to the measurements or to quench superimposing signals of unsuitable proteoliposomes during the measurements, the two the following assays were applied.

#### **2.5.10.1. Fluorescence assays**

The integrity of BetP-SL proteoliposomes after Bio-Bead/dialysis-reconstitution (2.5.7) was determined as described by Racher *et al.* (2001). This method bases on a special property of the polar fluorophore calcein (fluorexon) that is entrapped inside the proteoliposomes as a marker for the enclosed aqueous compartment of these lipid vesicles. Its main characteristic is the ability to self-quench: due to putative intermolecular interactions the fluorescence of calcein is reduced if a certain concentration is reached (30mM, Jayaraman *et al.*, 2001). Accordingly, calcein which is entrapped in intact liposomes at self-quenching concentrations gives no fluorescent signal, while calcein that leaks out of permeable liposomes gets diluted and displays an enhanced fluorescence.

For this purpose, proteoliposomes were slowly thawed at RT and collected by ultracentrifugation. 30mM calcein (Sigma-Aldrich, Munich, Germany) was diluted in 100mM  $KP_i$ , pH=7.5. The pH value of the calcein solution was adjusted to 7.2 by stepwise addition of 1M KOH. The proteoliposomes were dissolved in the calcein solution and extruded 15 times through polycarbonate filters (pore diameter 400 nm) to entrap 30mM calcein in the liposomal lumen. External calcein was removed by three gel filtration steps

using G75 sepharose (GE Healthcare, Munich, Germany) columns. Free calcein migrated slowly as a yellow fluorescent band through the column resin while the proteoliposomes with self-quenching internal concentrations of calcein (30mM) could be eluted first as an orange-colored band in 1-2ml 100mM  $KP_i$  buffer, pH=7.5. Fluorescence measurements were carried out with an Aminco Bowman Series 2 Spectrometer (SLM Aminco, Büttelborn) at an excitation wavelength of 495nm and an emission wavelength of 520 nm (slit width of 8nm). All samples were kept at RT.

### 2.5.10.2. Accessibility assays

Another method to simply test the integrity of proteoliposomes with incorporated BetP-SL was performed by the addition of a water soluble, polar spin relaxant to the external buffer that quenches the EPR signal upon collision with the nitroxide side chain of the MTS spin label attached to the protein (Altenbach *et al.*, 1994). If the analyzed proteoliposomes were intact, the addition of an appropriate amount of membrane impermeable quenchers like 50mM ChRomium-(III)-OXalate ( $CrOx$ ,  $Cr(C_2O_4)^{3-}$ ) to the external buffer (100mM  $KP_i$ , pH=7.5) of the liposomes would only lead to a signal decrease proportional to the amount of inside-out orientated BetP-SL proteins. However, if the whole EPR signal was quenched, the respective proteoliposomes were leaky (3.4.4, Results).

## 2.6. EPR measurements

The EPR measurements were carried out with three different spectrometers at the University of Osnabrück: A Magnostech Miniscope MS200 desktop machine (Magnostech Ltd., Berlin, Germany) and a Varian machine (Varian Inc., Palo Alto, CA, USA) for continuous wave (cw) experiments as well as a Bruker ELEXSYS spectrometer for pulsed EPR measurements (Bruker Biospin GmbH, Rheinstetten, Germany).

Room temperature continuous wave (cw) EPR spectra were recorded at a microwave frequency of 9.7GHz (X-Band) or 34GHz (Q-Band). For each experiment 15-20 $\mu$ l (cw EPR) or 30-50 $\mu$ l (pulsed EPR) of a solution with at least 50 $\mu$ M spin labelled BetP protein reconstituted in *E. coli* lipids were loaded into glass capillaries and manually inserted into the spectrometer. For pulsed EPR measurements the capillaries had to be frozen in liquid nitrogen prior to the application. Spectra were taken at the microwave power set between 1 and 5 milliwatt (mW) depending on signal intensity. The B-field modulation amplitude was set between 1.0 and 1.5G depending on the width of the lines of EPR spectra. If not indicated somewhere else, the following typical parameters were used:

#### Continuous wave EPR (at RT):

Time constant: 100 [ms]



Time sweep: 120-180 [ms]

Temperature: RT (23-25°C)

Pulsed EPR (DEER):

Temperature: ~50 K (~ -223°C, ~ -370°F)

### 3. Results

To cope with hyperosmotic stress induced dehydration of the cytoplasm, the secondary transport system BetP from *Corynebacterium glutamicum* is activated in less than one second. Thereby, it specifically imports its sole substrate glycine betaine as a compatible solute to restore the cells water balance and thus the essential cell turgor. Being independent of any accessory macromolecule, e.g. as signal detector, amplifier or transducer, BetP unifies altogether three properties of (i) a transporter, (ii) an osmosensor and (ii) an osmoregulator, i.e. it autonomously senses its stimulus (internal  $K^+$  concentration) and adapts its transport activity to the actual extent of osmotic stress (Rübenhagen *et al.*, 2000). Former studies showed that the C-terminal domain of the carrier plays a key role in sensing the stimulus and in the subsequent adaption process that regulates the activity of the protein (Peter *et al.*, 1998a; Schiller *et al.*, 2004b). To this regard, the construction of appropriate substitution mutants in the C-terminal domain of BetP revealed that both, the overall conformation and sterical orientation of the C-extension as well as the primary structure of the central part of this domain have an influence on the activation profile of BetP (Schiller *et al.*, 2006; Ott, 2005; Dissertation Ott, 2008). It was suggested, that structural changes within the C-domain as well as intramolecular interactions with other protein domains or the surrounding lipid phase are of particular importance for the activity regulation of the carrier. Furthermore, recent studies on a 2D crystal with BetP reconstituted in *E. coli* lipids as well as a 3D crystal with BetP in detergent suggested both, (i) a trimeric oligomerisation of the carrier in the native membrane and thus (ii) certain intermolecular protein-protein interactions upon BetP activation (Ziegler *et al.*, 2004; Ressler *et al.*, submitted; personal communication, C. Ziegler). Therefore, detailed information about the molecular dynamics within the C-domain and the respective influence on osmosensing and osmoregulation of the BetP carrier is of great interest for understanding the molecular mechanisms underlying these processes.

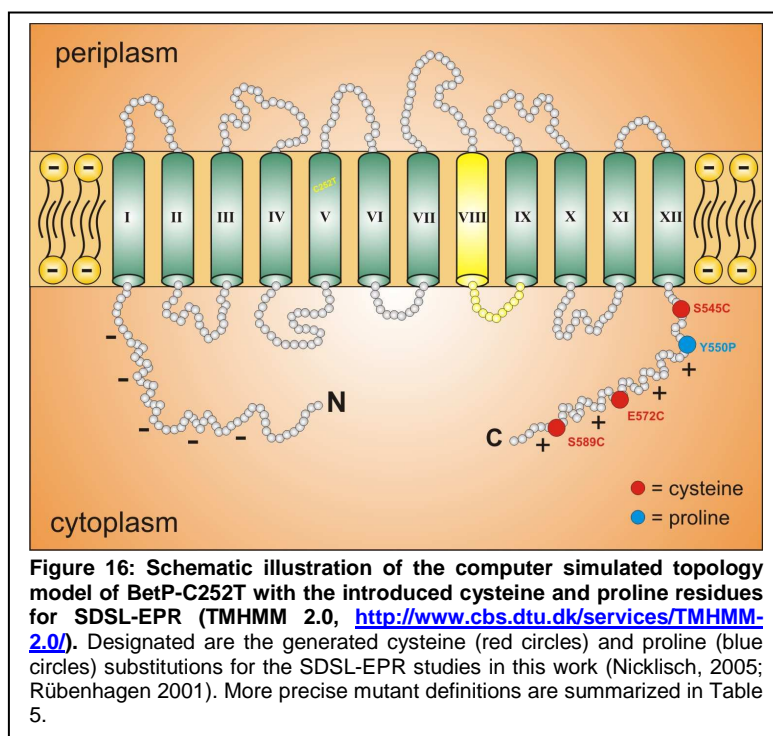
In order to probe whether and to which extent the C-terminal domain undergoes a conformational and/or sterical change upon salt stress, the spectroscopic technique of Site-Directed Spin Labelling-EPR (SDSL-EPR) was applied. Beside 2D-NMR (Nuclear Magnetic Resonance) and X-Ray crystallography, the SDSL-EPR is a complementary biophysical approach to study not only soluble, but also the challenging membrane protein systems (Hubbell *et al.*, 1998). In this approach native amino acids at desired sites in a given protein are replaced by cysteine residues which are then modified by nitroxide spin labels (Hubbell *et al.*, 2000). SDSL-EPR has been successfully applied to define elements of the secondary and tertiary structure of membrane proteins in solution and in

membranes (Hubbell *et al.*, 1998). Also, this method was used to characterize the global structure and the aggregation states of proteins by measuring of intra- and intermolecular distances (Perozo *et al.*, 1998; Mchaourab and Perozo, 2000). Moreover, SDSL-EPR was successfully used to determine the orientation and movements of individual segments of membrane proteins under physiological conditions and to characterize conformational changes that occur during protein function (Hubbell *et al.*, 2000; Rink *et al.*, 2000).

The present work is aimed to probe structure and structural changes of the C-terminal domain under hyperosmotic stress simulating conditions using SDSL-EPR. For this purpose, several site-directed mutants within the C-terminal domain of the BetP protein were constructed carrying the single site cysteine residues (see below). The following research was divided into four steps. (1) To confirm, whether the introduction of the spin label was not detrimental for the protein function, the sustained transport activity of each spin labelled BetP variant was studied. (2) The reconstitution of these mutants into *E. coli* lipids was optimized to obtain high yields of spin labelled and proper incorporated BetP protein for the EPR analysis at issue. (3) Continuous wave EPR studies were carried out to elucidate the (local) structure of the C-terminal domain and to determine structural changes during the reconstitution into liposomes as well as under hyperosmotic-induced BetP activation. (4) Pulsed EPR analysis was performed to determine intra- and intermolecular distances in single and double spin labelled, non-activated BetP mutants.

All EPR measurements and analysis were done under supervision of Dr. I. V. Borovykh in the laboratory of Prof. H.-J. Steinhoff (University of Osnabrück, Department of Physics).

### 3.1. Substitution mutants and strategic labelling



The polytopic topology model of BetP in Figure 16 displays the relative positions of each amino acid substitution for the construction of the single, double and triple mutants used in this work. Table 5 additionally summarises the respective suitability for the analysis of the structure and dynamics of the C-terminal domain by EPR spectroscopy (Nicklisch, 2005; Rübenhagen, 2001).

The present work will be concerned with three single cysteine mutants (BetP-S545C, -E572C and -S589C) to probe the local structure and local structural changes of the C-domain upon the hyperosmotic stress-induced activation of BetP as well as to determine distances within the non-activated carrier. To further analyse the overall conformation and orientation of the C-terminal extension, distances between two spin labels were measured in a double (BetP-S545C/S589C) and a triple (BetP-S545C/Y550P/S589C) mutants. Such a selection was based on the suggested positions of these amino acids in the C-domain: either at the beginning (BetP-S545C), in the centre and as well in the middle of a putative  $\alpha$ -helix (BetP-E572C) or at the end (BetP-S589C) of the C-terminal domain (Figure 16). The selection of the position 589 was justified by its location near the end of a 25 amino acids motif at the end of the C-terminal domain of BetP which was identified as a putative region involved in  $K^+$  sensing (Schiller *et al.*, 2004b). We expected rather pronounced structural/conformational changes in this region of the C-terminal domain when the BetP protein is activated. Position 572 was selected based on the recently suggested functional model of BetP activation in which the rise of the luminal  $K^+$  concentration induces conformational changes of the C-terminal domain in the region around residue 572 (Schiller *et al.*, 2006). In order to probe the importance of the membrane surrounding on the structure and function of the BetP protein we selected position 545 which is - based on the predicted protein topology and structure – supposed to be positioned near the membrane surface at the beginning of the C-domain (Figure 16). The introduction of a proline residue at position 550 was known to render the carrier

## Results

permanently active but insensitive to hyperosmotic stress (Schiller *et al.*, 2006). Thus, the relative distance between two strategically attached spin labels in a triple mutant (BetP-S545C/Y550P/S589C) compared to the respective distance in a mutant without the proline introduction (BetP-S545C/S589C) were studied for differences in the orientation and/or structure of the C-domain in a deregulated BetP carrier (for more details see section 3.5.6). In addition, former cryo-electron microscopy (cryo-EM) study of reconstituted as well as differential ultracentrifugation study of detergent solubilised BetP protein revealed that the carrier forms a trimer under the respective conditions (Ziegler *et al.*, 2004). Recent X-ray crystallography studies of crystallized BetP confirmed these results (Ressl *et al.*, submitted). However, at the moment there is no X-ray structure available for the BetP protein. Taking this into account, distance measurements for single and double spin labelled BetP should shed light on the structure and the arrangement of a functional BetP trimer in the membrane.

As a prerequisite for successful SDSL-EPR measurements, protein concentrations between 30-200µM are required. Even more important is a high labelling efficiency of the target cysteine residues in the protein under study. For this purpose the growth conditions, purification, and spin labelling steps for selected BetP single cysteine and cysteine/proline variants were successfully optimized (Nicklisch, 2005).

**Table 5: Constructed BetP mutants with the respective amino acid substitutions (Nicklisch, 2005; Rübenhagen, 2001).** The listed labelling efficiencies are specified in percentage (100% = all cysteine residues in a protein sample are labelled). The protein yield reflects the sum of expression, membrane incorporation and purification efficiency of a given Strep-BetP variant via StrepTactin MacroPrep FPLC purification and is specified in mg purified Strep-BetP protein per litre *E. coli* DH5α cell culture. Highlighted in yellow are the selected BetP mutants investigated via continuous wave and pulsed EPR spectroscopy in this work.

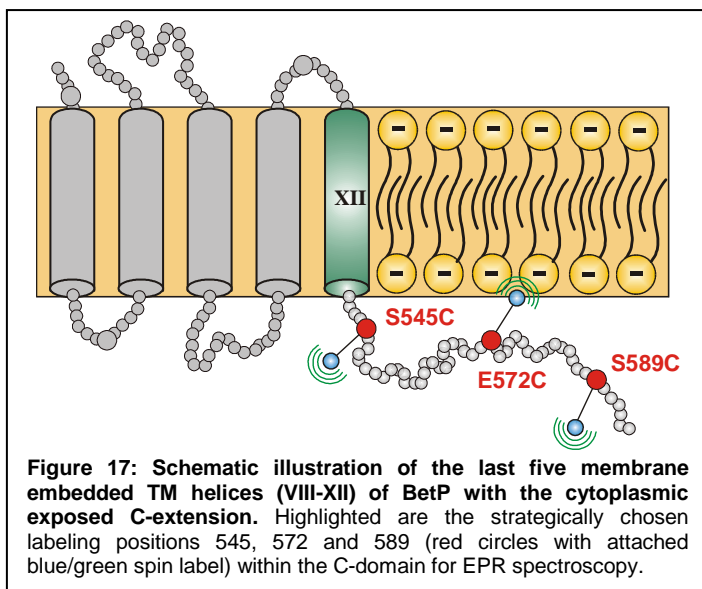
BetP variant	Amino acid substitution	SL efficiency	Protein yield
<b>Structure determination &amp; Monomer interactions</b>			
S61C *	Serine 61 -> cysteine 61	<10%	1.4-1.6mg/L culture
S545C	serine 545 -> cysteine 545	80-90%	1-1.5mg/L culture
E572C	glutamate 572 -> cysteine 572	50-80%	0.4-0.8mg/L culture
S589C	serine 589 -> cysteine 589	30-50%	1.2-1.3mg/L culture
<b>Intra &amp; Intermolecular Distances (functional protein)</b>			
S545C/S589C	double mutant (see above)	80-90% / 30-50%	1-1.2mg/L culture
<b>Intra &amp; Intermolecular Distances (deregulated protein)</b>			
S545C/Y550P/S589C	triple mutant (see above)	80-90% / 30-50%	0.3-0.5mg/L culture

Note:

- \* = probably this is a buried position; labelling procedure needs additional adjustment (work in progress).
- The mutant nomenclature from former studies was adopted (Nicklisch, 2005): the first letter represents the native amino acid followed by the respective position in the protein (counted from N->C) and finally the one-letter-code for the introduced amino acid. Double and triple mutations are separated via a slash.

The listed labelling efficiencies and protein yields in Table 5 are an average determination of all conducted cultivation and purification experiments for each mutant.

### 3.2. Activity regulation of BetP variants in *E. coli* lipids



As was mentioned above, strategic amino acid positions within the C-terminal domain were chosen for SDSL-EPR (Figure 17). To ensure that all used mutants (except BetP-E572C) were active, the functional activity of the spin labelled BetP proteins reconstituted in *E. coli* phospholipids (LPR=1:20) prior and/or after the EPR measurements was measured by

radiochemical transport measurements with [ $^{14}\text{C}$ ]-glycine betaine. The Activity measurements for these mutants were carried out with and without the attached spin label.

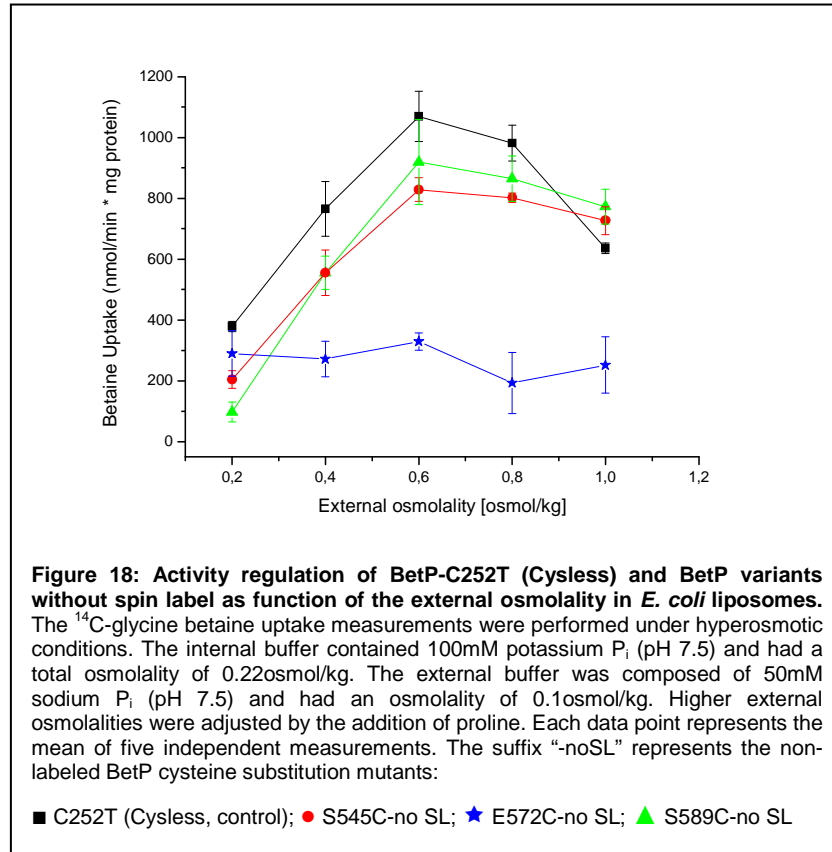
To determine BetP activity in proteoliposomes, the respective protein mutants were cultivated in *E. coli* DH5 $\alpha$  cells, purified using affinity chromatography, spin labelled on column and then reconstituted into *E. coli* lipids (see Materials and methods). Subsequently, the uptake of radioactively labelled [ $^{14}\text{C}$ ]-glycine betaine per time unit and amount of incorporated protein depending on the extent of external osmolality was determined. As a control, the activity for the cysteine-free mutant BetP-C252T were measured (C252T = Cysless = BetP mutant in which the only native cysteine at position 252 was changed to threonine; Rübenhagen *et al.*, 2001). The result of these control measurements is shown in the following figures for comparison. It was known, that this mutant is identical to the wildtype protein in terms of the  $K_M$  for sodium and betaine and its regulatory property in both, heterologously expressed in *E. coli* MKH13 cells as well as reconstituted in *E. coli* lipids (unpublished results).

#### 3.2.1. Non-labelled and spin labelled BetP variants S545C, E572C and S589C

Figure 18 shows the activation profiles of the unlabeled single cysteine variants BetP-S545C (red circles), BetP-E572C (blue stars) and BetP-S589C (green triangles) as well as the wildtype-like control profile of the BetP-Cysless (black squares) protein in proteoliposomes upon hyperosmotic shock. In agreement with the previous results of uptake measurements in *E. coli* MKH13 cells (Nicklisch, 2005), the single cysteine substitution in BetP-S545C and BetP-S589C had no influence on the regulation profile of

## Results

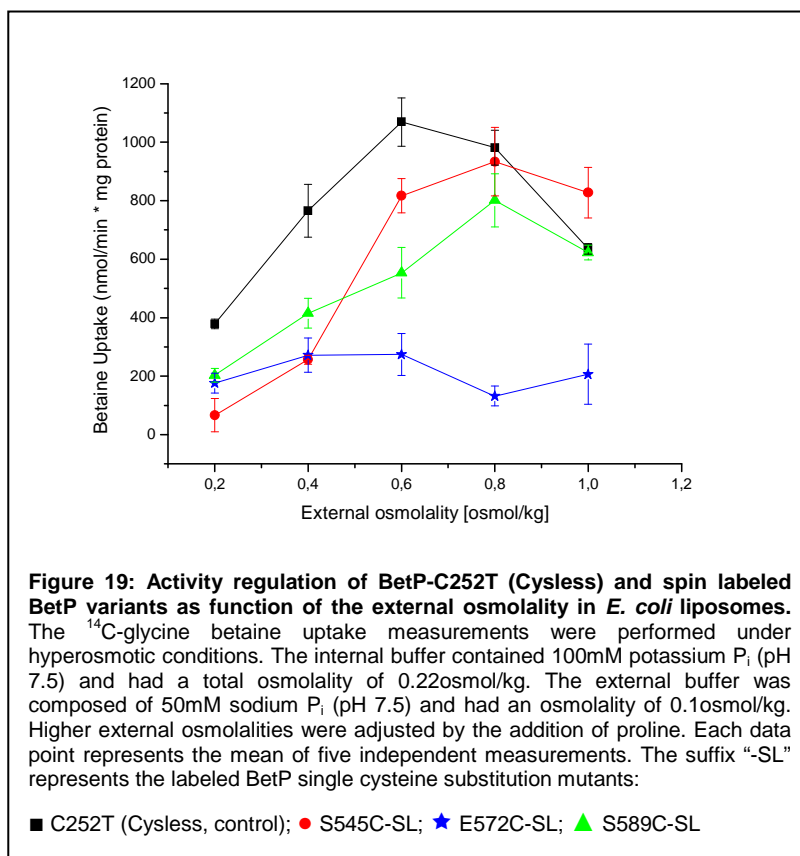
the reconstituted carriers. Hence, the maximal uptake rate was increasing when a higher hyperosmotic stress was applied. This regulation profile was similar to that of the control mutant (BetP-C252T). In other words, the respective activity curves showed the typical sigmoid progression with the optimum at an external osmolality of about 600mOsm/kg.



However, the maximal uptake rates of both, BetP-S545C (920nmol/min\*mg protein) and BetP-S589C (830nmol/min\*mg protein) were slightly lower than of the Cysless protein (1070nmol/min\*mg protein). Since these small differences in the total uptake rates at a given osmolality occur even with the same mutant, they most likely represent little variations in the sample preparations (e.g. different efficiencies of rightside-out reconstitution). In contrast but also in agreement with previous results, the uptake measurements for the BetP-E572C mutant showed a completely deregulated activity regulation, e.g. the transporter was unable to adjust its glycine betaine uptake rates to the external extent of osmotic stress (Figure 18, blue curve). Hence, the uptake rates of non-labelled BetP-E572C in *E. coli* lipids varied between 190-330(nmol/min\*mg protein) independent of the external osmolality. However, this distinct basic activity of the carrier mutant reconfirms, that the deregulated BetP variants are still functional transporters, but they lost the ability to sense their stimulus (potassium) and thus to suitably adjust their maximal uptake rates (Schiller *et al.*, 2006).

## Results

The next step was to check whether the activity of the respective mutants is affected by the attachment of a spin label. For this purpose, an aliquot of the same cell culture membrane fraction from each of the tested BetP-variants (Figure 18) was used, to covalently attach the reporter molecule (spin label) to the introduced cysteine residues during affinity chromatography (2.5.2 and 2.5.3). Subsequently these spin labelled BetP variants were reconstituted into *E. coli* liposomes transport measurements were carried out as described above. Figure 19 shows the respective uptake measurements of the spin labelled BetP variants S545C-SL (red circles), E572C-SL (blue stars) and S589C-SL (green triangles) reconstituted in *E. coli* liposomes under hyperosmotic conditions. The result of the control measurements for BetP-Cysless (black squares) is shown for comparison.



Again, similar to the unlabeled cysteine mutants, the regulation profile of the BetP-E572C-SL variant showed the same permanent activity of about 130-270(nmol/min\*mg protein) over the whole range of the applied hyperosmotic upshift. Thus, the presence of the spin label had no influence on the basic activity of this deregulated carrier. However, the regulation profiles of spin labelled BetP-S545C and BetP-S589C showed some differences compared to the uptake rates of the respective unlabeled proteins. Although both spin labelled BetP mutants were still osmoregulated, a shift of the activity optimum of



BetP-S545C-SL (930nmol/min\*mg protein) and BetP-S589C-SL (800nmol/min\*mg protein) from 600mOsmol/kg to 800mOsmol/kg was observed.

Since the uptake measurements revealed that the kinetic properties of all three BetP single cysteine variants could be sustained after the introduction of the paramagnetic spin probe, the next step was to provide a final concentration of highly purified spin labelled BetP protein after the incorporation into *E. coli* lipids that is suitable for high quality SDSL-EPR studies.

### 3.3. Optimization of the reconstitution process

As mentioned above, optimal protein concentration for SDSL-EPR is in the range of 30-200µM with near 100% labelling efficiency (e.g. nearly all proteins in a sample with its engineered cysteine residues are tagged with a paramagnetic spin label). For this purpose, the respective BetP variants were each heterologously expressed in *E. coli* DH5α cells, purified via affinity chromatography and subsequently reconstituted in *E. coli* lipids to obtain high yields of rightside-out orientated BetP protein in a native like environment (see Materials and methods).

To this regard, typical cultivation experiments finally led to yields of up to 1-1.5mg purified and spin labelled BetP protein per litre *E. coli* cell culture (Table 5). However, when reconstituted into *E. coli* lipids using the conventional reconstitution protocol according to Rigaud *et al.* (1995), we unexpectedly observed protein loss up to 90%. This was confirmed by protein concentration determination assays and SDSL-EPR spectroscopy, e.g. the signal/noise ratio was considerably lower as expected and estimated from the initially supplied protein amount (see below). Since the former kinetic characterizations of BetP mutants by transport measurements did not rely on high protein amounts in the proteoliposomes, this detrimental phenomenon did not attract the attention up to the present EPR studies.

It was assumed that the SM2-Bio-Beads did not only absorb the excess of detergent but also trap a large amount of the hydrophilic and strongly adhesive BetP transporter (personal communication, S. Morbach and V. Ott). To avoid such unfavourable high protein loss, an alternative reconstitution assay on the basis of the work of Philippot *et al.* (1983) was developed and applied to BetP. Beside the respective verification using the protein concentration determination assay (Amido Black, Schaffner and Weissmann, 1973), a comparison of both reconstitution methods (Rigaud *et al.*, 1995 and Philippot *et al.*, 1983) was studied using cw-EPR spectroscopy in terms of signal and thus protein loss.

### 3.3.1. Signal loss during SM2-Bio-Bead reconstitution

The high spin label mobility and thus the sharp lines in the EPR spectrum of the reconstituted BetP-S589C-SL mutant allowed the detection and qualitative analysis of subtle changes in the relative signal amplitude as an indicator for protein loss during the respective reconstitution method. For this purpose, a defined amount of the BetP-S589C-SL sample (about 300 $\mu$ l) was collected at several time points (the same for both samples) during both reconstitution procedures and subsequently the corresponding EPR signal was measured. For both methods the same protein (BetP-S589C-SL) and *E. coli* lipid batches with equal amounts for each reconstitution assay were used.

Neither changes of Bio-Beads during the incubation nor dilutions of the samples were carried out in both procedures. This means that changes of the signal intensities could only be induced by the absorption of BetP by Bio-Beads. Since changes of the EPR signal intensity are proportional to the changes in the sample concentration, the overall signal intensity of a defined amount of sample after each reconstitution process could be used to determine the relative reconstitution efficiency of a particular assay.

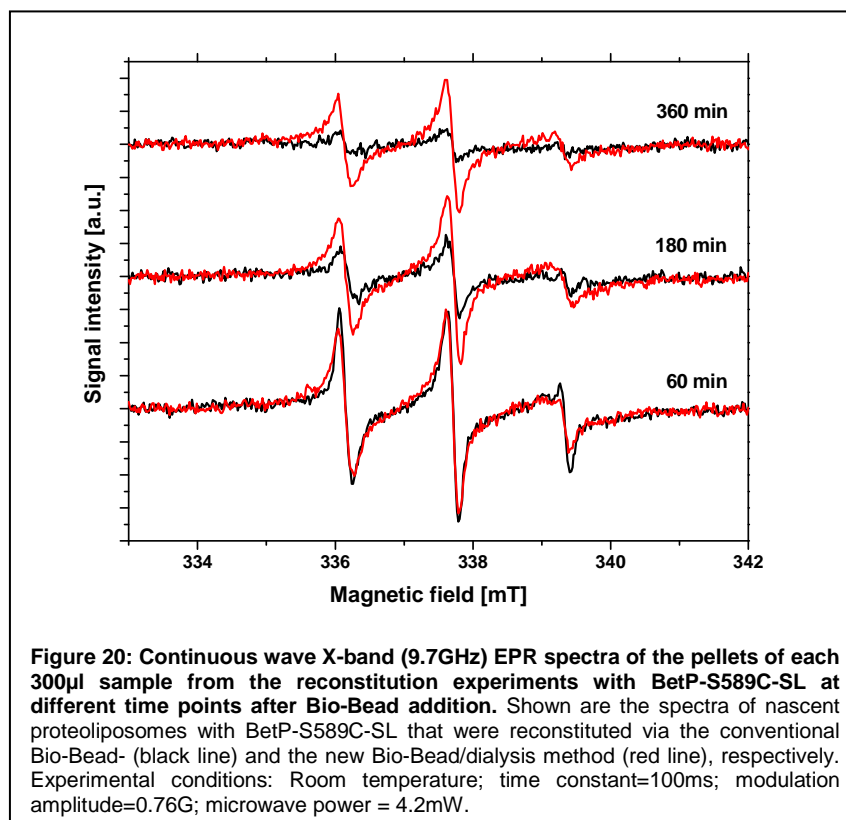


Figure 20 depicts the EPR spectra of the reconstituted BetP-S589C-SL samples with the conventional (black curve) and the new (red curve) reconstitution method after 60min, 180min and 360min of the initial Bio-Bead addition. Although the relative signal intensities

## Results

after 60min of Bio-Bead treatment did slightly differ in amplitudes (Figure 20, cp. black and red lines at 60min), the longer incubation with the hydrophobic adsorbent led to significant signal loss when the conventional reconstitution assay was used. On the contrary, reconstitution with the new Bio-Bead/dialysis method resulted only in about 20-30% of signal loss during the first 6 hours of incubation (Figure 20, black and red curves at and 360min).

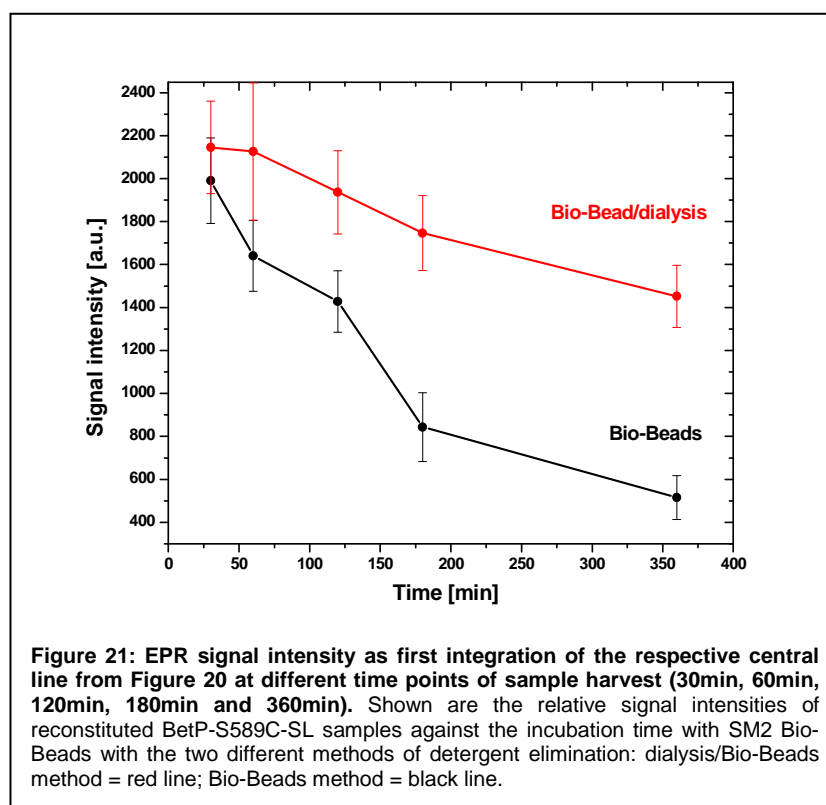
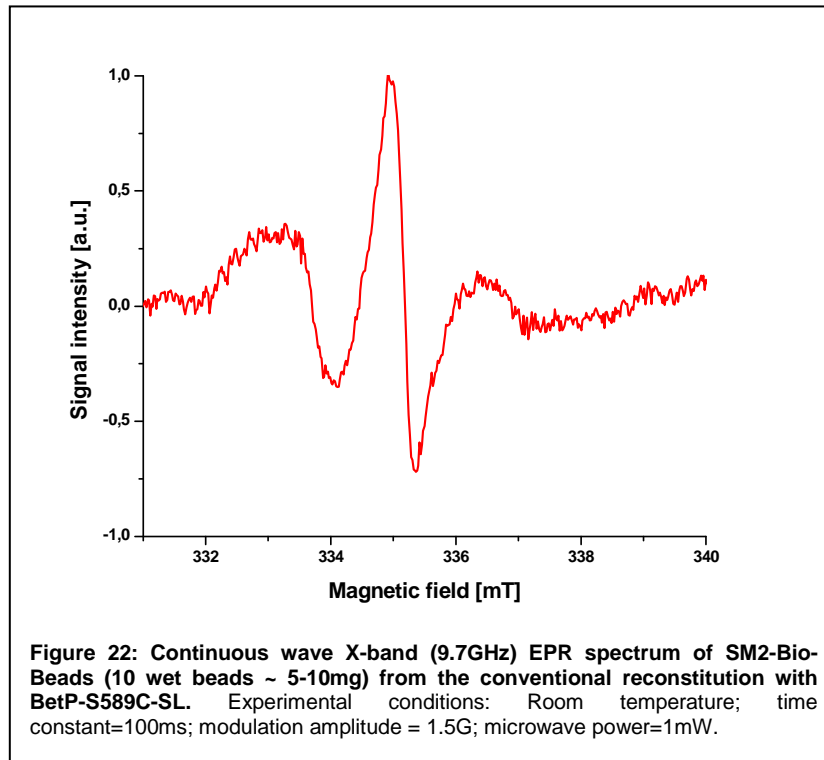


Figure 21 shows the signal intensity (value of the first integral of the central EPR line) for both preparation methods plotted as a function of time (zero time is the moment of adding Bio-Beads). The results indicate that protein loss occurs in both reconstitution methods. However, already after 6 hours of incubation less than 30% of the initially applied protein amount could be recovered with the conventional Bio-Bead reconstitution assay, whereas about 70% of all deployed BetP-S589C-SL protein could be detected at the same time in the sample from the new Bio-Bead/dialysis reconstitution procedure (Figure 21, cp. black and red curve).

To check if the residual BetP protein in both experiments adsorbed to the Bio-Beads, several pieces of Bio-Beads (a few mg) from the conventional reconstitution assay were collected and the EPR spectra of these Bio-Beads were measured. Under the current experimental conditions, native Bio-Beads showed no EPR spectra (data not shown). On

contrary, Bio-Beads used for detergent removal in the conventional method showed very pronounced EPR spectra which is attributed to the spin labelled BetP protein adsorbed during the reconstitution procedure (Figure 22).



Taken into account that in the performed reconstitution experiment a total amount of about 150-200mg Bio-Beads was used, the high signal/noise ratio from only a few mg of Bio-Beads (Figure 22) confirms the adsorption of large amounts of BetP to the polystyrene beads during the conventional reconstitution process. Interestingly, the spectral line shape of the adsorbed BetP-S589C-SL protein changed from the sharp 3-line-spectrum (=high spin label mobility) to a broad spectrum that reflects a highly restricted mobility of the spin label (cp. Figure 22 and Figure 23). This indicates that at least this part of the C-extension is involved in the adsorption process. Analogous experiments carried out with the BetP-E572C-SL mutant showed similar EPR spectra when the respective BetP protein adsorbed on Bio-Beads. Altogether these results showed that probably the whole C-extension is the “sticky” protein domain and a contact point for the absorption (Figure 57).

### 3.4. Mobility profiles of C-terminal BetP variants

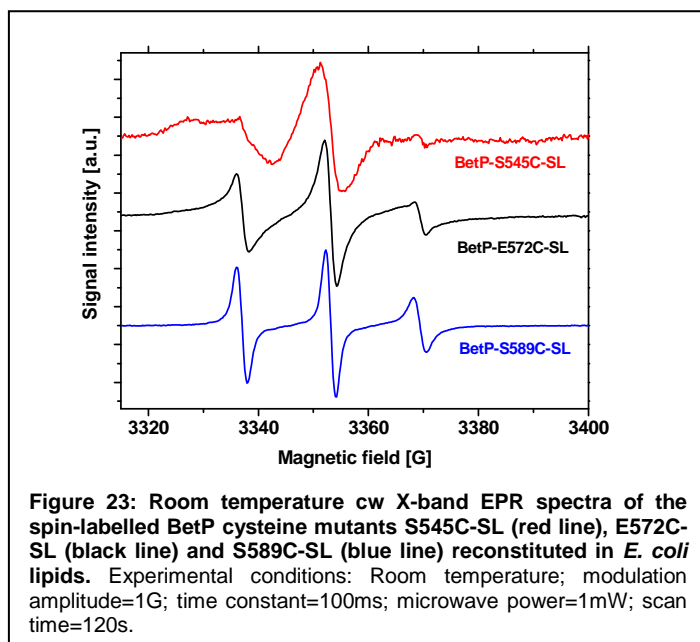


Figure 23 shows the cw-EPR spectra of three spin labelled cysteine mutants of BetP reconstituted in *E. coli* lipids (for more details see Nicklisch, 2005). A graduated increase in the mobility was observed when the spin label position was moved from the beginning (S545C-SL) to the centre (E572C-SL) and to the end (S589C-SL) of the C-terminal domain. This screening was in agreement with the relative amino

acid positions referring to the known topology model (Figure 16). However, these preliminary results with samples created by a suboptimal reconstitution procedure (2.5.6, Materials and methods) significantly limited advanced EPR studies.

By means of the new established Bio-Bead/dialysis procedure it was possible to reproduce previous findings with respect to the spin label mobility profiles of the strategically introduced cysteines within the C-domain of the reconstituted BetP variants (Figure 23). Additionally, it provided the opportunity to increase the signal/noise ratio of each sample such as subtle mobility changes of samples in detergent and in *E. coli* lipids could be monitored and compared to each other. To this regard the next chapter deals with the comparison of the spin label mobility for both, (i) solubilised BetP variants and (ii) for the corresponding mutants reconstituted in liposomes. This comparison aimed to identify whether the incorporation of BetP into *E. coli* lipids has an effect on the respective spin label mobility profile for a given BetP variant and thus to reveal probable lipid-protein interactions within the C-terminal domain.

#### 3.4.1. Quantification of the spin label mobility

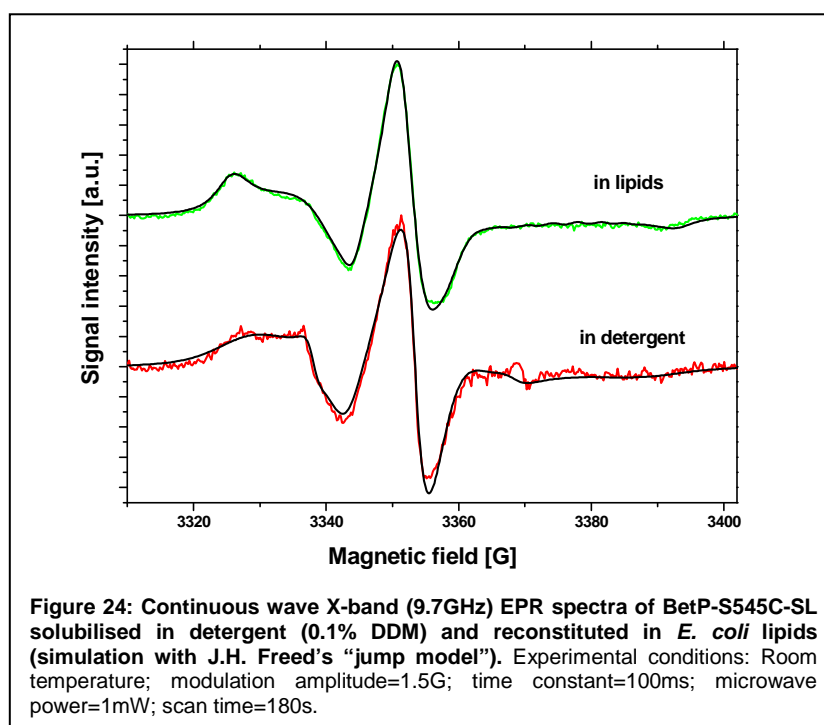
The quantitative analysis of the EPR spectra was carried out using a program developed by J. H. Freed (“jump model”; Freed, 1976). In most cases two components with two different rotational correlation times ( $\tau_1$  and  $\tau_2$ ) can be identified (for details see Appendix). Each component describes the dynamic properties of a covalently linked spin label and provides hints to a possible spin label rotation (and/or jumps) at the respective amino acid position. In general it can be stated that the shorter the rotational correlation time, the higher the mobility of an attached spin label and *vice versa*. If there is only one dedicated

sphere (for example, the same environment and no restriction for motion from nearby protein domains), the respective EPR spectrum can be simulated by only one single component. However, in most cases a mixture of rotational degrees of freedom is possible for a spin label, and a second  $\tau_2$  component (with a different correlation time) has to be introduced to simulate a spectrum properly. This can be for example due to restrictions from the surrounding of the protein or due to structural changes during function of the protein. The simulation and comparison of both parameters before and after protein activation (e.g. via salt shock in the case of BetP) can thus provide information about conformational changes at the respective spin label position, e.g. a changing the solvent exposure or a changing the structure of protein domain in the vicinity of the spin label.

The following results concerning the spin label mobility profiles of the single cysteine variants BetP-S545C-SL, BetPE572C-SL and BetPS589C-SL will be divided in two parts: (1) A qualitative and quantitative analysis as well as comparison of the respective spin label mobility of each BetP variant in different environments (solubilised in detergent or reconstituted in *E. coli* lipids) and (2) a qualitative study of the putatively different spectral lineshapes (and thus spin label mobility) of each reconstituted BetP mutant before and after the carrier activation by an hyperosmotic upshift in the external buffer.

### 3.4.2. Comparison of the spin label mobility in detergent and in *E. coli* lipids

#### 3.4.2.1. BetP-S545C-SL



A pronounced difference in the shape of the EPR spectra was observed for the spin label at position 545 in the C-terminal domain of BetP for the sample in detergent and in proteoliposomes (Figure 24). Both spectra showed a strong restriction of the spin label mobility and exhibited two spectral components which describe a higher ( $\tau_1$ ) and lower ( $\tau_2$ ) mobility. The correlation times determined from the simulation using the jump dynamical model were  $\tau_1=3.8\text{ns}$ ,  $\tau_2=16\text{ns}$  for BetP-S545C-SL in detergent and  $\tau_1=15\text{ns}$ ,  $\tau_2=52\text{ns}$  for the protein reconstituted in lipids. According to the respective correlation times, this revealed a nearly 4fold decrease in the spin label mobility upon the reconstitution into liposomes. In addition to the correlation time, also the relative amplitudes of the fast and slow components changed: The amplitude of the fast component nearly vanishes when the protein is inserted into the lipids (Figure 25). This result is in agreement with the suggested structure of the BetP protein in its lipid environment: the spin label at position 545 is placed near the beginning of the C-terminal extension and should “sense” a putative interaction of this domain with the membrane. As a result we may conclude that structure and/or conformation of the C-extension is different in detergent and in lipid environment and that the structure of this part of protein domain is strongly confined by the lipid environment (“lipid effect”).

#### 3.4.2.2. BetP-E572C-SL

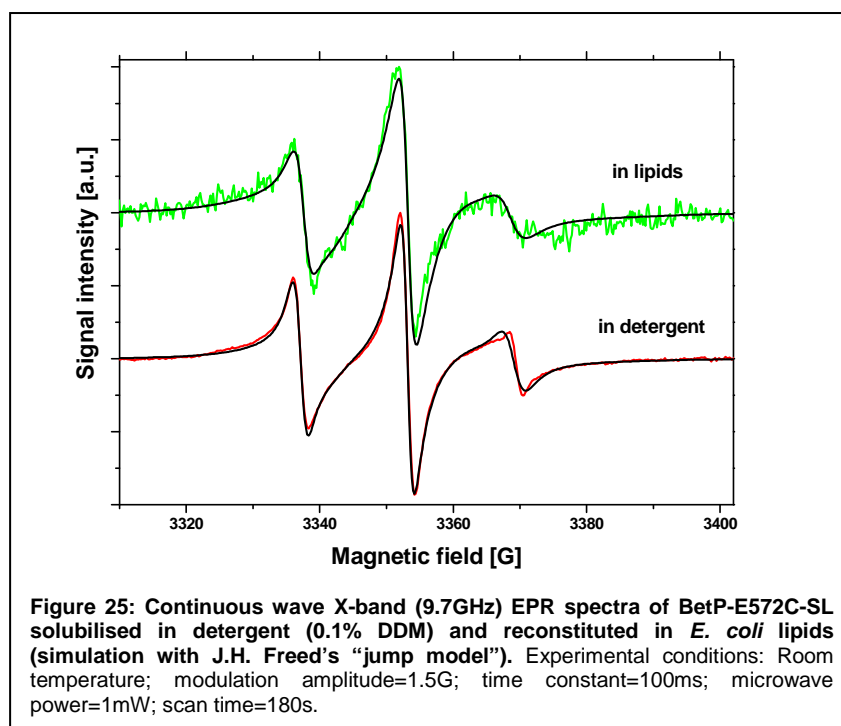
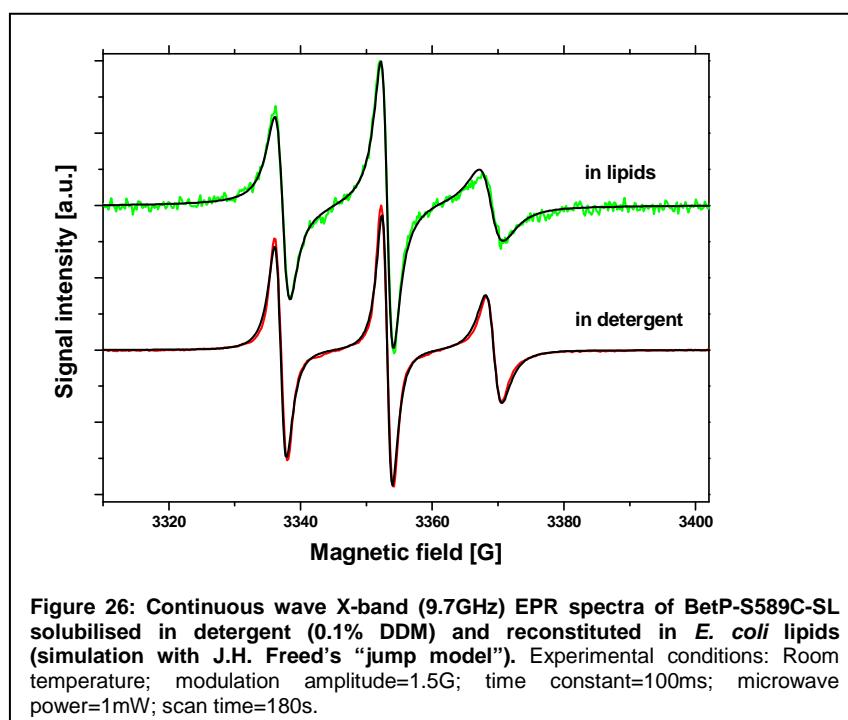


Figure 25 shows the comparison of the EPR spectra of the spin label attached to position 572 of the C-terminal domain measured for samples in lipid and in detergent. The effect of

the membrane environment on the mobility of this C-terminal region was less visible than for position 545 but still present. According to the respective simulation results, both EPR spectra, in detergent and in lipid environment, consisted of two components similar to position 545. The correlation times determined from the respective simulation were  $\tau_1=2.0\text{ns}$ ,  $\tau_2=8.3\text{ns}$  for BetP-E572C-SL in detergent and  $\tau_1=2.9\text{ns}$ ,  $\tau_2=9.5\text{ns}$  for the protein reconstituted in lipids. Again, when BetP is reconstituted into *E. coli* lipids we observed an approximately 1.5fold increase in the time constant for the fast component ( $\tau_1$ ) with almost no effect of the reconstitution into lipids on the slow component ( $\tau_2$ ). The comparison of the time constants for BetP-S545C-SL and BetP-E572C-SL indicated that the spin label mobility at position 572 is much less restricted compared to position 545. The mobility of the spin label at position 572 is about twofold higher than that at position 545 when the respective BetP cysteine mutants were solubilised in detergent and even 5fold higher when the two BetP variants were reconstituted in lipids. This increased mobility of the spin label at position 572 is in agreement with the suggested location in the centre of the flexible C-domain of BetP (Figure 17).

#### 3.4.2.3. BetP-S589C-SL



The effect of reconstitution on the spin label mobility at position 589 is shown in Figure 26. When the BetP protein was solubilised in detergent we obtained a perfect fit with only one component with a correlation time of  $\tau=1.2\text{ns}$ . However, when the BetP protein was reconstituted in lipids, we had to add a small amount (not more than 10%) of a slow



## Results

component with  $\tau_2=10.2\text{ns}$  to obtain a good fit. This small addition of a slow component also changed the correlation time for the fast component to  $\tau_1=2.2\text{ns}$  (Table 6). As depicted in Figure 26, the mobility of the spin label at position 589 is higher compared to the respective spin label mobility of BetP-S545C-SL and BetP-E572C-SL (Figure 24 and Figure 25). According to the calculated fast components ( $\tau_1$ ) of the simulated EPR spectra from BetP-S589C-SL, the corresponding spin label mobility is about 1.5fold higher compared to the BetP-E572C-SL mutant and about 7fold higher compared to the respective spin label mobility of BetP-S545C-SL. This is in agreement with the fact that this position is close to the end of the C-terminal extension. To our surprise we also observed an effect of the reconstitution into *E. coli* lipids on the spin label mobility at this end position. A possible explanation could be that somehow this end of the C-terminal part is not reaching out into the medium but rather stays in the vicinity of the lipid bilayer and/or protein.

We concluded, that the reconstitution of the spin labelled BetP variants into *E. coli* lipids resulted in a decrease of the spin label mobility for all three mutants (Figure 24-Figure 26, cp. red and green lines). This indicated a direct or indirect interaction of BetP with the surrounding lipids and/or structural changes of the protein in the vicinity of the C-terminal domain upon reconstitution. The degree of these changes is strongly depending on the position of the spin label within the C-terminal extension, but the tendency of an increasing mobility along the C-domain moving from the membrane to the distal end is still present.

For better comparison, Table 6 summarizes the calculated correlation times for all three investigated BetP mutants (S545C-SL, E572C-SL and S589C-SL) solubilised in detergent and reconstituted into liposomes.

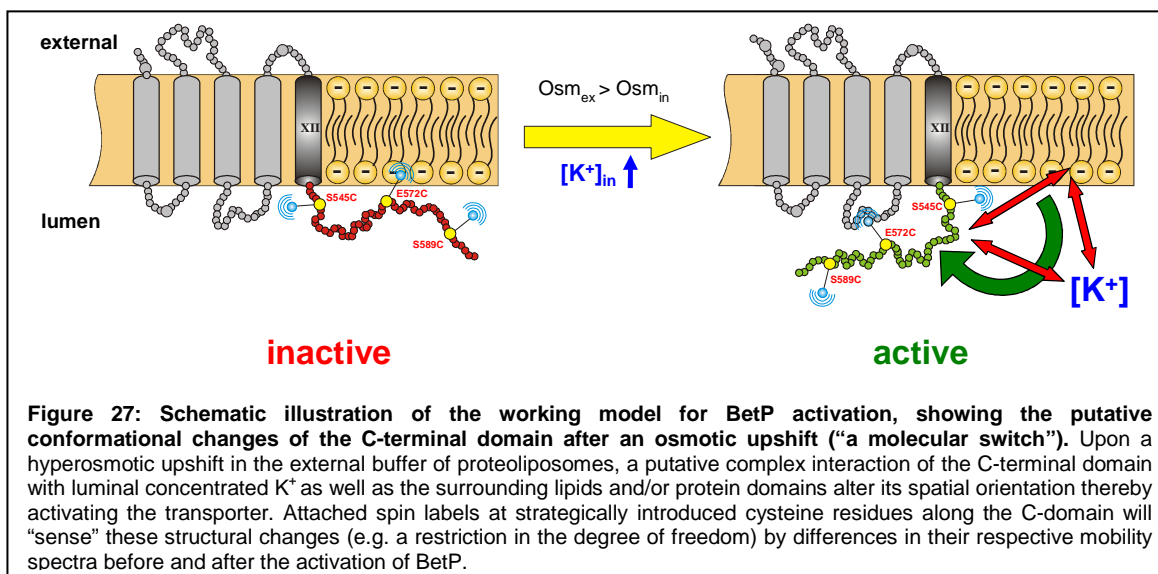
**Table 6: Rotational correlation time components  $\tau_1$  and  $\tau_2$  from spin labelled BetP variants in detergent and reconstituted in *E. coli* lipids (proteoliposomes).** The respective time constants were derived from EPR spectra simulations carried out with the "jump model" of J. H. Freed (Freed, 1976).

BetP variant	in detergent *		in <i>E. coli</i> lipids	
	$\tau_1$	$\tau_2$	$\tau_1$	$\tau_2$
S545C-SL	3.8ns	16ns	15ns	52ns
E572C-SL	2.0ns	8.3ns	2.9ns	9.5ns
S589C-SL	1.2ns		2.2ns	10.2ns

Note:

- \* = 0.1% n-dodecyl- $\beta$ -D-maltopyranoside (Solgrade, Anatrace Inc., USA)

### 3.4.3. Salt induced mobility changes



The next step was the study of mobility changes at each spin labelled amino acid position (545, 572 and 589) during an external osmotic upshift in the proteoliposomes using cw X-band (9.7GHz) EPR spectroscopy. Thereby, the type and extent of the mobility profile alterations from each BetP mutant were studied in detail to describe the putative C-domain movements as a tendency. However, due to time restrictions, the following results will show the qualitative identification of changes in the respective spin label mobility profiles by differences in the spectral broadening or sharpening upon the applied hyperosmotic stress. The corresponding rotational correlation times will be calculated by the “jump model”-software from J.H: Freed (work in progress).

Figure 27 shows the basic idea underlying the EPR study of salt-induced mobility changes within the C-domain and/or in the vicinity of this domain. To apply an osmotic upshift, the external buffer of the proteoliposomes (internal buffer = external buffer = 100mM  $KP_i$ , pH 7.5) was supplemented with different salts (NaCl, KCl) or zwitterionic solutes (proline, glycine betaine) at concentrations sufficient to fully activate BetP (based on activity measurements, section 3.2). Thereby, 660mM of the ionic compounds NaCl and KCl have an osmolality of about 1.3osmol/kg, whereas 1M of the amino acid proline or the amino acid derivative glycine betaine corresponds to about 1osmol/kg. The increase of the external osmolality should lead to a water efflux out of the proteoliposomes and consequently to an increase of the luminal  $K^+$  concentration that activates BetP. In other words, sensing of the potassium stimulus could probably induce an altered conformation and/or orientation of the C-domain which leads to an activation of the carrier (Figure 27). Such pronounced changes might subsequently generate a new sterical challenge for a given amino acid position and its corresponding spin label in terms of mobility restriction

or disentanglement. If so, the superposition of the spectra of each inactive and hyperosmotically activated BetP mutant will provide information about the mobility changes upon salt stress.

### 3.4.3.1. BetP-S545C-SL (the beginning of the C-domain)

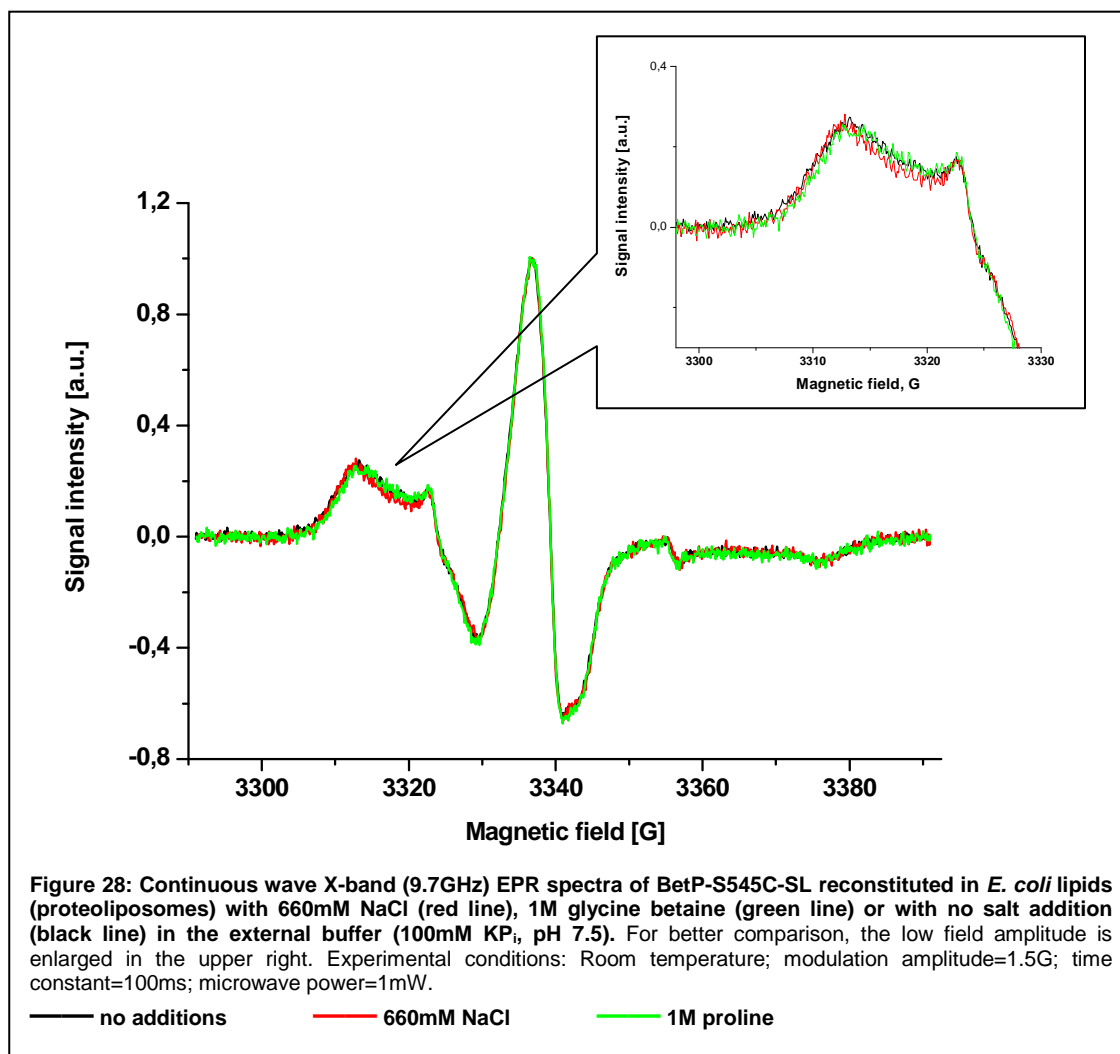


Figure 28 shows the X-band EPR spectra of BetP-S545C-SL reconstituted into *E. coli* proteoliposomes without (black line) and in the presence of externally added salt 660mM NaCl (red line) and zwitterionic 1M proline (green line). The enlarged low field lines of the spectra (Figure 28, upper right) show, that neither the addition of activating amounts of NaCl (red line) nor proline (green line) to the external buffer of the proteoliposomes induced significant changes in the respective spin label mobility profile compared to the control sample (black line). The EPR measurements carried out in the presence of 660mM KCl or 1M glycine betaine showed similar results (data not shown).

This probably indicates – as expected from the topology model - that the structure of this part of the C-terminal domain does not change upon hyperosmotically induced BetP

activation. Also, it may indicate that changes of the protein structure in the vicinity of this spin label are very small.

### 3.4.3.2. BetP-E572C-SL (in the centre of the C-domain)

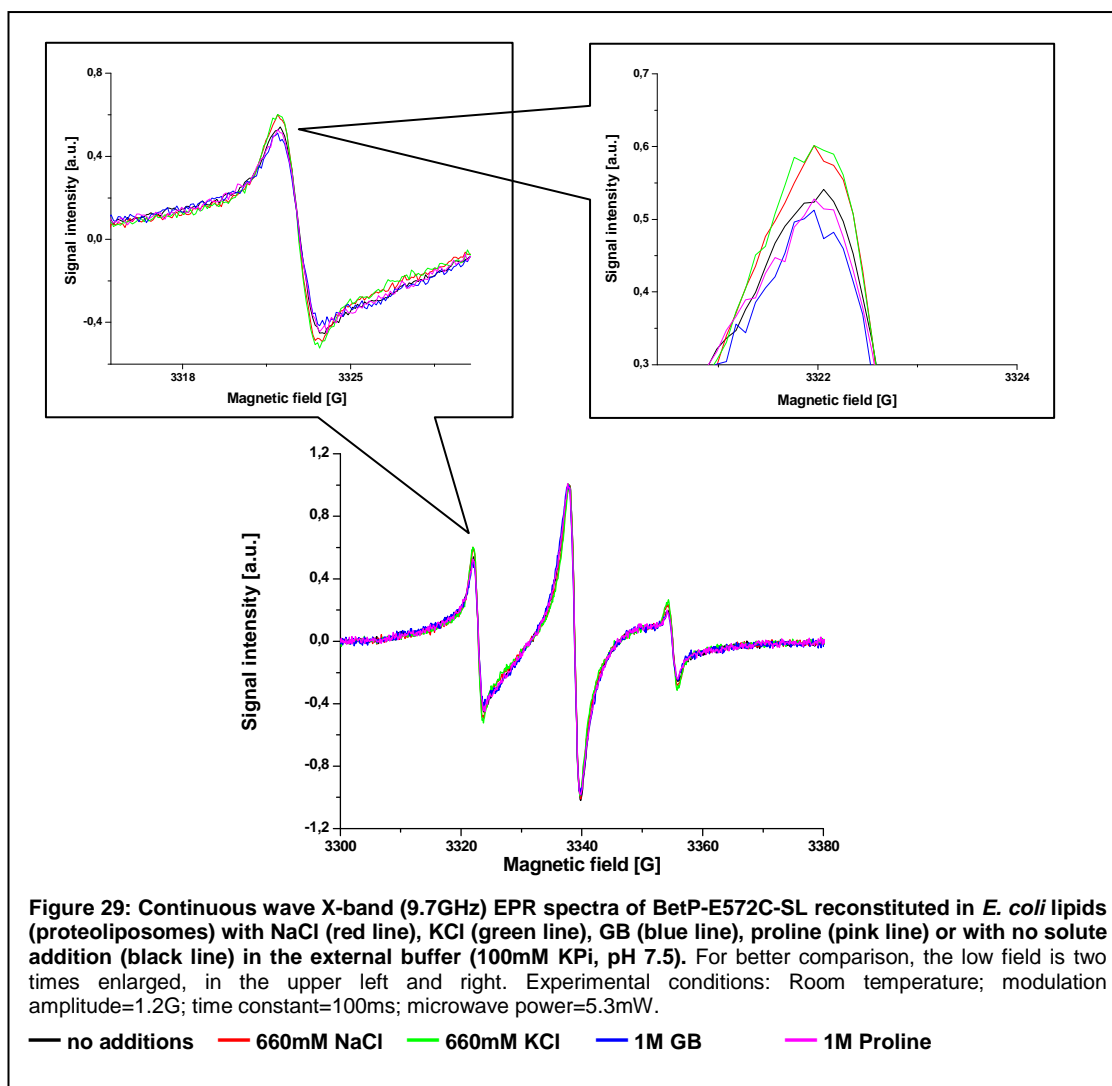
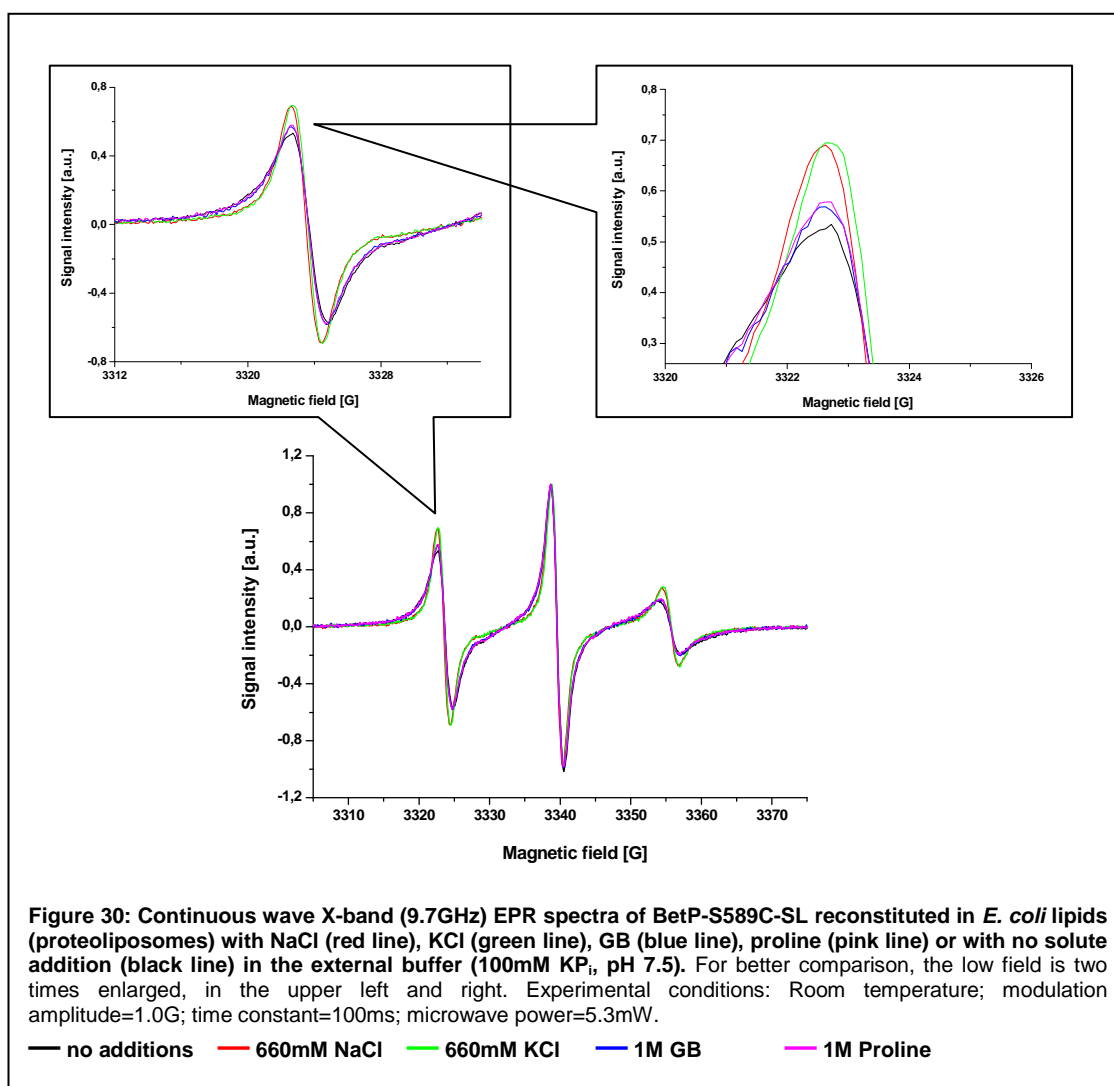


Figure 29 shows the EPR spectra of reconstituted BetP-E572C-SL under non-activating conditions (black line) and upon the hyperosmotically-induced carrier activation. The spectra shown in this figure are slightly different from those shown in Figure 25, because some sharp lines around 3323G and 3358G are visible now. This may be caused due to interfering signals from a small admixture of non-bound spin label (less than a few %) and/or due to a small admixture of unsuitable proteoliposomes with spin labelled BetP protein that may superimpose the spectra (e.g. leaky proteoliposomes, see section 3.4.4). The addition of the solutes glycine betaine (“GB”, blue line) and proline (pink line) to the external buffer had no effect (or only a weak effect) on the respective spin label mobility at position 572. However, if the external buffer was supplemented with activating amounts of NaCl (660mM, red line) or KCl (660mM, green line), an increase in the amplitude

(sharpening) of the low and high field lines were visible, indicative of a higher spin label mobility. Due to some admixture of unbound spin label and/or leaky liposomes it was unclear, if a certain hyperosmotic stress effect on the structure of the C-domain and thus the spin label mobility at position 572 was indeed present. It has to be noted that a small admixture of unbound spin label is also visible in the EPR spectra of BetP-S545C-SL (cp. Figure 28 and Figure 24).

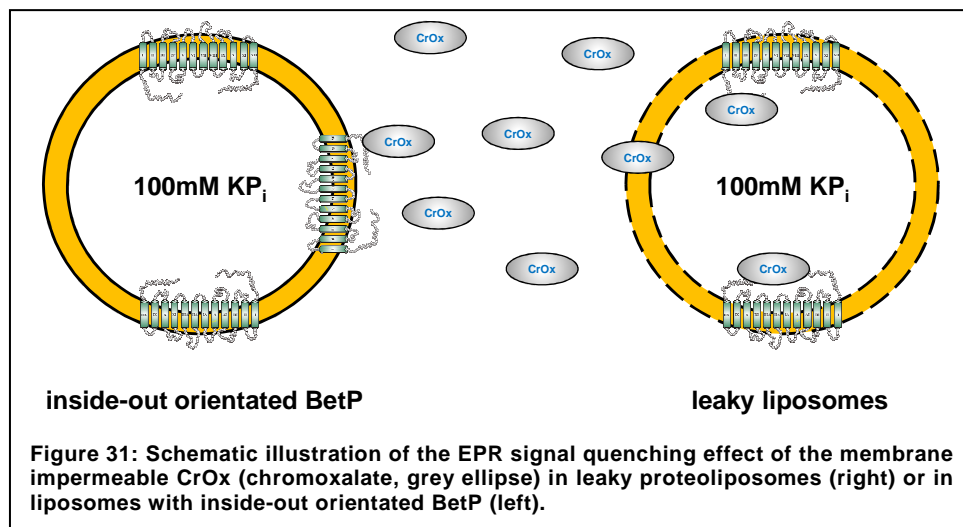
### 3.4.3.3. BetP-S589C-SL (close to the end of the C-domain)



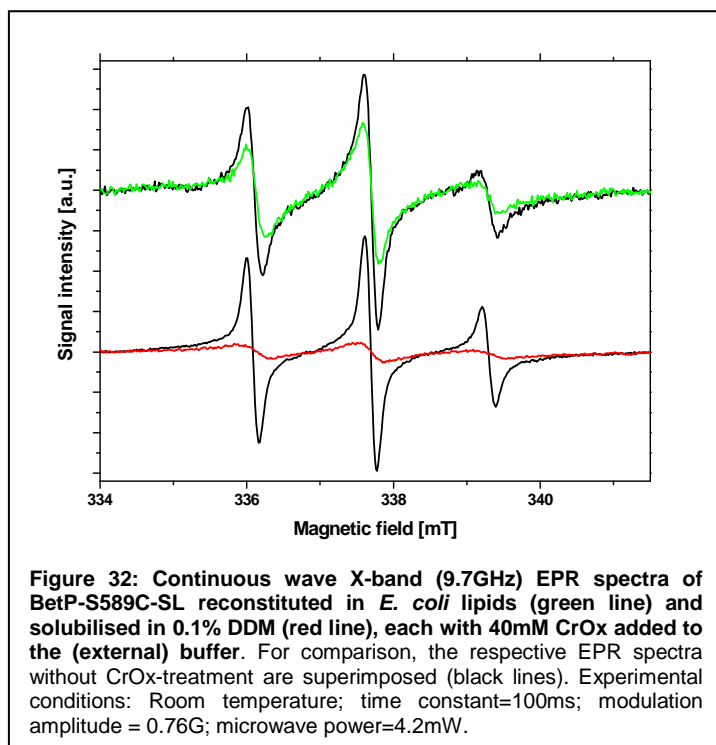
Applying an external osmotic upshift by adding activating amounts of NaCl (660mM, red line), KCl (660mM, green line), glycine betaine (1M, blue line) or proline (1M, pink line) to the external buffer of proteoliposomes with incorporated BetP-S589C-SL led to strong changes in the shape of the EPR spectra detected from a spin label at this position. These changes were reflected in a sharpening of all three hyperfine lines compared to the untreated sample (Figure 30). In particular, this spectral sharpening (= higher spin label mobility) was more pronounced when the salts NaCl and KCl were used as hyperosmotic

stress-inducing compounds in the external buffer than using the zwitterionic solutes glycine betaine and proline (Figure 30, cp. the amplitude of the red or green line with that of the blue or pink line).

These findings were congruent in terms of a higher solute-induced mobility effect on the spin label with an increasing distance to the fixed lipid/protein interface within the C-domain of BetP according to the suggested activation model (Figure 27). However, it still remained to be elucidated why the salts NaCl and KCl were able to induce a much higher spin label mobility as hyperosmotic stress-causing supplements in the external buffer of the proteoliposomes than the zwitterionic (= exhibit no net charge at physiological pH) solutes glycine betaine and proline. One possible explanation is that the charged extensions of inside-out orientated BetP or of BetP in leaky proteoliposomes might electrostatically interact with the salt ions (Figure 31). This putative interaction might induce a spectral sharpening (= high spin label mobility) that superimposes the mobility spectra of intact proteoliposomes with rightside-out orientated BetP during the conducted activation experiments. To discriminate between these putatively direct electrostatic effects and a potassium-stimulated mobility effect during BetP activation, a simple method to quench signals deriving from differently orientated BetP-trimers and from BetP in leaky liposomes was introduced.



### 3.4.4. Electrostatic interactions of salt with the C-domain and/or lipids



For this purpose, a hydrophilic paramagnetic quencher called CrOx (chromate-(III)-oxalate,  $K_3Cr(C_2O_4)_3 \cdot 3H_2O$ , Sigma Aldrich GmbH, Germany) was used. The addition of CrOx induces a broadening of the EPR spectra due to the spin-spin interactions of its own paramagnetic centre with the spin label. The higher the accessibility (collision frequency) of the spin labels to the aqueous phase the stronger the quenching effect of CrOx. Figure

32 shows the effect of CrOx-addition (40mM) on the EPR spectra from two different BetP-S589C-SL samples: (1) solubilised in detergent (red line) and (2) reconstituted into *E. coli* lipids (green line). When BetP is reconstituted into proteoliposomes, about 20% decrease of the signal is observed upon the addition of 40mM CrOx to the external buffer (Figure 32 upper spectra). On the contrary, the addition of the same amount of CrOx to solubilised BetP protein led to a signal decrease of about 95% (Figure 32, bottom spectra), verifying the quenching effect of CrOx on accessible spin label positions in the detergent sample. The addition of CrOx to the external buffer of proteoliposomes with incorporated spin labelled BetP variants should induce significant signal quenching only in two cases: (1) if some of the proteoliposomes are leaky and thus making the C-domain of incorporated BetP accessible for the membrane-impermeable quencher and (2) if inside-out orientated BetP is present in the liposomes with its spin labelled C-domain facing the external solvent (Figure 31).

Thus, similar measurements as described above were performed in the presence of an appropriate amount of CrOx to observe spectral changes (= changes in spin label mobility) and thus a putative C-domain movement only due to the (indirect) BetP activation upon a hyperosmotic upshift in the external medium. Hence, no EPR signals would be detected from all differently orientated (inside-out) BetP proteins and from carriers reconstituted into leaky liposomes.

### 3.4.4.1. Salt effect on BetP-S589C-SL reconstituted into *E. coli* proteoliposomes in the presence of CrOx

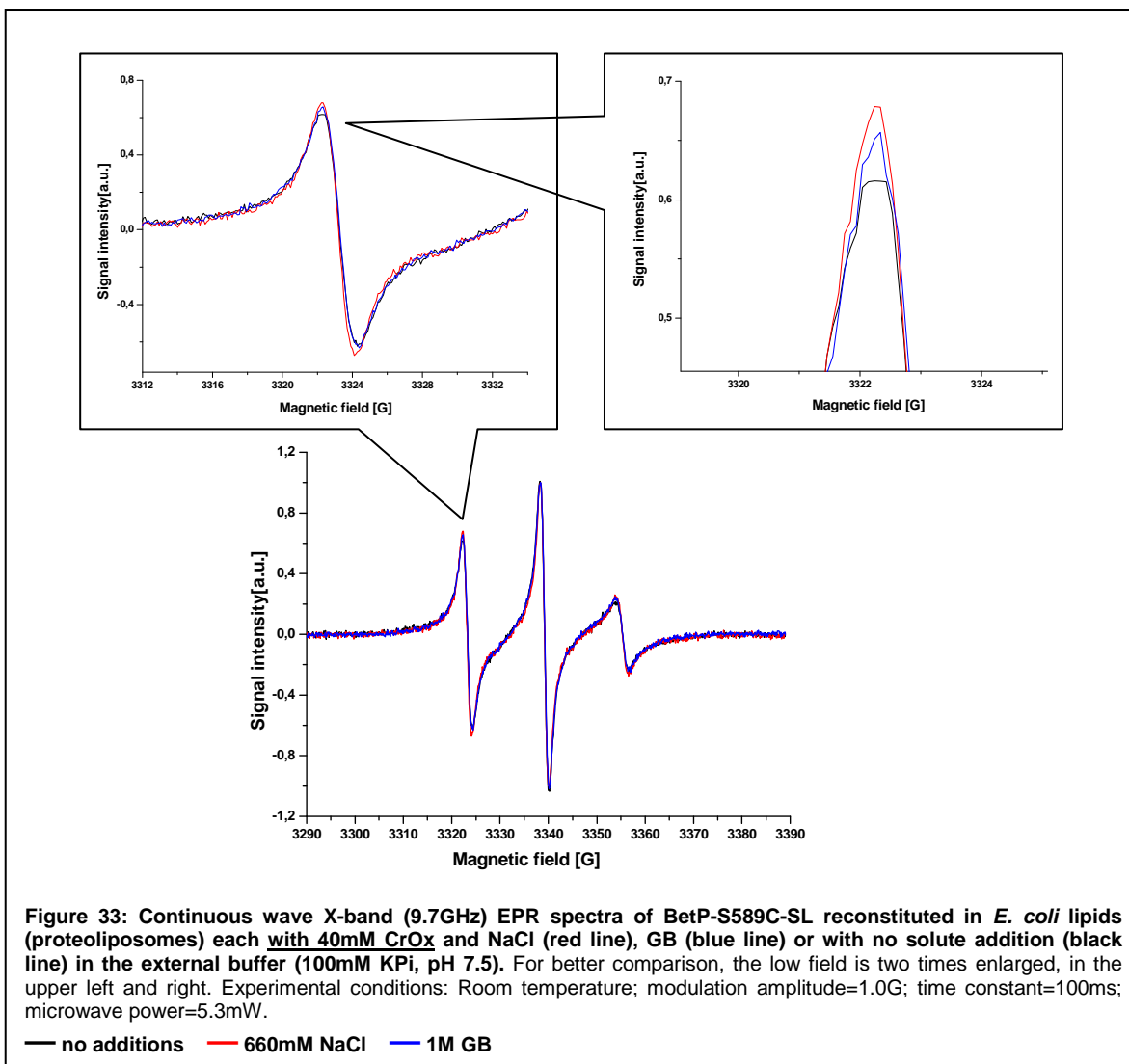


Figure 33 shows the EPR spectra of the spin label at position 589 (close to the terminal end of the C-domain) of reconstituted BetP without (black line) and upon a hyperosmotic upshift in the external buffer. Here again, hyperosmotic stress is applied by the addition of different kinds of solutes in the external buffer (ionic and zwitterionic solutes). In contrast to Figure 30, all these measurements were carried out in the presence of 40mM CrOx in the external buffer to quench interfering signals of unsuitable (leaky or with opposite carrier orientation) BetP proteoliposomes (Figure 31).

As visible in the corresponding EPR spectra (Figure 33, inserts) the hyperosmotic upshift-induced mobility effect on the spin label in BetP-S589C-SL is less pronounced but still present as compared to the “unquenched” sample (cp. Figure 30 and Figure 33). An increase in the spin label mobility upon the addition of the zwitterionic solute (1M GB, blue line) as well as the ionic solute (660mM NaCl, red line) is indeed present. However, the



effect of salt on the conformation and/or orientation of the C-domain, i.e. the increase in spin label mobility, at this end position is still more pronounced than the respective effect of zwitterionic solutes (Figure 33).

### 3.4.4.2. Salt effect on BetP-E572C-SL reconstituted into *E. coli* proteoliposomes in the presence of CrOx

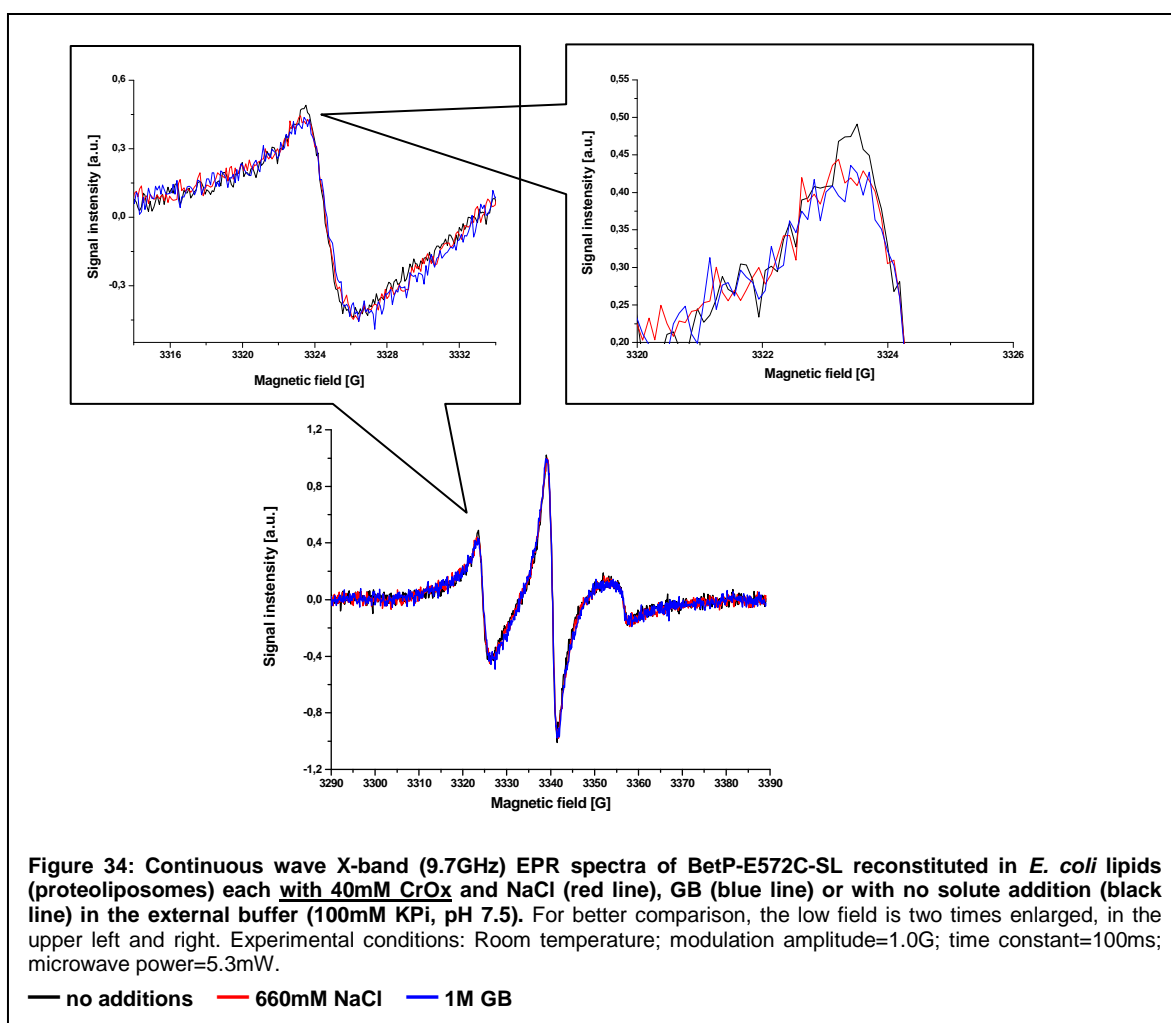


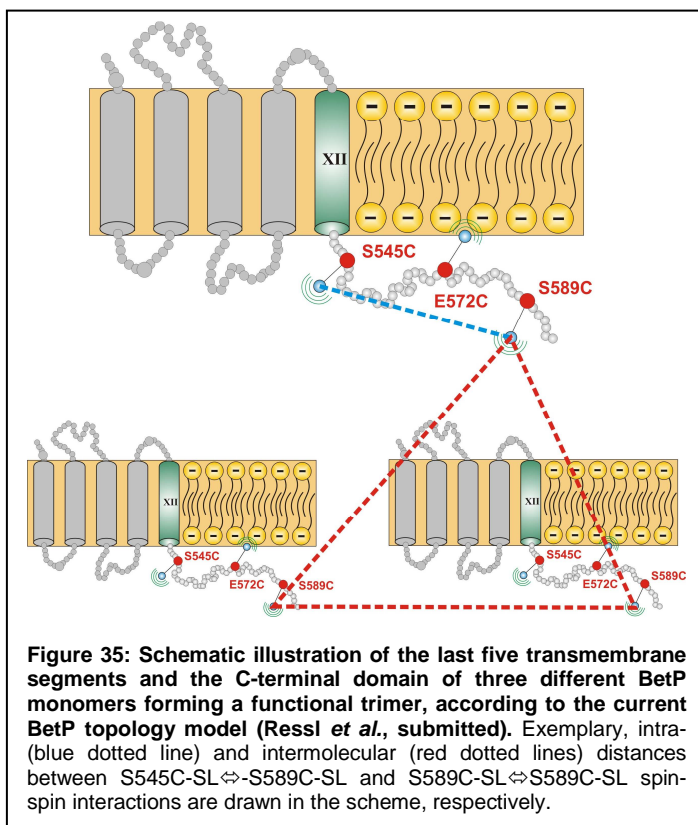
Figure 34 shows the EPR spectra of the spin label attached to position E572 in the presence of 40mM CrOx with different hyperosmotic upshift-inducing supplements (NaCl, GB) in the external buffer of the respective proteoliposomes.

Interestingly and in contrast to the previous results (Figure 29), in the presence of CrOx the mobility of the spin label at position 572 is decreasing as visible from the diminished amplitude and the increased line width of the respective low field peaks (cp. Figure 29 and Figure 34). This may be attributed to a restricted mobility of the spin label at this position resulting in a broader EPR spectrum upon the application of a hyperosmotic upshift. The mobility effect is nearly same for both kinds of solutes (ionic and zwitterionic). Since the permanent activity of this BetP mutant was proven to be independent of the external

increase in osmolality, such changes in the spin label mobility and thus in the structure and/or orientation of the C-domain were unexpected if we suggest an involvement of C-domain dynamics in the activity regulation process of BetP (Figure 27). However, more detailed studies are needed to prove this effect (see Discussion, work in progress).

We conclude that the hyperosmotic stress-induced mobility changes for the spin labels at positions 589 and 572 could still be detected in the presence of CrOx. However, these changes were different from those observed in the absence of the quenching agent. In particular, the direction of changes still remained the same for the spin label at position 589 (e.g. an increasing mobility with and without CrOx). In contrary, a slight decrease of the spin label mobility of BetP-E572C-SL was observed in the presence of the quenching agent.

### 3.5. Distance measurements with BetP variants



The study of the salt induced mobility changes (see above) revealed that during the activation process of reconstituted BetP protein some structural changes within the C-terminal domain occurred. Although these local changes were in agreement with our suggested topology and activation model of BetP, the global information about tertiary or quaternary structural changes and/or relative movements of the C-domain upon the hyperosmotic stimulation was still missing. At the moment no X-ray structure is available for the BetP protein. As

mentioned in the introduction, SDSL-EPR in combination with DEER is widely used for determination of inter- and intramolecular distances in proteins solubilised in detergent or incorporated in a lipid surrounding as well as for the study of global structural changes during protein function (Jeschke *et al.*, 2004; Hustedt and Beth, 1999, Jeschke and Polyhach, 2007).

Thus, in this work the DEER technique was applied to study intra- and intermolecular distances in the BetP carrier. Distance measurements are based on the detection of the amplitude of interactions between two or more spins. To make this possible, at least two spin labels have to be introduced in one protein. In addition, spin-spin interactions can be measured if a single spin labelled BetP monomer forms sufficiently packed aggregates (oligomeric structure) that allow detecting dipole-dipole couplings. It was already known, that BetP is forming a trimer in detergent and upon reconstitution into *E. coli* lipids (Ziegler *et al.*, 2004). With this in mind DEER measurements were carried out to probe both, (i) intermolecular distances between single spin labelled positions within the C-domain of each BetP monomer (Figure 35, red dotted lines) and (ii) intramolecular distances between two spin labels within the same C-extension of each monomer (Figure 35, blue dotted lines).

The latter distance determination experiments were chosen to prove if an altered C-domain conformation may be responsible for a correct stimulus sensing and/or signal transduction of BetP. The aim was to identify the distances between two spin labels attached to cysteine residues at the beginning (545) and close to the end (589) of the C-terminal domain in two different mutants: (i) a double mutant (BetP-S545C/S589C) exhibiting the intramolecular S545C $\leftrightarrow$ S589C distance in an osmotically regulated BetP carrier and (ii) a deregulated triple mutant (BetP-S545C/Y550P/S589C) with a putatively different S545C $\leftrightarrow$ S589C distance due to the intermediate proline introduction. It was suggested, that the proline introduction at position 550 may alter the conformation and/or orientation of the C-domain rendering the respective carrier mutant insensitive to the osmotic stimulus (Figure 11). If this is true, these changes were expected to be quantifiable by the different S545C $\leftrightarrow$ S589C distances in the two constructed BetP mutants.

The DEER analysis for each conducted experiment was performed as described in the literature (Jeschke and Polyhach, 2007; for more details see Appendix). In short, the measured dipolar evolution function  $V(t)$  was separated into the form factor  $F(t)$  and the background factor  $B(t)$ . Dividing  $V(t)$  by the fitted  $B(t)$  function leads to the contribution of the form factor  $F(t)$  to the overall spin echo signal (equation (13), Appendix). In the derived Gaussian distance distribution the (highest) probability  $P(r)$  is then plotted as a function of the determined distance  $r$  with a standard deviation that can be qualitatively derived from the broadening of the bell-shaped curve (Gauss curve).

### 3.5.1. BetP-S545C-SL in *E. coli* liposomes

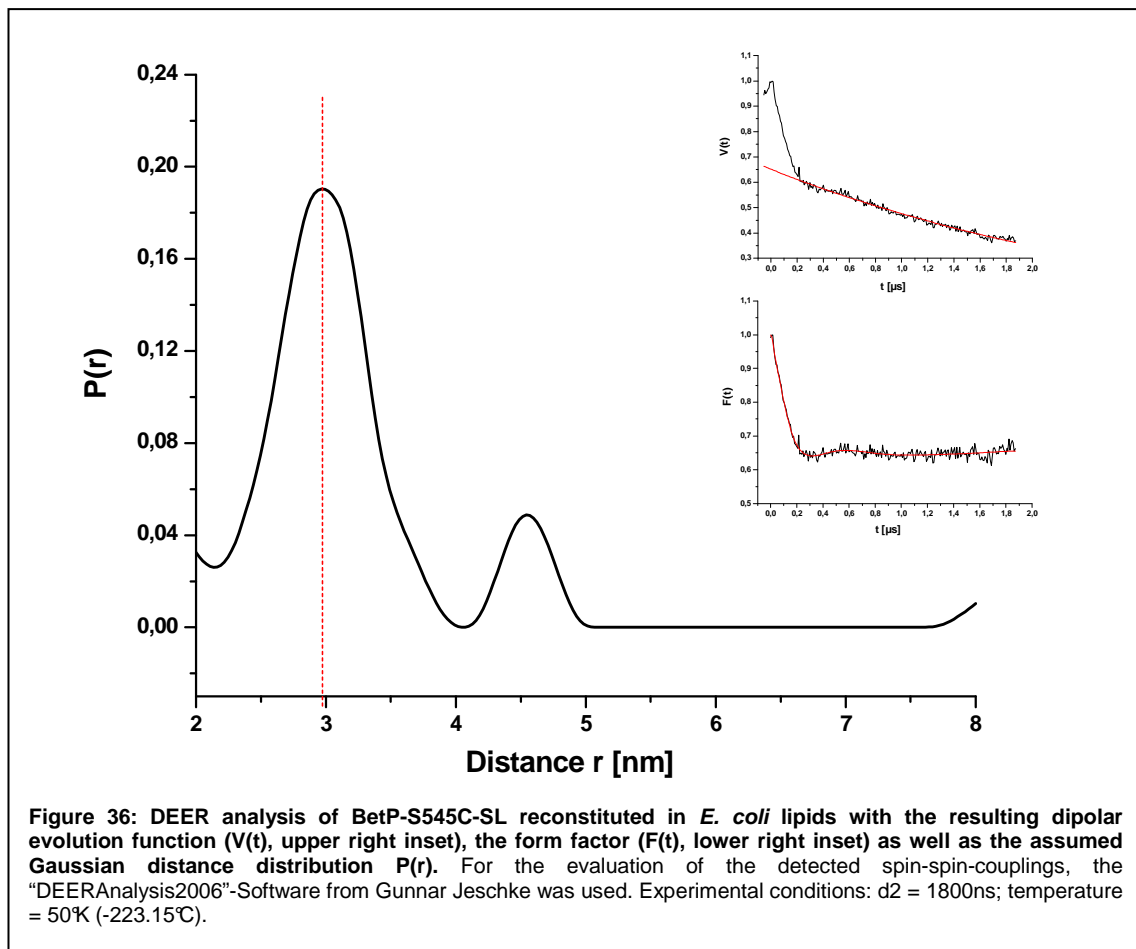


Figure 36 shows the experimental results of four-pulse DEER measurements (insert) and results of the analysis of this experiment with BetP-S545C-SL reconstituted in *E. coli* lipids (proteoliposomes). This result shows that a distance of  $30 \pm 5 \text{\AA}$  is observed in the single labelled BetP variant incorporated into proteoliposomes. Since no second spin label was present in one BetP monomer, the distance we measured had to be originated from intermolecular interactions between different BetP monomers. In addition to the main peak, a small peak with lower amplitude was observed at a distance of about  $45 \text{\AA}$  (Figure 36). However, the position of this additional peak varied from experiment to experiment carried out with the same BetP-S545C-SL mutants ( $45\text{-}50 \text{\AA}$ , Figure 54, Figure 55, Figure 56, Appendix).

### 3.5.2. BetP-S545C-SL in detergent

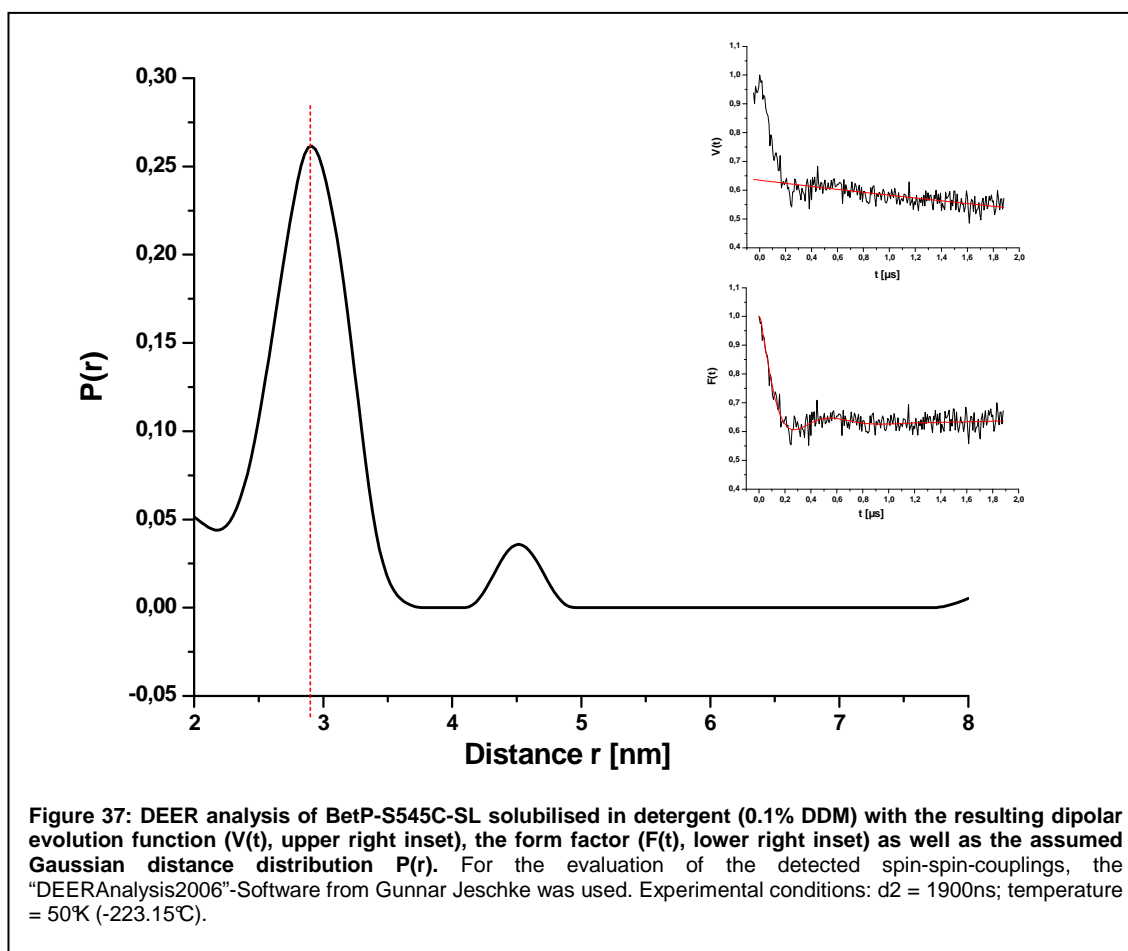
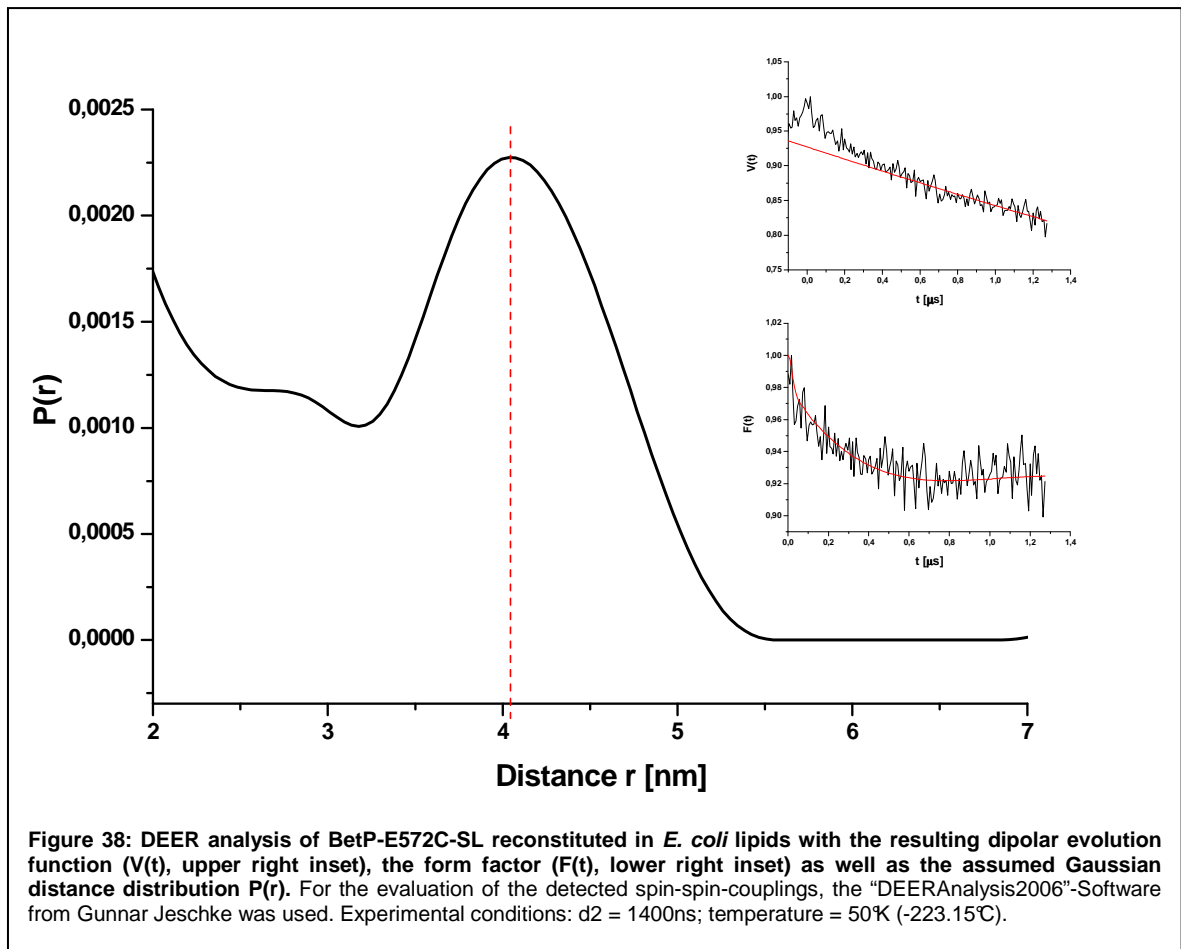


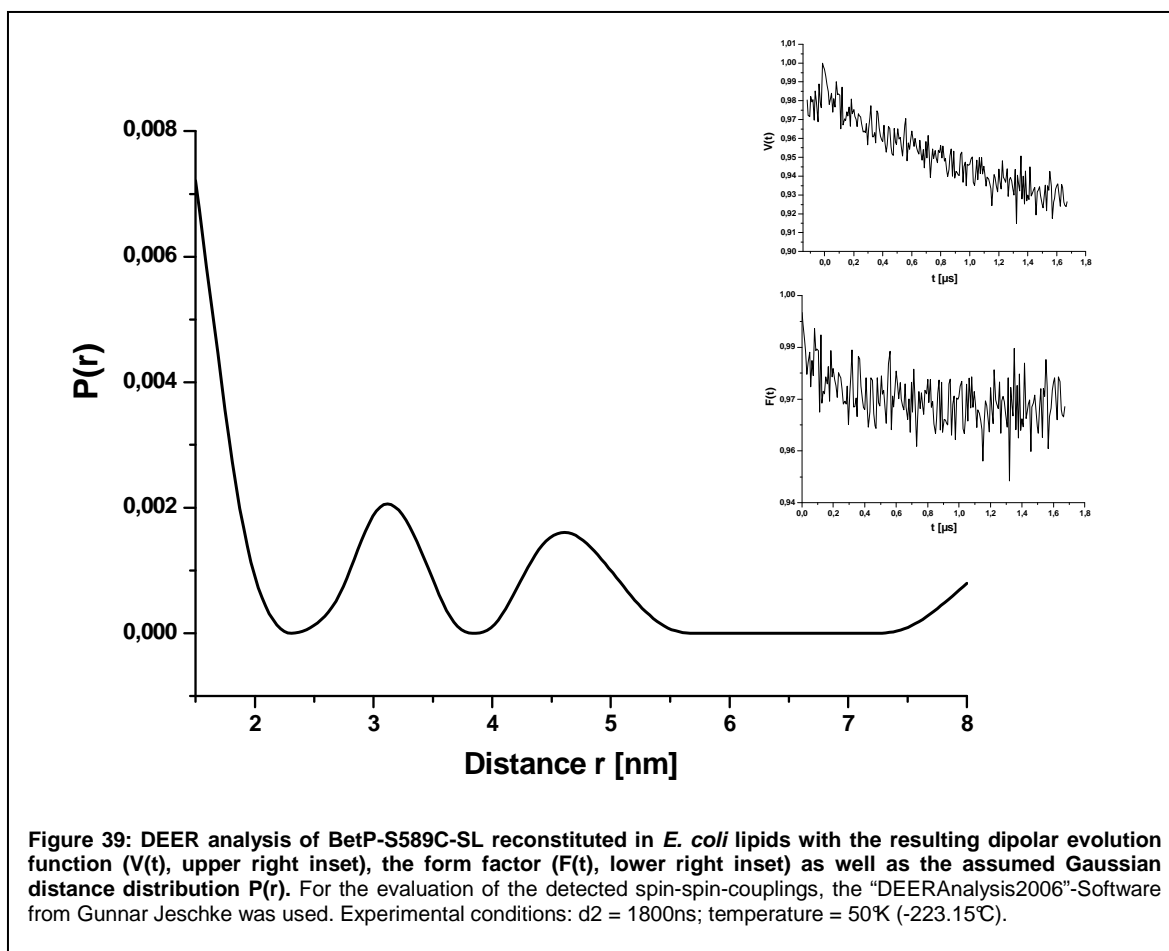
Figure 37 shows the DEER trace and the respective results of the analysis for BetP-S545C-SL solubilised in 0.1% DDM. Prior to the reconstitution of the above measured BetP-S545C-SL variant (Figure 36) an aliquot of the same purified protein was retained for the DEER analysis with a corresponding sample solubilised in detergent. The analysis showed a mean distance of  $29 \pm 5 \text{ \AA}$ , which was more or less identical to the observed spin-spin distance in the membrane embedded BetP-S545C-SL sample (Figure 36).

### 3.5.3. BetP-E572C-SL in *E. coli* liposomes



The results of the DEER analysis for the spin labelled BetP-E572C mutant are shown in Figure 38. The analysis of time resolved traces revealed a mean distance of  $40 \pm 8 \text{Å}$  between the spin labels at position 572 (centre of the C-extension) in the BetP trimer. For the moment the signal/noise ratio does not allow to draw a final conclusion about the distance measured in this sample (Figure 38, inserts; work in progress). It has to be noted that according to the suggested topology model, the spin label at this centre position within the C-domain exhibits more rotational freedom than the spin label at position 545 (Figure 35), resulting in much broader distance distribution (cp. Figure 36 and Figure 38). The presence of various spin label conformations in a given sample can affect the DEER time trace and mask the frequency of the main oscillation (Jeschke and Polyhach, 2007). However, these preliminary results indicated that indeed some spin-spin interactions between the spin labels attached to the position 572 of different BetP monomers occurred.

### 3.5.4. BetP-S589C-SL in *E. coli* liposomes



The respective DEER trace and the results of the analysis for the BetP-S589C-SL sample are shown in Figure 39. Due to the low labelling efficiency for this sample (less than 30%) the signal/noise ratio was very low (Figure 39, inserts). It was not possible to detect an oscillating  $V(t)$  curve and to properly fit the background function  $B(t)$  (for more details see Appendix; Jeschke and Polyhach, 2007). However, due to the presence of a relatively long decaying echo signal (cp. insert in Figure 39 with insert in Figure 36), we could rule out a distance below  $50\text{\AA}$  (personal communication, I. Borovykh). Future experiments with samples exhibiting a higher labelling efficiency are needed to confirm these results. In addition, the spin label at this position (near the C-terminus) showed a high mobility indicating a large space available for the spin label motion (Figure 30). As result, a broad conformational distribution can be expected for the spin label at this position, resulting in the absence of any modulation pattern in the DEER trace (Jeschke and Polyhach, 2007). Also, it is important to note that the common freezing of a DEER sample down to  $50\text{K}$  can induce additional distance distributions which have been observed to affect the resulting modulation pattern.

### 3.5.5. BetP-S545C/S589C-SL in *E. coli* liposomes

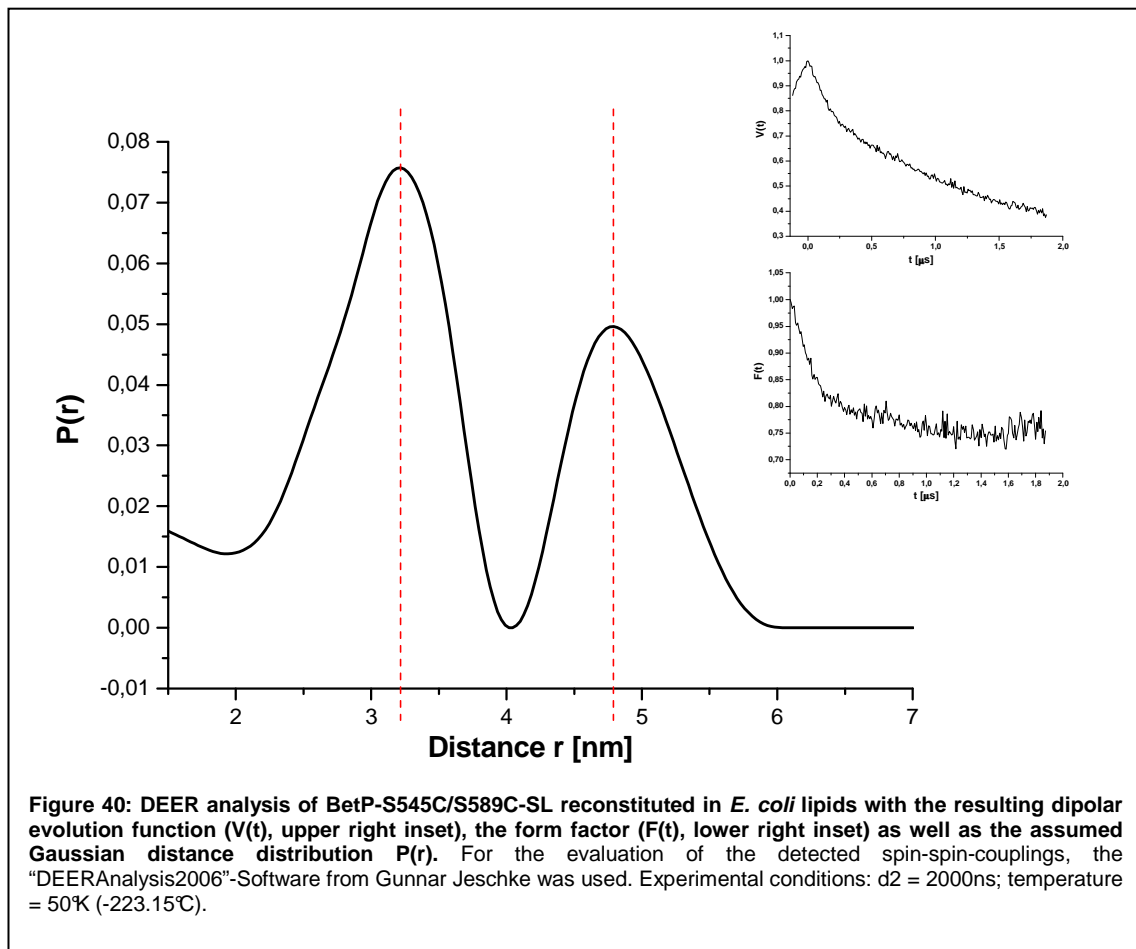
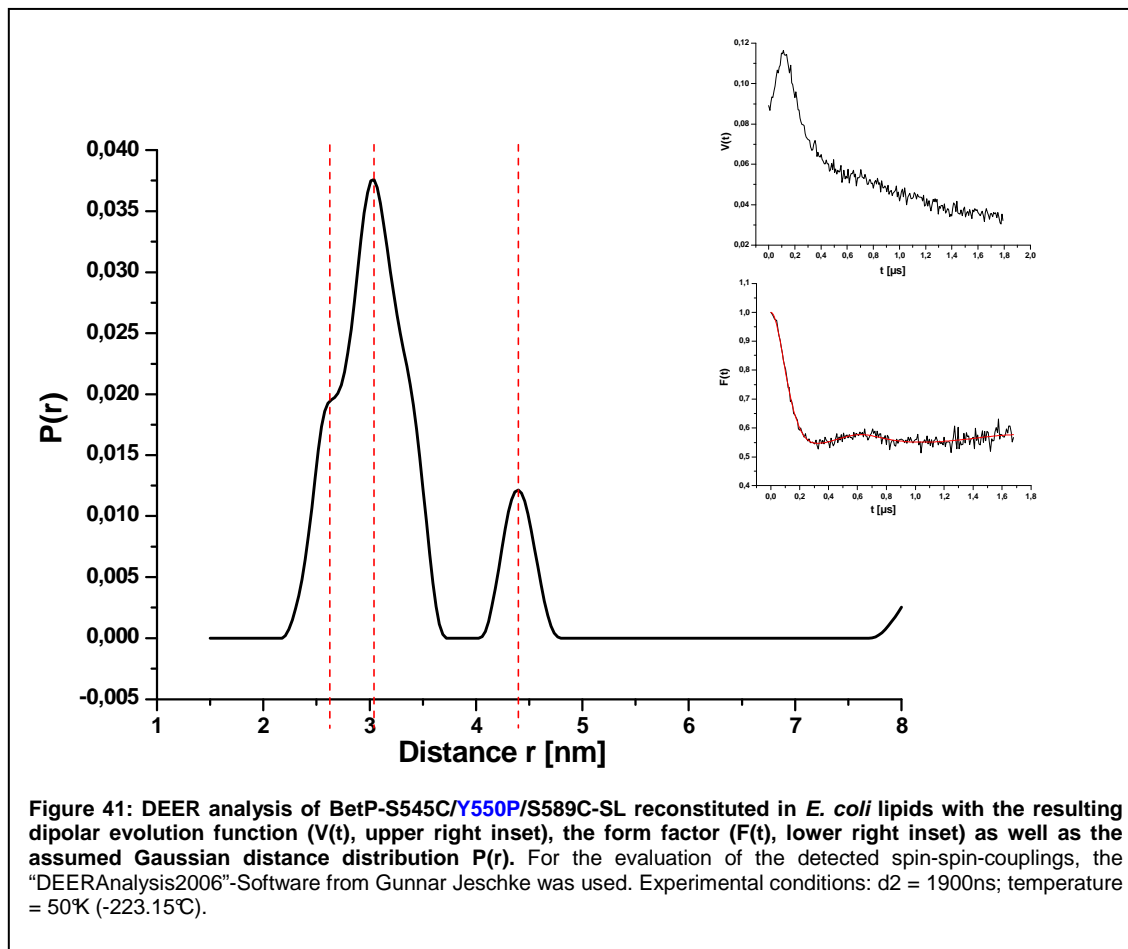


Figure 40 shows the results of the DEER study for a double spin labelled cysteine mutant (BetP-S545C/S589C-SL). Here, in addition to the already observed distance of about  $30\text{\AA}$  (position 545) we detected an additional peak with a mean distance of about  $47\text{\AA}$ . Due to the fact, that we were not able to determine a distinct intermolecular distance between the single spin labelled 589 positions in the BetP trimer (Figure 39), the second distance of about  $47\pm 5\text{\AA}$  (Figure 40) may be attributed to an intramolecular distance between the spin labels attached to position 545 and 589 in the same BetP monomer. Since the signal/noise ratio for the single labelled BetP-S589C mutant was rather low, we still cannot completely rule out that interactions of the spin labels at position 589 in different BetP monomers of the trimer are responsible for this additional distance. Currently work is in progress to confirm these results.



### 3.5.6. S545C/Y550P/S589C-SL in *E. coli* liposomes



An additional mutant of interest was the triple mutant BetP-S545C/Y550P/S589C. The introduction of a proline at position Y550 leads to a permanently active (deregulated) transport protein (Schiller *et al.*, 2006). This triple mutant was used to probe the hypothesis changes in the structure/orientation of the C-terminal domain during the activation process of BetP (Figure 27). For this purpose and as mentioned above, the intra- and intermolecular distances of the "quasi-wildtype" protein BetP-S545C/S589C (Figure 40) and the deregulated triple mutant BetP-S545C/Y550P/S589C (Figure 41) had to be compared to each other.

Figure 41 shows the results of DEER measurements for the triple mutant BetP-S545C/Y550P/S589C. The respective analysis revealed the presence of two distinct distances, a short distance of about  $30 \pm 5 \text{ \AA}$  and a greater distance of about  $44 \pm 3 \text{ \AA}$ . The short distance may be assigned to the S545C-SL  $\leftrightarrow$  S545C-SL interaction in the trimer (cp. Figure 36 and Figure 41). The second distance of  $44 \pm 3 \text{ \AA}$  could appear due to the interaction of spin labels at position 545 and S589C within the same BetP monomer. Interesting is the fact that although the short distance (S545C-SL  $\leftrightarrow$  S545C-SL) did not change for these two samples, the larger distance was about  $3 \text{ \AA}$  less in the triple mutant

## Results

sample compared to the double mutant BetP-S545C/S589C-SL (cp. Figure 40 and Figure 41). The distance distribution was nearly the same for the intermolecular interactions of spin labels at position 545. On the contrary, the observed standard deviation ( $\sigma$ ) of the DEER analysis carried out for BetP-S545C/Y550P/S589C-SL had nearly half the amount compared to BetP-S545C/S589C-SL (3Å vs. 5Å, Table 7). This can be induced for example by the presence of a different sterical conformation of the C-terminal domain in the cysteine/proline mutant. In addition, a pronounced shoulder is visible at the left side of the main peak (distance about 27Å). Currently, the origin of this shoulder is not clear. Further research is necessary to confirm these results.

Table 7 summarizes the determined spin-spin distances of all single and double spin labelled BetP variants studied in this work.

**Table 7: Summary of the computed spin-spin distances of the DEER EPR analysis (DEERAnalysis2006, Jeschke) on spin labelled BetP variants reconstituted in *E. coli* lipids (proteoliposomes).**

BetP variant	Mean distance	Standard deviation
	r [Å]	$\sigma$ [Å]
S545C-SL	30	5
S545C-SL-detergent	29	5
E572C-SL	40	8
S589C-SL	n.d.	n.d.
S545C/S589C-SL	32	6
	47	5
S545C/Y550P/S589C-SL	26	4
	30	5
	44	3

## 4. Discussion

The structural and functional characterization of the osmoregulated transporter BetP from *Corynebacterium glutamicum* is in the focus of the presented work. Under hyperosmotic conditions, this secondary carrier imports its substrate glycine betaine into the cell. Interestingly, BetP is able to sense the osmotic challenge by monitoring the increase of the cytoplasmic K<sup>+</sup> concentration as well as to subsequently adjust its import activity to the extent of externally applied osmotic stress. Former studies revealed that – to a certain extent – the integrity and primary structure of the C-terminal domain of BetP are crucial for a correct stimulus sensing and/or signal transduction (Peter *et al.*, 1998a; Schiller *et al.*, 2004b; Ott, 2008). In depth analysis with proline substitutions within a putative  $\alpha$ -helical stretch which is located in the centre of the C-domain showed that also the conformation and relative orientation of this domain is essential for the activity regulation of the transporter (Schiller *et al.*, 2006). Recently, it was suggested that the interaction of the C-extension with other domains of the protein, structural changes in the vicinity of the C-terminal domain as well as interactions between BetP monomers in the oligomeric state may be important for the function of the carrier (Ressl *et al.*, submitted).

In order to further analyze the structure and function of the C-domain during the activation process of BetP, an SDSL-EPR-based spectroscopic study of the transporter and in particular of distinct positions at the beginning (545), in the centre (572) or the end (589) of the C-terminal domain was carried out under activating and non-activating conditions. In the scope of this work was the detailed analysis of the general structural properties as well as time-resolved motions of the C-domain during BetP-activation. For this purpose and as a prerequisite for all performed EPR measurements, first the sustained functionality of each spin labelled BetP cysteine variant was verified by radiochemical uptake measurements with [<sup>14</sup>C]-glycine betaine and compared to the control mutant BetP-C252T (“cysless”) with its wildtype-like activity regulation profile. In addition, an efficient reconstitution of these mutants into *E. coli* lipids in terms of a high yield of rightside-out orientated, spin labelled BetP protein was established to obtain enough highly purified material for the SDSL-EPR studies. Preliminary distance measurements between two spin labels within the same C-domain of the same BetP monomer (intramolecular distance) or between different single spin labelled BetP monomers in their oligomeric state were performed to further confirm the trimer aggregation of the reconstituted transporter (Ziegler *et al.*, 2004; Ressler *et al.*, submitted).

## 4.1. Activity regulation of BetP variants in *E. coli* lipids

The combination of both, (i) Site-Directed Spin Labelling (SDSL) and (ii) Electron Paramagnetic spin Resonance (EPR) spectroscopy was used to provide specific information on the structure and environment of genetically engineered cysteine residues within the C-terminal domain of the secondary transporter BetP. Since no crystal structure of the protein is published to date, the selection of the single cysteine mutants for the aims of this thesis was based on the so far suggested topology model of the BetP carrier (Figure 9). Hence, the three chosen positions should provide a consecutive screen of the presumably different mobility of spin labels attached to introduced cysteines at the beginning (545), in the centre (572) or close to the end (589) of the 55 amino acid comprising C-terminal domain.

As an initial step, a sulfhydryl-specific spin label containing a stable free radical had to be covalently linked to the cysteine of interest which in turn can then be used as the EPR-detectable probe. However, the influence of the spin label attachment on the structural and kinetical properties of the respective carrier variant had to be investigated to assure a functional conformation that does not impair the native activation process of the protein. For this purpose, the catalytic activity of each spin labelled and non-labelled BetP mutant reconstituted in *E. coli* lipids was determined via radiochemical transport measurements. In doing so, the maximal uptake rates for [<sup>14</sup>C]-glycine betaine as a function of the applied osmotic upshift for each variant were determined and compared to the wildtype-like regulation profile of the BetP-C252T (“cysless”) protein as control.

### 4.1.1. Comparison of the regulatory properties of non-labelled and spin labelled BetP variants S545C, E572C and S589C

As expected from the corresponding *in vivo* experiments (Nicklisch, 2005), the respective activation profiles of the non-labelled reconstituted BetP cysteine variants looked almost the same. When reconstituted in *E. coli* lipids, BetP-S545C and BetP-S589C showed a regulation profile similar to the wildtype-like BetP-C252T mutant, while the BetP-E572C mutant was deregulated. Thus, a cysteine substitution at the beginning (position 545) or close to the end (position 589) of the C-domain did not influence the autonomous activity regulation property of the BetP carrier incorporated in liposomes. Likewise, the deregulated activation profile of BetP-E572C in *E. coli* lipids showed a (permanent) uptake rate, but the mutant was still unable to adapt its maximal activity to the increase in the external osmolality.

The corresponding spin labelled BetP variants could sustain their normal osmoregulation profile in the case of BetP-S545C-SL and BetP-S589C-SL or their deregulated activation profile in the case of BetP-E572C-SL. This proved that the spin labels attached to position

545 or 589 did not induce a sterical hindrance or a general impairment of the stimulus detection and/or signal transduction process. Concerning the spin labelled position 572, the sustained permanent activity after the spin label introduction did not seem to influence the transport process. Since the non-labelled BetP-E572C mutant already exhibits a deregulated activation profile, a particular influence of the spin label attachment on the stimulus sensing and signal processing properties of this BetP mutant cannot be separated from the effect of the cysteine introduction at position E572.

Interestingly, the spin label attachment seemed to lead to a shift in the sensitivity towards the stimulus detection, as already observed in N-terminal deletion mutants or in proteoliposomes with a higher share of negatively charged lipids (Peter *et al.*, 1997; Schiller *et al.*, 2006). The activation optimum was reached at an external osmolality of 600mosmol/kg with the non-labelled BetP mutants and at 800mosmol/kg with the spin labelled variants (cp. Figure 18 with Figure 19). Due to the fact that both, (i) the N-terminal extension and (ii) the surrounding phosphatidylglycerol lipids in the proteoliposomes possess negative charges, which seem to be involved in the sensitivity of stimulus perception, electrostatic interactions may play a certain role in the adaptive osmoregulation process of the BetP transporter. Since the MTS spin label only comprises an uncharged pyrrole ring as well as a sterically shielded paramagnetic electron (four surrounding methyl groups, Figure 49) an electrostatic influence can be ruled out as an origin for the putative sensitivity shift. However, the attachment could also restrict particular conformational degrees of freedom within the BetP protein that might hinder a proper stimulus sensing. Due to the fact, that in the studied single cysteine BetP variants only one small substituent per monomer was attached, it is rather unlikely that the small spin probe caused a sterical restriction that might influence the overall regulation profile to such an extent. However, in the case of ProP from *E. coli* all attempts to attach single spin labels at different positions within the carrier led to an inactive protein and thus prevented the application of SDSL-EPR for the functional carrier (J. Wood, personal communication). It has to be noted, that different batches of *E. coli* lipids were used in the activity measurements for labelled and non-labelled BetP mutants. In an "old" lipid batch unavoidable lipid oxidation products due to radical abstraction or the formation of peroxides, may cause both, (i) an improper incorporation of the BetP protein or (ii) an increase in the permeability of the liposome bilayer (Zhang *et al.*, 1993; Zuidam *et al.*, 2003). Both chemical degradations may thus lead to physical changes of the proteoliposomes that may induce the observed shift in (osmo-) sensitivity. In addition, the degree of purification in each lipid batch varies to a certain extent (Avanti Polar Lipids manufacturer, personal communication). A higher degree of purification leads to a higher fraction of negatively charged PG in the *E. coli* extract, which in turn was already

observed to render BetP more insensitive to its stimulus (<http://www.avantilipids.com/LipidsByExtraction.asp>; Schiller *et al.*, 2006; Rübenhagen *et al.*, 2000). However, this observed activation optimum shift to higher osmolality in the presence of a spin label needs additional confirmation (work in progress).

We conclude that the introduction of a spin label at amino acid positions 545 and 589 did not impair the BetP function and thus allowed the further study of these mutants using SDSL-EPR. In addition, the analogous modification (i.e. spin label attachment) of the BetP-E572C protein had no influence on its deregulated activation profile, e.g. its permanent activity independent of the applied hyperosmotic stress was conserved.

## 4.2. Optimization of the reconstitution process

By means of SDSL-EPR analysis it became obvious that the direct contact to the hydrophobic SM2 Bio-Bead resin promotes BetP absorption and that this phenomenon was responsible for the high protein loss during the conventional reconstitution process developed by Rigaud *et al.* (1995).

According to a common interpretation of the reconstitution process, the incorporation of membrane proteins in pre-solubilised *E. coli* liposomes occurs during the first minutes after the addition of the solubilised protein and should be more or less complete before the addition of the Bio-Beads (Rigaud *et al.*, 1988b, 1998). However, in our case the polystyrene beads even seemed to “extract” the already incorporated BetP out of the liposomes during reconstitution. Since pre-saturation of the Bio-Beads with lipids, an increase of the adsorption rate due to higher temperatures or a higher number of batches (Rigaud *et al.*, 1997) as well as the application of low protein concentrations did not lead to a significant improvement, a new alternative method was developed here for BetP reconstitution. The task was to ensure high reconstitution efficiency in terms of both, (i) a high protein recovery and (ii) functional rightside-out incorporation into *E. coli* lipids. Since the direct contact to Bio-Beads was responsible for the high protein loss, a separation of the protein-lipid-detergent micelles and the hydrophobic absorbent was obligatory. For this purpose, a reconstitution by dialysis was suggested to circumvent this problem. A dialysis bag with a suitable cut-off (e.g. 50kDa for BetP trimer with ~180kDa) allowed the detergent removal by size exclusion. However, the critical micelle concentration (cmc, minimal detergent concentration at which micelles form) of the used detergent DDM is rather low (0.5mM, Le Maire *et al.*, 2000) and led to high dilution factors and a prolonged dialysis time. A combination of dialysis and Bio-Bead addition to the external buffer was known to significantly accelerate a dialysis reconstitution process and was thus applied and optimized for the reconstitution of BetP (according to the basic idea of Philippot *et al.*,

1983). By comparison of the relative EPR signal amplitudes of spin labelled BetP variants during the reconstitution with the conventional and with the new Bio-Bead/dialysis method it was possible to quantify relative protein loss and efficiency of the two methods.

This SDSL-EPR study revealed that during the conventional reconstitution about 75% of the BetP-S589C-SL protein was adsorbed to the Bio-Beads after 6h hours of Bio-Bead incubation. In contrast to this, only 30% protein was lost during the Bio-Bead/dialysis reconstitution after 6h of incubation (Figure 21). Similar results were obtained for the BetP-E572C-SL mutant (data not shown). After 24 hours of reconstitution (=end of procedure) we obtained an about 5-8 times higher amount of reconstituted spin labelled BetP protein when the new Bio-Bead/dialysis method was applied as compared to the conventional reconstitution assay. Although during the Bio-Bead/dialysis method no direct contact and thus adsorption of BetP to the Bio-Beads could occur, a certain extent of protein loss was still observable (Figure 21). The subsequent measurement of the Bio-Beads from the dialysis buffer revealed that no spin labelled BetP protein was adsorbed (data not shown). Reasons for this might be attributed to the used dialysis membrane. The permeability of such a spongy matrix of cross-linked polymers mainly depends on the molecular shape, degree of hydration or solubilisation, ionic charge, and polarization of the protein species to be retained. Although the respective Molecular Weight Cut-Off (MWCO) is an indirect measure of the retention performance, it is more precisely determined as the solute size that retains to at least 90% ("Membrane selection guide", Spectrum Labs, <http://www.spectrapor.com/>). Thus, possible explanations for the protein loss could be that (i) a small amount of BetP monomers (64,2kDa), trimers (~180kDa) or even lipid-protein-detergent micelles were extracted from the dialysis bag and distributed in the dialysis buffer at concentrations which were too low to be measured by EPR spectroscopy (500mL external buffer volume and only a few mg of Bio-Beads were used for the reconstitution) or (ii) - most probably - a certain amount of BetP adsorbed to the dialysis membrane (CE, cellulose ester) and could not be recovered after the reconstitution. Thus, a small but unavoidable extent of protein loss has to be considered and included in every design of future reconstitution procedures with the Bio-Bead/dialysis method.

Interestingly, the spectral line shapes of the two BetP variants E572C-SL and S589C-SL looked nearly similar (broad EPR spectra, typical for spin labels with restricted mobility), when adsorbed to the Bio-Beads (Figure 57, Appendix). This led to the conclusion that at least a major part or even the whole C-domain is strongly interacting (binding to) with the hydrophobic resin and supports the former suggestions of being "sticky" to various kinds of surfaces (V. Ott and S. Morbach, personal communication). It raises the question, if

such a “sticky” agent had to be shielded under native conditions to function as a flexible and “switch”-like sensor in the BetP protein? It may be noted, that such an ability of Bio-Beads to strongly absorb BetP protein can be used in future experiments, for example, to remove inside-out orientated BetP trimers from the proteoliposomes. This method may be used to improve the quality of future transport measurements and EPR analysis.

EPR spectroscopy revealed that the final yield of reconstituted spin labelled BetP was low (around 10-20% of the starting amount) using the conventional reconstitution assay. Although some protein loss was also observed in the new established Bio-Bead/dialysis method, the final recovery of proper incorporated spin labelled protein was about 70%. Consequently, this new method was preferred for further reconstitution procedures. Thus, separation of the hydrophobic adsorbent and BetP protein by a dialysis bag with a proper cut-off (e.g. 50kDa for BetP trimers with a total molecular mass of about 180kDa) seems to be crucial for a high efficient reconstitution into *E. coli* lipids to sustain the calculated LPR (lipid-to-protein ratio) necessary for high quality cw- and pulsed EPR measurements. It was shown that direct contact between Bio-Beads and the BetP protein results in a strong absorption of the carrier to Bio-Beads. In particular, it was deduced that the C-terminal domain is involved in this process.

### 4.3. Mobility profiles of C-terminal BetP variants

To reveal putative protein-protein or protein-lipid interactions during reconstitution into *E. coli* lipids, the EPR spectra of each of the three spin labelled BetP variants (S545C-SL, E572C-SL, S589C-SL) solubilised in detergent were compared to the spectra of the respective mutant when reconstituted in liposomes. Beside a qualitative analysis of the spectral lineshapes (relative broadening or sharpening), a spectral analysis using a program developed by J. H. Freed (“jump model”; Freed, 1976) was performed to quantify the rotational correlation times of each spin labelled BetP protein and to allow a relative comparison of both, (i) the general spin label mobility at the three spin labelled positions within the C-domain in two different environments (in detergent and in lipids) and (ii) the relative increasing or decreasing of the spin label mobility from each BetP mutant in detergent compared to the reconstituted sample.

Due to sample heterogeneity and different rotamers of the spin label side chain, in most cases two or even more correlation time components can be derived from a given EPR spectrum (Guo *et al.*, 2007). In particular, this reorientational motion (correlation time) of the nitroxide radicals arises from different contributions: (i) internal dynamic modes of the side chain, (ii) local protein backbone fluctuations, (iii) interactions with neighbouring side chains, and (iv) conformational changes and rotational diffusion of the entire protein (Beier



and Steinhoff, 2006). Since the latter contribution can be suppressed by simply increasing the viscosity of the protein solution (Timofeev and Tsetlin, 1983), side-chain motions and local backbone fluctuations affect a given EPR mobility spectrum to the greatest extent. The proper incorporation of the BetP variants into *E. coli* liposomes should have a similar effect as to increase the viscosity in soluble protein solutions. In addition, it was expected that the membrane protein would adapt its native and probably more rigid conformation in liposomes compared to the more flexible conformation in detergent that may be reflected in a decreasing spin label mobility.

#### 4.3.1. Lipid effects in BetP-S545C-SL, -E572C-SL and -S589C-SL

Results obtained with the BetP-S545C-SL mutant with the spin label attached to a cysteine residue suggested that this position is in close vicinity to the membrane/protein interface and thus showed a restricted mobility spectrum in both environments, when solubilised in detergent and when reconstituted in *E. coli* lipids. This was indicated by a broad spectral lineshape and two slow rotational correlation time components. The rotational correlation time component  $\tau_1$  of BetP-S545C-SL in detergent reveals a weak immobilization with a value of 3.8ns, whereas the second component  $\tau_2$  (16ns) hints to an intermediate mobility of the respective side chain motion (Figure 52 and Figure 53; Steinhoff, 1990; Beier and Steinhoff, 2006). However, the incorporation in *E. coli* lipids leads to a pronounced decrease in spin label mobility of both spectral components, indicating an intermediate ( $\tau_1 = 15$ ns) or even strong ( $\tau_2 = 52$ ns) spin label immobilization at position 545 after the reconstitution. Thus, reconstitution of BetP-S545C-SL seemed to lead to a tighter package and/or a certain sterical hindrance via lipid shielding or to a partial hinged position of amino acid position 545 that reduces the respective spin label mobility. This result is confirming the suggested (based on topology analysis) position of this amino acid in the protein structure.

Unlike the other two studied cysteine mutants (BetP-S545C-SL, BetP-S589C-SL), BetP-E572C-SL is a deregulated carrier variant. This mutant still shows some low level of constant activity, but it is not able to adapt its maximal uptake rate to the extent of osmotic stress it is exposed to. In this mutant the spin label is attached to a cysteine located in the centre of a putative  $\alpha$ -helix which is assumed to be situated in the middle of the C-terminal domain (Figure 11). When the BetP mutant is reconstituted into lipids, we observed a 1.5 fold increase in the time constant for the fast component ( $\tau_1$ ) with almost no effect of lipid on the slow component ( $\tau_2$ ). Thus, the effect of reconstitution into lipids on the dynamics of the spin label at position 572 is less pronounced than for the label attached to position 545. The comparison of the respective time constants for both single spin labelled reconstituted mutants (BetP-S545C-SL and BetP-E572C-SL) indicated that the mobility of

the spin label at position 572 is much less restricted. The time constants for the fast and slow components of BetP-E572C-SL were about two times lower (=higher spin label mobility) compared to the results from BetP-S545C-SL. This is in agreement with the suggested structure of the C-domain: position 572 is located near the centre of the flexible C-terminal extension. These results indicated (i) a more flexible structure of the C-domain at positions 545 and 572 in the solubilised BetP protein and (ii) a less effect of reconstitution on the structure and spin label mobility at position 572 in the reconstituted BetP sample. Thus, with correlation times of  $\tau_1 = 2.9\text{ns}$  and  $\tau_2 = 9.5\text{ns}$  in *E. coli* lipids, the attached spin label at position 572 showed a weak or intermediate immobilization (Figure 52).

The spectral simulation of BetP-S589C-SL in detergent revealed only one fast correlation time component with  $\tau_1=1.2\text{ns}$ . This hinted to a nearly free reorientational motion of the attached spin label if the protein is solubilised. The incorporation into *E. coli* lipids decreased this fast  $\tau_1$  component nearly twofold ( $1.2\text{ns} \Rightarrow 2.2\text{ns}$ ) and additionally revealed the presence of a second (slow) component  $\tau_2$  with  $10.5\text{ns}$ . Compared to the E572C-SL mutant, this indicated that positions 572 and 589 have a similar overall flexibility after reconstitution. Since both positions showed a pronounced lipid effect that seemed to restrict both spin label mobilities to the same extent, these two parts of the C-terminal extension may exhibit a similar relative orientation, e.g. in parallel to the lipid bilayer and/or protein plane. In addition, the absence of the second (immobile) spectral component in the solubilised BetP-S589C-SL sample may indicate, that the position 589 is more exposed or freely tumbling when the protein is solubilised in detergent. The incorporation into lipids however may lead to pronounced interactions with protein or lipid surroundings that induce sample heterogeneity, e.g. different reorientational dynamics of the nitroxide group for position 589 that expose the second correlation time component. However, it is important to note that the spin label in position 589 is supposed to be located close to the end of the C-domain. Depending on the secondary structure of the C-domain and a suggested perpendicular orientation to the lipid plane, we would expect a distance of about  $40\text{\AA}$  or even more from position 589 to the rigid lipid/protein interface. Thus, no effect of the reconstitution into *E. coli* lipids on the spin label mobility at this terminal position would be expected. This further supports the idea of a relative orientation of the whole C-domain that is parallel or close to the lipid or protein plane in the reconstituted, non-activated BetP transporter.

The preliminary results from the “lipid effects” on the spin label mobility of the three cysteine positions within the C-domain of BetP revealed that all three positions showed a decrease in spin label mobility upon reconstitution into *E. coli* lipids, indicating a more rigid

conformation of the whole C-terminal extension in a lipid environment. However, it was rather unexpected to observe a pronounced mobility restriction for the spin label attached to the terminal end of the C-domain (S589C-SL) after incorporation into lipids. Taking this into account, the 55 amino acid comprising C-terminal domain of the non-activated carrier is not supposed to be freely tumbling in the cytoplasm but rather to stay in the vicinity of the lipid surface (e.g. in parallel to the lipid plain) or of other protein domains that might restrict its degree of freedom. As a result, a shearing movement of the C-terminal domain upon activation might be more reasonable than a free tumbling switch (Figure 47).

To further confirm the observed “lipid effects” for each of the analysed spin label positions within the C-domain of BetP, power saturation measurements would be necessary in future experiments. With this technique the solvent exposure or the relative orientation towards lipid and protein phases of an attached spin label can be estimated. A dimensionless accessibility parameter  $\Pi$  is deduced from the different collision frequencies of the respective spin label with paramagnetic quenchers and allows a separation between the different grades of spin label interactions in a tagged protein sample (Altenbach *et al.*, 1994; Malmberg and Falke, 2005).

#### **4.3.2. Salt induced mobility changes of BetP-S545C-SL, BetP-E572C-SL and BetP-S589C-SL**

Characterization of the mobility profiles of the three single spin labelled BetP variants S545C-SL, E572C-SL and S589C-SL under non-activating conditions (without salt/osmotic stress) in detergent and reconstituted in liposomes was in agreement with the suggested topology model (Figure 17). The next step was to analyse the respective mobility changes of the consecutive spin label positions within the C-domain after a hyperosmotically stimulated carrier activation. This study addressed the question whether the C-terminal extension indeed undergoes conformational changes and/or sterical reorientations during the activation process of the protein. If so, these putative dynamics could lead to a change of interaction partners (surrounding lipid or protein domains) before and after the osmotic upshift and thus allow monitoring osmostress-induced spin label mobility changes in a given EPR spectrum. Due to time restriction, a quantitative analysis of the EPR data from the present salt effect measurements could not yet be conducted (work in progress). Thus, the following discussion will be based on a qualitative interpretation of the spin label mobility derived from the relative spectral broadening or sharpening of the detected EPR lines.

Applying activating amounts of NaCl (660mM) or proline (1M) did not have a pronounced effect on the mobility profile of the spin label attached to position 545 compared to the

untreated sample (Figure 28). Since the amino acid position 545 is supposed to be located in close vicinity to the rigid lipid/protein interface, the respective spin label mobility was not expected to be significantly affected during a putative reorientation of the C-extension upon BetP activation. This result indicated that changes of the protein structure in the vicinity of this spin label position were either very small or not present.

The hyperosmotic BetP-E572C-SL activation by the addition of proline (1M) or glycine betaine (1M) to the external buffer of the respective proteoliposomes had only a small or no effect on the spectral line shape of the spin label at this position. These results are in agreement with the known deregulated activity regulation profile of BetP-E572C-SL if we suggest, that changes in the structure or orientation of the C-domain are necessary for a proper BetP activity regulation (Figure 19). Hence, we did not expect strong structural changes and thus no changes in the spin label mobility at this position in the presence or absence of activating amounts of osmolytes. However, the analogous stimulation with salts (NaCl, KCl, 660mM each) showed some increase in the spin label mobility compared to the untreated sample. This suggested a certain effect of salt on the conformation of at least the central part of the C-domain. It was known from former transport measurements with BetP heterologously expressed in *E. coli* MKH13 cells that salt as hyperosmotic upshift-inducing solute was more potent in activating the BetP carrier and hence led to higher maximal uptake rates than non-ionic solutes (personal communication, S. Morbach and R. Krämer). However, it was unclear if these small effects were related to structural changes within the central part of the C-domain due to BetP activation or due to a salt effect on unbound spin label in the sample. Also, we could not exclude that this increase in spin label mobility occurred due to the presence of leaky liposomes or liposomes with inside-out orientated BetP trimers in the sample (see below and 4.3.3).

In contrast to the experiments with the spin label at position 545 and 572, an osmotic upshift (with both kinds of solutes, ionic and zwitterionic) applied to proteoliposomes with incorporated BetP-S589C-SL were able to induce a pronounced increase of spin label mobility compared to the untreated sample (Figure 30). However, the effect of salts was about 2-3 times stronger than that of the zwitterionic solutes. It has to be noted, that the osmotic strength of both kinds of triggers differed by about 30%, e.g. the buffer supplemented with salt (NaCl, KCl) exhibited a total osmolality of 1.3osmol/kg whereas the osmotic upshift with zwitterionic solutes (GB, proline) was carried out with a total osmolality of 1osmol/kg in the external buffer. Since both values of osmotic strength should be sufficient to fully activate BetP, such pronounced differences in the spin label mobility induced by ionic and zwitterionic solutes were rather surprising. At this point, the presence of an unspecific salt effect was suggested.

We conclude that the SDSL-EPR study of putative salt-induced mobility changes at spin labels attached to three different positions in the C-terminal domain of BetP indicated that a salt and/or osmotic effect is present. This effect(s) is (are) depending on both, (i) the compound used to create the osmotic upshift and (ii) the position of the spin label in the protein structure. Upon the osmotically induced activation of each BetP variant, a higher increase in spin label mobility was detected with a greater distance of the spin label position from the fixed membrane position. In particular, the osmotic upshift resulted in hardly any mobility changes of the spin label attached to position 545, only weak effects on the spin label at position 572 and a strong increase in the spin label mobility at position 589. These changes are indicative of an altered, more flexible conformation at least in the centre (E572C) and at the end of the C-terminal domain (S589C) after a hyperosmotically-induced activation of BetP. It also may indicate a weaker interaction of this protein domain with other domains in the same monomer (and/or with domains in other BetP monomers) as well as a weaker interaction with the surface of the surrounding lipids. These findings are in agreement with the suggested working model for the BetP activation process (Figure 27).

During this study a new question was raised: Why are the salts NaCl and KCl able to induce a greater mobility effect on the respective spin label than the zwitterionic solutes glycine betaine and proline, when used as hyperosmotic upshift-inducing supplements in the external buffer of the proteoliposomes (Figure 33). BetP activation (and thus the suggested C-terminal motions) was thought to be only induced by the increase in the internal  $K^+$  concentration due to the hyperosmotically induced water efflux out of the proteoliposomes (Figure 15, Materials and Methods). Thus, it was rather unexpected, that both kinds of osmolytes with a comparable osmolality of 1osmol/kg (proline, GB) and 1.3osmol/kg (NaCl, KCl) affected the studied protein domain in such a different way. Two possible explanations for this phenomenon may be envisaged; both are related to a direct electrostatic interaction of salt ions with accessible spin labels that might induce a higher mobility effect. Such putative interactions might only occur in the case of (1) different orientations of BetP in the proteoliposomes (e.g. a population of proteoliposomes with a mixture of inside-out and rightside-out orientations) or (2) if a small amount of the proteoliposomes was leaky (see below and Figure 31, Results).

In addition, the slightly higher osmolality and ionic strength (30%) of the salt may exert a direct or indirect influence on the membrane and/or protein conformation because also the internal concentration of  $K^+$  is increasing during the hyperosmotic upshift. Since proteoliposomes behave like ideal osmometers, the changes in the external osmolality are directly proportional to the volume changes during vesicle shrinkage (White *et al.*, 2000).

Thus, the calculated final internal potassium concentrations in the respective BetP-proteoliposomes might be about 550mM applying an external osmotic upshift with 1M of the zwitterionic compounds GB and proline as well as about 700mM using 660mM NaCl or KCl as hyperosmotic stress-inducing agents (Rübenhagen *et al.*, 2001). Taken this into account, a combination of both, a direct electrostatic effect of salt ions on the external side of the proteoliposomes as well as the (indirect) higher osmotic effects (increased cation and potassium concentration) of the salt may be responsible for the above mentioned differences in spin label mobility.

#### **4.3.3. Salt effects on reconstituted BetP variants in the presence of CrOx**

To rule out the possibility that leaky liposomes or liposomes with inside-out orientated BetP protein could facilitate a direct electrostatic interaction of the external salt ions with both charged extensions of the investigated BetP variants (Figure 9), “quenching” amounts of Chromium Oxalate (CrOx, 40-50mM) were exemplarily added to the external buffer of hyperosmotically “shocked” BetP-S589C-SL and BetP-E572C-SL proteoliposomes. Such an experiment allows discriminating between indirectly induced mobility effects (across the liposome membrane) on spin labels within the C-terminal domain of BetP and putatively superimposing mobility effects that might derive from a direct electrostatic salt/C-domain interaction during the hyperosmotic upshift using salt in the external buffer. Due to the fact that the sharp EPR spectra of BetP-S589C-SL and BetP-E572C-SL are much more sensitive to even small mobility effects, these two mutants were chosen for all control experiments concerning the different spin label mobility changes induced by salts and solutes (Figure 23). Since all EPR signals from spin labels in leaky liposomes or in liposomes with inside-out orientated BetP trimers were quenched, the changes in the shape of the EPR spectra of each spin label were related to hyperosmotic stress induced conformational changes within the C-domain of rightside-out orientated carriers.

Upon the addition of CrOx to the external buffer of BetP-S589C-SL proteoliposomes, the relative amplitude of the respective EPR spectra was much smaller compared to the untreated sample (cp. Figure 30 and Figure 33, full spectra). As an important result of this experiment it was shown, that in the presence and absence of CrOx, the spin label mobility changes (monitored by changes of the amplitude of the low field EPR line) still had the same direction for ionic and zwitterionic solutes as hyperosmotic upshift-inducing compounds, i.e. an increase in spin label mobility. However, slight differences were still visible: in both cases (with and without CrOx addition) the amplitude in the spectrum derived from the proteoliposomes treated with zwitterionic solutes (GB, proline) was

smaller. This difference in relative amplitude (salt vs. zwitterionic solute) was significantly reduced upon CrOx addition, which was supposed to be related to the lower osmolality compared to the used salt (see above).

When similar measurements were performed with the spin label at position 572, both, ionic and zwitterionic solutes exerted a similar effect on the respective spin label mobility (Figure 34), but the observed effect was in the opposite direction to the one detected for the spin label at position 589. A small decrease of the respective low field amplitude was detected, which indicated that the mobility of the spin label at position 572 is slightly decreasing, when an osmotic stress is applied. Such an effect on the spectral lineshape can be expected, for example, if the central region of the C-domain moves closer to other protein domains or to the surface of the membrane upon BetP activation. However, when a cysteine is inserted at this particular position, the respective BetP variant loses the ability to be activated by a hyperosmotic upshift. As mentioned above and according to the currently suggested model for BetP activation we did not expect pronounced mobility changes within the C-domain of a deregulated BetP carrier. To circumvent this problem, in future experiments it will be necessary to study another engineered BetP mutant with a cysteine introduction in close vicinity to position 572, which exhibits a wildtype-like activity regulation.

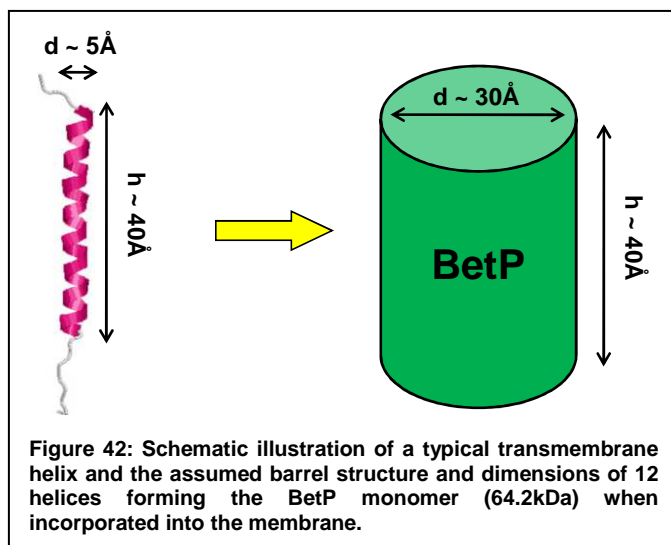
We conclude that the CrOx treatment ensured the presence of a population of intact, salt-impermeable proteoliposomes with correctly incorporated and spin labelled BetP protein. Thus, the detection of changes in the spectral lineshape upon hyperosmotic stress could be related to structural changes in the C-terminal domain of reconstituted BetP or in the close vicinity of this domain leading to sterical restrictions for the attached spin labels. The pronounced effect on the respective spin label mobility of BetP-S589C-SL and BetP-E572C-SL was diminished in the CrOx-treated proteoliposomes. However, a slightly higher mobility for the spin label at position 589 was observed, when the osmotic upshift was induced by salt instead of zwitterionic solutes (Figure 33). This difference can most likely be attributed to a 30% higher total osmolality of the external buffer supplemented with salt. In general, the mobility changes of the spin label at position 589 in the presence of CrOx had the same tendency compared to the changes observed in the absence of the relaxing agent (i.e. higher spin label mobility). In contrast to this, the trend of the respective spin label mobility at position 572 was different with and without the addition of the quenching agent to the external buffer. In the absence of CrOx, a salt-induced osmotic upshift led to a higher spin label mobility, while a zwitterionic-induced upshift had nearly no effect (Figure 29). The addition of CrOx to the external buffer of BetP-E572C-SL proteoliposomes caused a significant decrease in the spin label mobility using both, either

ionic or zwitterionic compounds for the osmotic upshift. It has to be noted, that the extent of the mobility restriction was nearly the same as indicated by the similar amplitude of the respective EPR spectra (Figure 34). The results in the absence of CrOx indicated, that salt seems to directly interact with the C-terminal domain of BetP, leading to a higher spin label mobility at positions in the centre (572) and at the end (589) of the extension. This may be the case, if the high salt concentration (660mM) impairs or even destroys intramolecular salt bridges or other ionic interactions of the C-domain with other protein domains and/or with the surrounding phospholipid headgroups of the membrane (Ressl *et al.*, submitted). However, the used salts for applying the hyperosmotic upshift, could not yet been tested in transport measurements with proteoliposomes. If KCl would be used as a hyperosmotic stress inducing compound, the crucial outwardly directed potassium potential cannot be established during the uptake measurements (electrical gradient). On the other hand, if NaCl would be used, an influence of the co-substrate on the transport process could not be ruled out.

These putative ionic as well as the zwitterionic effects have to be “titrated” in future experiments. Several concentrations (osmotic and ionic strength) of the salts have to be examined for their degree of increasing spin label mobility at a defined position (e.g. S589C). These measurements have to be performed in the absence and presence of CrOx and some other quenching agents (e.g. NiEDDA). In this context, the corresponding osmotic strengths of zwitterionic solutes have to be used for the application of osmotic upshifts and the effects on the respective spin label mobility have to be compared to the results from the salts-induced upshift measurements. A well-defined dependence of the applied solute concentration on the respective spin label mobility in CrOx-“quenched” proteoliposomes should finally be able to define both, (i) an intrinsic potency of salts to induce higher spin label mobility and (ii) a relationship between BetP activity and the respective spin label mobility at selected sites within the C-terminal domain.



#### 4.4. Distance measurements with BetP variants



Beside its catalytic function of glycine betaine import, BetP can autonomously sense its activating stimulus (osmosensor) and adjust its activity to the extent of the triggering osmotic stress (osmoregulator). However, the molecular mechanisms of osmosensing and signal transduction were barely investigated to date. Former studies

on C-terminal truncation and substitution mutants revealed that this domain of the transporter has a crucial function in the osmosensing and osmoregulation process of BetP. The question came up, if particular structural changes within the C-domain and/or dynamical interactions between the C-domain and surrounding lipid or protein domains might be responsible for a proper stimulus sensing and/or signal transduction.

The preliminary DEER studies in this work focused on the elucidation of the structural properties of the non-activated BetP carrier. For this purpose, the intermolecular distances between single spin labelled BetP monomers should allow the discrimination of multiple distance distributions detected in double or triple spin labelled cysteine mutants in the present work and for future SDSL-DEER investigations on BetP. Thus, the studies were split in two parts: (1) the detection of distances within single spin labelled BetP variants to derive intermolecular and/or intramolecular spin-spin interactions as “standard”-distances, and (2) a study on the influence of a proline introduction at position 550 on the distance between two strategically introduced cysteines at the beginning (position 545) and close to the end (position 589) of the C-terminal domain in a double (BetP-S545C/S589C-SL) and triple (BetP-S545C/Y550P/S589C-SL) mutant. The proline introduction was known to render the corresponding BetP variant deregulated, i.e. permanently active but insensitive to its activating stimulus. This triple mutant (BetP-S545C/Y550P/S589C-SL) thus exhibits a (permanently) active conformation and/or orientation of the C-domain that should be studied and quantified by DEER analysis.

For all following structural analysis of the BetP protein it will be assumed that the 12 transmembrane helices of a single monomer are arranged like a barrel in the membrane leading to a mean diameter of about 30 Å (Figure 42). In addition, the results from the continuous wave EPR measurements concerning the lipid- and salt/solute-induced effects on the respective spin label mobility within the C-domain suggested rather a shearing

degree of freedom close to other protein domains and/or the lipid membrane plane for the whole C-terminal extension. Furthermore it was already proven, that BetP is forming a homo-trimer in detergent and upon reconstitution into *E. coli* lipids (Ziegler et al., 2004; Ressler et al., submitted).

#### 4.4.1. BetP-S545C-SL

Four independent pulsed EPR measurements with the corresponding DEER analysis of BetP-S545C-SL reconstituted in *E. coli* lipids confirmed that the mean distance between the individual 545 positions within a reconstituted BetP trimer is about  $30 \pm 5 \text{ \AA}$ . According to the suggested barrel structure of one BetP monomer (Figure 42), the known trimeric state in *E. coli* lipids (Ziegler et al, 2004) as well as the determined spin-spin distance of about  $30 \text{ \AA}$ , the beginning of the C-terminal domain of each monomer within the trimer is most likely orientated inwardly, i.e. the amino acid positions 545 are facing the interfaces of each adjacent monomer (Figure 43).

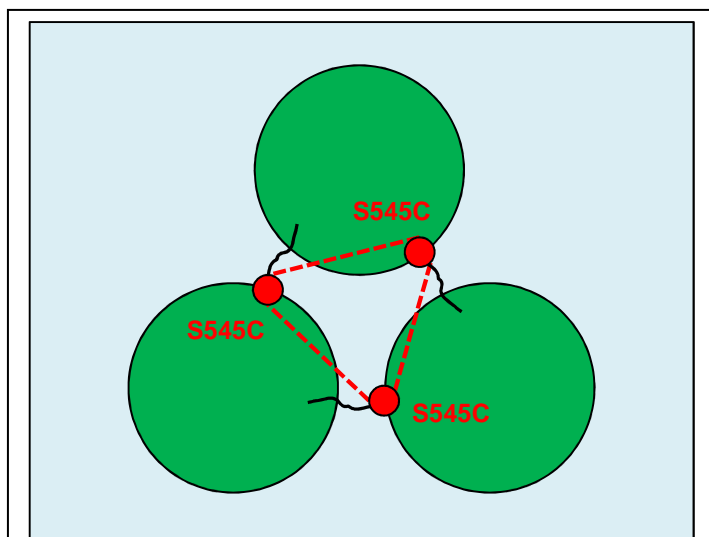


**Figure 43: Schematic illustration of three single BetP monomers forming the functional trimer in the liposomal membrane.** The suggested intermolecular spin-spin distance between the S545C-SL positions (red circles) is depicted as red-dotted line. The beginning of each C-domain is shown as a black line.

SDSL-DEER thus confirmed that BetP is in an oligomeric state (e.g. trimer) when it is reconstituted in liposomes. In addition, the results of the DEER study for BetP-S545C-SL in detergent revealed a mean S545C-SL  $\leftrightarrow$  S545C-SL distance of  $29 \pm 5 \text{ \AA}$  (Figure 37). This distance is in line with the respective results from the reconstituted mutant (Figure 36). The detection of spin-spin interactions in this sample

indicated that BetP is also forming oligomers when it is solubilised in detergent. It is important to note, that the inward orientation of the position 545 in each C-domain is also conserved in the detergent samples. Thus, an oligomeric state of BetP-S545C-SL could be shown with the same sample in detergent and functionally reconstituted in *E. coli* lipids as confirmed by subsequent transport measurements (Figure 19).

#### 4.4.2. BetP-E572C-SL

The respective distance measurements with BetP-E572C-SL reconstituted in *E. coli* lipids revealed a mean spin-spin distance of  $40 \pm 8 \text{ \AA}$ . It has to be taken in to account that the E572C position is situated in the middle of a putative  $\alpha$ -helical stretch. According to the respective crystal structure of BetP, this stretch is supposed to form a rigid cylindrical secondary structure element ( $\alpha$ -helix) which is not bendable (Ressl *et al.*, submitted).

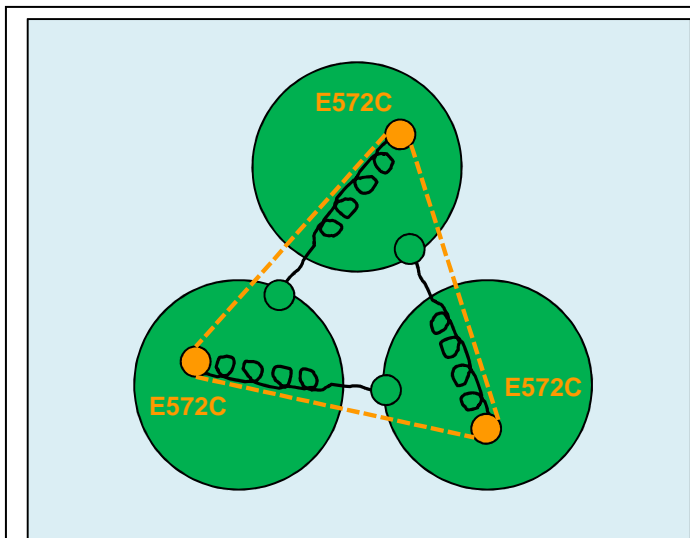


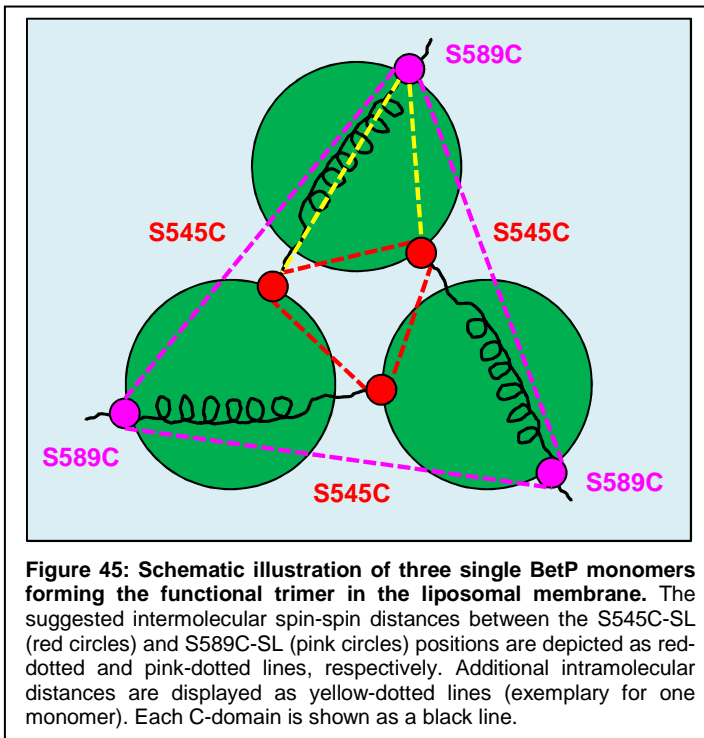
**Figure 44: Schematic illustration of three single BetP monomers forming the functional trimer in the liposomal membrane.** The suggested intermolecular spin-spin distance between the E572C-SL positions (orange circles) is depicted as orange-dotted line. Each partly displayed C-domain is shown as a black line.

Thus, this intermolecular distance could be achieved, if each C-terminal domain of one monomer would somehow overlie the adjacent BetP monomer (Figure 44). If they were sticking out to the surrounding lipids or folded over the same monomer, the E572C-SL  $\leftrightarrow$  E572C-SL distance would be much greater (approximately  $60\text{-}80 \text{ \AA}$ , Figure 47). However, the determined distance could also be obtained, if the C-domains would be

orientated perpendicular to the membrane (Figure 47, model D). According to the results from the continuous wave EPR measurements in this work (see above), the current hypothesis about the C-terminal dynamics during the activation process of BetP (Ressl *et al.*, submitted) as well as the determined distance by DEER analysis of BetP-E572C-SL, Figure 44 displays the suggested “adjacent overlies” orientation of the C-terminal extension (Figure 47). This model is already adjusted to the previous results with BetP-S545C-SL and thus represents a successive refinement of the suggested relative C-domain orientation in the BetP trimer.

#### 4.4.3. BetP-S545C/S589C-SL

Unfortunately the respective DEER analysis from the BetP-S589C-SL single mutant did not lead to any significant signal resolution and hence distance distributions. However, the used  $d_2$ -time of 1800ns (Table 9, Appendix) suggests an intermolecular spin-spin distance of at least  $45 \text{ \AA}$  or more. Future experiments with a higher labelling efficiency will reveal this distance, if the distance between the spin labelled 589 positions within a non-activated BetP trimer are generally accessible within the range of the detection limits of pulsed EPR spectroscopy.



The respective analysis of the double mutant BetP-S545C/S589C-SL revealed two distinct distances of  $32\pm 6\text{\AA}$  and  $47\pm 5\text{\AA}$ . Due to the fact, that we could not determine a distinct intermolecular distance between the single spin labelled 589 positions in a BetP trimer (Figure 39), it was difficult to accurately assign the measured distances to an intra- or an intermolecular spin-spin coupling in this double mutant. However, the calculated shorter distance of about  $32\pm 6\text{\AA}$

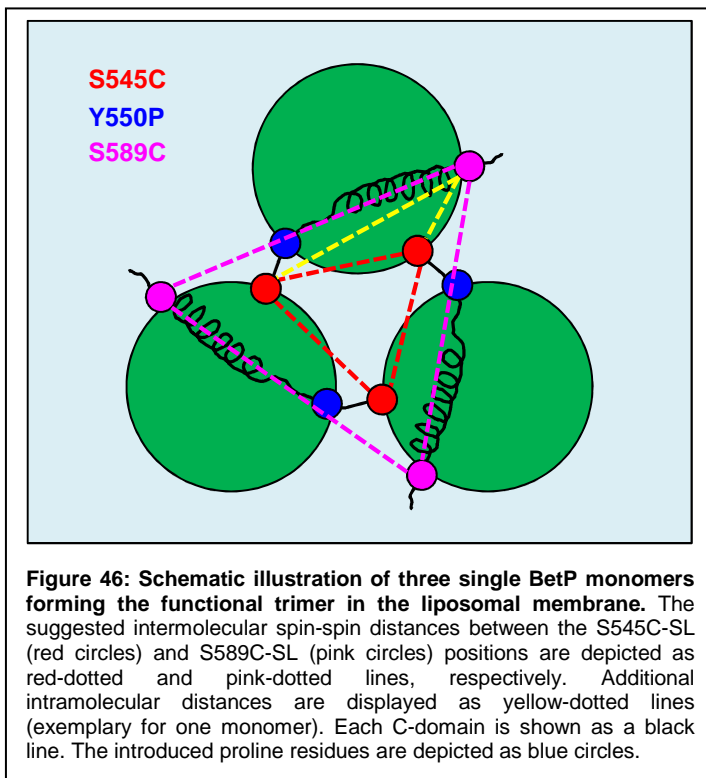
(Figure 40) fits well to the already determined intermolecular S545C-SL  $\leftrightarrow$  S545C-SL interactions (Figure 36,  $30\pm 5\text{\AA}$ ). Thus, the second distance of about  $47\pm 5\text{\AA}$  (Figure 40) may in principle represent three different interactions: (i) an intermolecular S589C-SL  $\leftrightarrow$  S589C-SL interaction, (ii) an intramolecular S545C-SL  $\leftrightarrow$  S589C-SL interaction or (iii) an intermolecular S589C-SL  $\leftrightarrow$  S545C-SL interaction (Figure 45).

However, based on the suggested “adjacent-overlie” model (see above), an intermolecular S589C-SL  $\leftrightarrow$  S589C-SL distance would be greater than about  $60\text{\AA}$  and thus hardly detectable by pulsed EPR spectroscopy (Figure 45, pink-dotted line). On the other hand, the suggested rigid  $\alpha$ -helical stretch of about 32-34 amino acids would separate the intramolecular positions 545 and 589 by a distance of at least  $50\text{\AA}$  (right-handed helical structure with 3.6 residues per turn and a corresponding translation of  $1.5\text{\AA}$ ) plus 10 amino acids in extended or coil form. So this distance as well as the intermolecular S589C-SL  $\leftrightarrow$  S545C-SL interactions will be reasonable candidates for the second distance determined in the double mutant (Figure 45, yellow-dotted lines).

In general, large distances between two spin labels in a protein domain under study have to be partitioned in smaller distance segments by the introduction of an intermediate spin label to obtain a suitable triple cysteine mutant (e.g. BetP-S545C/R574C/R589C-SL). Such a segmental analysis of the distances within the C-terminal domain can then be summarized and compared with the intermolecular distances in the corresponding single spin labelled mutants (e.g. BetP-S545C-SL, BetP-R574C-SL and BetP-S589C-SL), to clearly separate putative dipole-dipole couplings between adjacent BetP monomers.

#### 4.4.4. BetP-S545C/Y550P/S589C-SL

Similar to the respective single proline mutant (BetP-Y550P), the introduction of a proline at position 550 within the double mutant BetP-S545C/S589C renders the transporter permanently active (Nicklisch, 2005; Schiller *et al.*, 2006). This BetP-S545C/Y550P/S589C-SL triple mutant is thus unable to respond to a higher external osmolality with an increased uptake rate (Nicklisch, 2005). It was suggested, that the introduction of a proline at the beginning of the C-domain (amino acid position 550) might alter its whole conformation and/or relative orientation towards the surrounding protein or lipid domains. A comparison of the intramolecular S545C-SL  $\leftrightarrow$  S589C-SL distance in the double and triple mutant enabled us to make a statement on relative movements or conformational changes of the C-terminal domain after the introduction of the proline.



The respective DEER analysis of BetP-S545C/Y550P/S589C-SL revealed three distances of  $44 \pm 3 \text{ \AA}$ ,  $30 \pm 5 \text{ \AA}$  and of  $26 \pm \text{ \AA}$ . The  $30 \text{ \AA}$  distance strongly points at the already determined intermolecular S545C-SL  $\leftrightarrow$  S545C-SL distance (Figure 43). The detected spin-spin interactions in the range of about  $44 \text{ \AA}$  were slightly shorter than the large distance observed in the double mutant BetP-S545C/S589C-SL ( $47 \text{ \AA}$ , Figure 45). This may result from two different sterical alterations: the

introduction of the proline may lead to a kink within the C-domain that (i) brings the C-terminal ends in a BetP trimer in close vicinity to each other, resulting in a shorter intermolecular S589C  $\leftrightarrow$  S589C distance of about  $44 \text{ \AA}$  or in contrary (ii) tears them far apart (where a intermolecular S589C  $\leftrightarrow$  S589C distance would be beyond the detection limit) to reveal a certain intramolecular S545C  $\leftrightarrow$  S589C distance of about  $44 \text{ \AA}$  (Figure 46, long yellow-dotted line). Interestingly, a third distance was observed in the sample with a mean value of about  $26 \text{ \AA}$  (Figure 41). Taken this into account, the latter assumption seems to be more likely if the third distance may derive from additional intermolecular S589C-SL  $\leftrightarrow$  S545C-SL spin-spin interactions (Figure 46, short yellow-dotted line). Currently, i.e. with the present signal/noise ratio, we cannot exclude that the shortest

distance (26Å) is the intramolecular distance between the spin labels at positions 545 and 589, since some indication of a similar distance is also visible in Figure 40 (asymmetric peak shape at about 32Å). An additional possible combination of spin labelled interaction partners in the investigated triple mutant would be the following: (i) the S545C↔S589C distance within the C-domain of the same monomer is 26Å, (ii) the intermolecular S545C↔S545C distance is 30Å and (iii) the additional distance of 44Å represents either a S545C↔S589C or a S589C↔S589C spin-spin interaction, both from different monomers in the trimer (Figure 46).

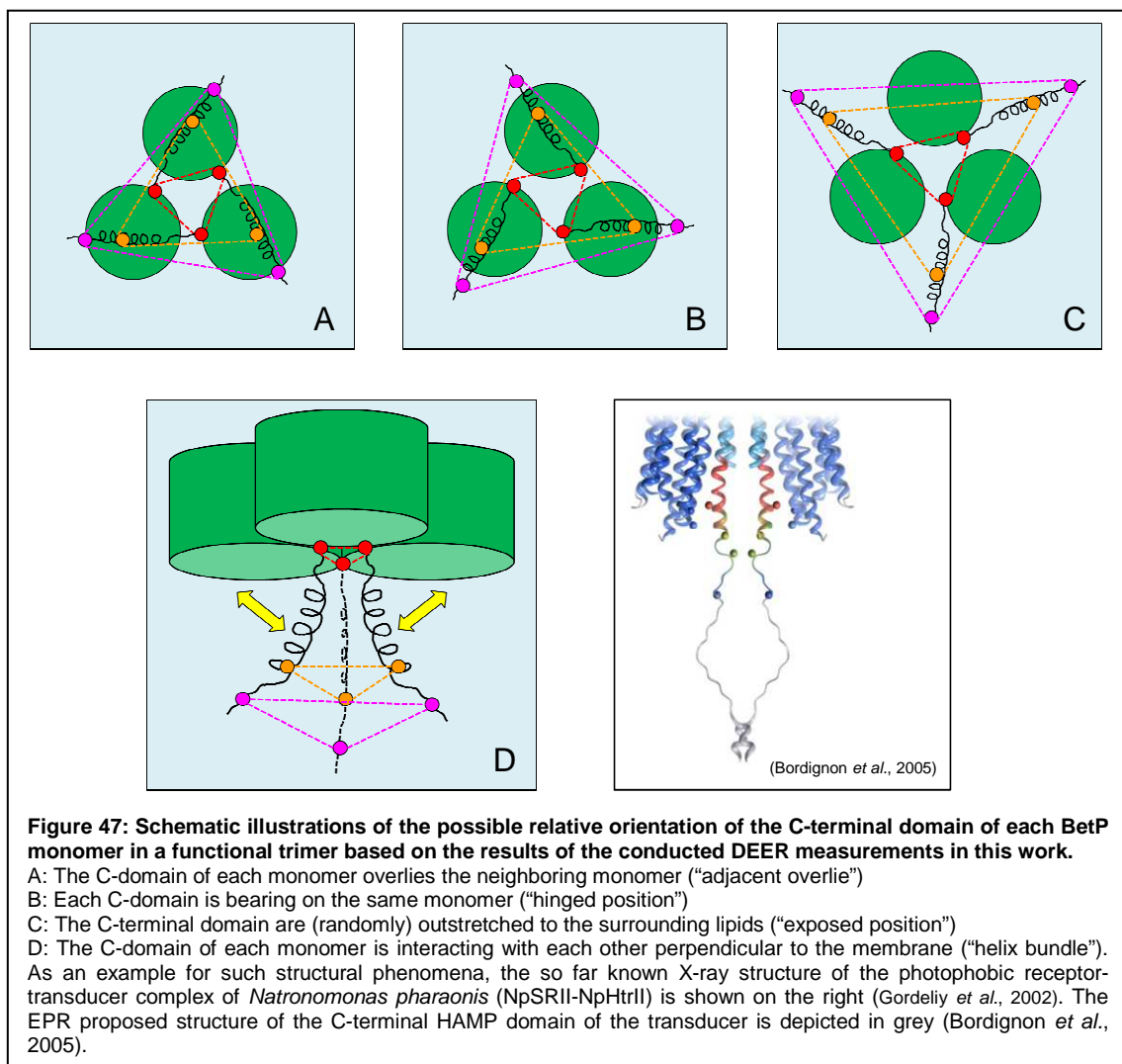
To further support the considerations on the conformation of the C-terminal domain and the relative orientation towards the adjacent monomer, the above mentioned consecutive analysis of spin label mobility within the C-domain is required and also further coordination points for spin labels have to be considered. In addition, except for the BetP-S545C-SL mutant, the other distance measurements need additional confirmation. Subsequently, the distances have to be determined in the activated carrier proteins and compared to the results from the same non-activated BetP mutants to gain further information about the extent and direction of C-domain movements during the activation process.

**Table 8: Summary of the computed spin-spin distances of the DEER EPR analysis (DEERAnalysis2006, Jeschke, 2006) on spin labelled BetP variants reconstituted in *E. coli* lipids (proteoliposomes).**

BetP variant	Mean distance r	Standard deviation $\sigma$
	[Å]	[Å]
S545C-SL	30	5
S545C-SL-detergent	29	5
E572C-SL	40	8
S589C-SL	n.d.	n.d.
S545C/S589C-SL	32	6
	47	5
S545C/Y550P/S589C-SL	26	4
	30	5
	44	3

Based on the results from the cw- and pulsed EPR studies carried out in this work, in principle a choice of possible “working” models for the relative orientation of the C-terminal domain within a functional BetP trimer can be outlined (Figure 47):

(A) the C-domain of each monomer is overlapping the neighbouring monomer (“adjacent overlies”), (B) the C-extension is positioned on the same monomer (“hinged position”), (C) the C-terminal part of each BetP monomer is randomly extended to the surrounding lipid plane (“exposed position”) or (D) the cytoplasmic C-domains in a putative BetP trimer arrange as loosely interacting helix bundles (“helix bundle”) in analogy to the rod-shaped cytoplasmic domains of the NpHtrII transducer from *Natronomonas pharaonis* (Figure 47, lower right; Bordignon *et al.*, 2005) or the chemoreceptors Tsr and Tar from *E. coli* (Kim *et al.*, 1999).



However, with regard to the determined intermolecular E572C ↔ E572C distance of about 40 Å in the respective single cysteine variant, the “exposed” model (Figure 47C; Table 8) seems rather unlikely. If all three C-extensions in a trimer would be equally outwardly directed (perpendicular to the trimer centre, but in parallel to the lipid plane) the distances

between the spin labelled positions 572 of each monomer would be greater than 50-60Å and thus not detectable in the described EPR experiment ( $d_2=1400$ ns, corresponding to maximal detectable distance  $\sim 42$ Å, Table 9). In addition, if a randomly exposed orientation would be correct, the detected E572C $\leftrightarrow$ E572C distance would be much more distributed (i.e. isotropic; Jeschke and Polyhach, 2007).

Concerning the other three proposed models (Figure 47A, B, D) no clear discrimination can yet be made on the basis of the results from the mobility and distance measurements in this work. However, recent results from the crystallized BetP trimer strongly supports the idea of an “adjacent overlie” model (Ressl *et al.*, submitted). It was shown, that at least the C-terminal domain of one monomer is interacting with the cytoplasmic surface of the adjacent monomer in the respective crystal. Also, this model predicts a shearing degree of freedom rather than a tumbling flexibility for the C-terminal domain of the BetP transporter which is in line with the measured mobility changes during the hyperosmotic upshift studies in this work (see above).

## 4.5. Future aspects

Publication of the BetP crystal structure will provide the best basis for the construction of new cysteine mutants of the carrier that are suitable to refine the general structural properties and intramolecular dynamics during the activation process.

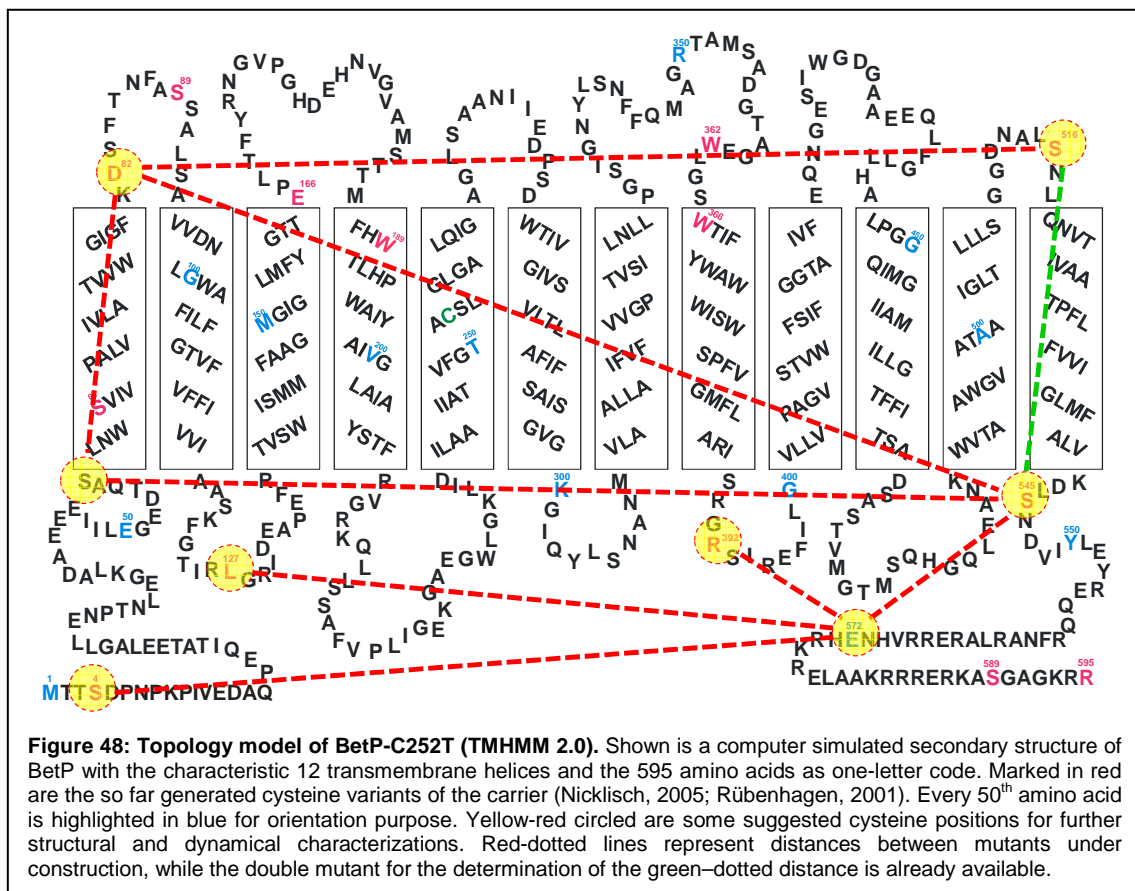
With regard to the salt induced mobility changes, new mutants within the C-terminal domain have to be engineered and tested for functionality, spin label efficiency and finally for their changes in spin label mobility upon a hyperosmotic BetP activation (Figure 48; e.g. S545C/E572C, D82C/E572C, S4C/E572C, others). For this purpose, a set of EPR techniques is available to probe (i) the accessibility to paramagnetic quenchers and thus the solvent exposure of a spin labelled position, (ii) the local mobility profile of the spin label side chain, and (iii) a polarity profile of the direct environment (Biswas *et al.*, 2001; Malmberg and Falke, 2005; Hustedt and Beth, 1999). The combination of these techniques should allow clear statements on the relative movement of the whole C-domain during the activation process of the transporter.

Concerning the distance measurements, new single, double or even triple cysteine mutants will be constructed along the C-domain as well as at strategic positions within the neighbouring protein areas (e.g. the cytoplasmic exposed loops, N-terminal domain, etc.). Mutants with substitutions of fixed amino acid positions close to the membrane (Figure 48, S545C, S57C = not yet constructed, D82C, S516C), within the internal loops (e.g. L127C, R392C) or in the N-terminal domain (e.g. S4C, others) in combination with a second introduced cysteine position in the C-domain (e.g. E572C, Figure 48) will allow a more detailed analysis of the relative distances changes and thus of the C-terminal motions



within the trimer upon BetP activation. For structural analysis, also transmembrane distances of introduced cysteine residues close to the membrane/protein interface will be determined (e.g. S516C/S545C, S57C/D82C = not yet constructed). Finally, the introduction of spin labels close to the suggested substrate binding site and/or transport tunnel (TM IV and TM VIII; Ressler *et al.*, submitted; Vinothkumar *et al.*, 2006; e.g. W362C, W366C, W362C/W366C, kindly obtained from Jonna Hakulinen, group of Dr. C. Ziegler, MPI Frankfurt) will allow a time-resolved analysis of the substrate and co-substrate binding and/or transport process through the carrier (Wegener *et al.*, 2000; Jeschke *et al.*, 2004).

In general, a direct interaction of the C-domain with the surrounding protein domains and/or membrane lipids can be investigated by both, (i) spin-spin interactions from two or more spin labels introduced at suggested interacting sites in the protein or (ii) by a comparison of the mobility spectrum from a distinct spin labelled cysteine position within the C-domain of BetP with the respective spectrum of a BetP mutant with the same cysteine introduction, but varying additional properties like truncations (e.g. N-terminal domain, protein loops), a different lipid composition in the proteoliposomes and/or amino acid substitutions at putative interacting sides.



## 5. Summary

The putative intra- and intermolecular protein dynamics during the activation process as well as general structural properties of the secondary carrier BetP from *Corynebacterium glutamicum* were studied in this work. Previous work indicated that the integrity, conformation, and/or relative orientation of the C-terminal domain of BetP are crucial for a correct stimulus sensing and/or signal transduction during the activation process. The structural properties in the immediate environment of three strategically introduced cysteine residues at the beginning (S545C), in the centre (E572C) and close to the end (S589C) of the C-domain were analysed by EPR spectroscopy under activating (using continuous wave (cw-) EPR) and non-activating (using cw- and pulsed EPR) conditions. The investigation of the activity regulation revealed that all mutants were active in proteoliposomes and showed the expected regulation behaviour. A wildtype-like activity regulation was observed in the case of BetP-S545C-SL and BetP-S589C-SL, whereas BetP-E572C-SL showed a constant uptake rate independent of the applied hyperosmotic stress. The establishment and optimization of a new reconstitution assay for the BetP protein led to a 6-7-fold higher yield of in *E. coli* lipids incorporated spin labelled BetP compared to the conventional method. It furthermore revealed a pronounced adsorption of BetP to the Bio-Beads during reconstitution with a strong involvement of the charged C-domain. The SDSL(Site-Directed Spin Labelling)-EPR studies on the selected single cysteine mutants within the C-terminal domain of BetP showed higher spin label mobility with increasing distance to the lipid/protein interface. Significant differences in the spin label mobility at all three positions were observed when solubilised BetP protein was reconstituted into *E. coli* lipids. This indicated that the structure/conformation of the C-terminal domain of BetP depends on its direct surrounding. Only weak changes in the shape of the respective EPR spectra were observed for spin labels attached to positions 545 and 572, but a significant increase in the spin label mobility at position 589 upon a hyperosmotically-induced BetP activation. This increase in the spin label mobility could be a first indication of structural and/or conformational changes close to the end of the C-terminal domain induced by the activation of BetP.

Preliminary distance measurements were carried out using SDSL-DEER (Double Electron-Electron Resonance) spectroscopy. The results of these measurements showed that: (1) an intermolecular distance of about 30Å was obtained for spin-spin interactions within single spin labelled BetP-S545C-SL. This result confirmed that BetP is forming an oligomer (most probably a trimer) in the lipid environment and thus in its functional state; (2) when similar measurements were performed for this sample in detergent we obtained nearly the same distance between the spin labelled positions 545. These results

confirmed that the global structure of BetP is virtually the same in both environments, reconstituted in lipids or solubilised in detergent. Due to poor signal/noise ratios, the other distance measurements indicated, that the distance between spin labels at position 589 is around or above 50Å, while the spin-spin interactions within the single spin labelled BetP-E572C-SL mutant revealed a distance of about 40Å. Further work is in progress to confirm these results. When the double spin labelled BetP-S545C/S589C-SL mutant was studied, two distance peaks were derived from the detected signal. While the shorter distance could be assigned to the intramolecular S545C⇔S545C distance, the additional signal could be attributed to an intramolecular S545C⇔S589C interaction. When the deregulated triple mutant BetP-S545C/Y550P/S589C was analysed, a difference in the two mentioned distances was observed compared to the double mutant. It was suggested that the proline introduction at position 550 had an effect on the structure and/or orientation of the C-domain.

The results described in this work are in agreement with the current hypothesis of BetP activation and with yet unpublished data of the crystal structure of the carrier.

---

## 6. References

- Abe, S., Takayama, K., and Kinoshita, S. (1967).** Taxonomical studies on glutamic acid-producing bacteria, *J. Gen. Appl. Microbiol.* 13, 279-301.
- Allaby, M. (1994).** The Concise Oxford Dictionary of ecology, New York: Oxford University Press.
- Altenbach, C., Flitsch, S. L., Khorana H.G., and Hubbell, W. L.: (1989).** Structural studies on transmembrane proteins. 2. Spin labelling of bacteriorhodopsin mutants at unique cysteines, *Biochemistry* 28, 7806-7812.
- Altenbach, C., Greenhalgh, D.A., Khorana, H.G., and Hubbell, W.L. (1994).** A collision gradient method to determine the immersion depth of nitroxides in lipid bilayers: application to spin-labelled mutants of bacteriorhodopsin, *Proc. Natl. Acad. Sci. USA* 91(5), 1667-1671.
- Anishkin, A. and Kung, C. (2005).** Microbial mechanosensation, *Curr. Opin. Neurobiol.* 15(4), 397-405.
- Ankri, S., Serebrijski, I., Reyes, O., and Leblon, G. (1996).** Mutations in the *Corynebacterium glutamicum* proline biosynthesis pathway: a natural bypass of the proA step, *J. Bacteriol.* 178, 4412-4419.
- Arakawa, T. and Timasheff, S. N. (1985).** The stabilization of proteins by osmolytes, *Biophys. J.* 47, 411-414.
- Bakker, E. P. (1993).** K<sup>+</sup> Transport Systems: Cell K<sup>+</sup> and K<sup>+</sup> Transport Systems in Prokaryotes, in: *Alkali Cation Transport Systems in Prokaryotes* (Bakker, E. P., Herausgeber), CRC Press, 205-224.
- Ballal, A, Basu, B., and Apte, S.K. (2007).** The Kdp-ATPase system and its regulation, *J. Biosci.* 32(3), 559-568.
- Banaszak, L. (2000).** Foundations of Structural Biology, Academic Press, San Diego, CA.
- Becker, M. (2007).** Untersuchungen zum Kaliumtransport in *Corynebacterium glutamicum*, diploma thesis, University of Cologne.
- Beier, C. and Steinhoff, H.J. (2006).** A structure-based simulation approach for electron paramagnetic resonance spectra using molecular and stochastic dynamics simulations, *Biophys. J.* 91(7), 2647-2664.
- Berliner, L. J. (1976).** **Spin Labelling. Theory and applications**, An international series of monographs and textbooks, Molecular Biology.
- Berrier, C., Coulombe, A., Szabo, I., Zoratti, M., and Ghazi, A. (1992).** Gadolinium ion inhibits loss of metabolites induced by osmotic shock and large stretch-activated channels in bacteria, *Eur. J. Biochem.* 206, 559-565.
- Berrier, C., Besnard, M., Ajouz, B., Coulombe, A., and Ghazi, A. (1996).** Multiple mechanosensitive ion channels from *Escherichia coli*, activated at different thresholds of applied pressure, *J. Membr. Biol.* 151, 175-187.

- Bezanilla, F. and Perozo, E. (2002).** Structural biology. Force and voltage sensors in one structure, *Science* 298(5598), 1562-1563.
- Biemans-Oldehinkel, E., Doeven, M.K., and Poolman, B. (2006).** ABC transporter architecture and regulatory roles of accessory domains, *FEBS Lett.* 580(4), 1023-1035.
- Birnboim, H.C. and Doly, J. (1979).** A rapid alkaline extraction procedure for screening recombinant plasmid DNA, *Nucleic Acids Res.* 7, 1513-1523.
- Biswas, R., Kühne, H., Brudvig, G.W., and Gopalan, V. (2001).** Use of EPR spectroscopy to study macromolecular structure and function, *Sci. Prog.* 84(Pt 1), 45-67.
- Booth, I. R. and Louis, P. (1999).** Managing hypoosmotic stress: aquaporins and mechanosensitive channels in *Escherichia coli*, *Curr. Opin. Microbiol.* 2, 166-169.
- Bordignon, E., Klare, J.P., Doebber, M., Wegener, A.A., Martell, S., Engelhard, M., and Steinhoff, H.J. (2005).** Structural analysis of a HAMP domain: the linker region of the phototransducer in complex with sensory rhodopsin II, *J. Biol. Chem.* 280(46), 38767-38775.
- Borovykh, I.V., Ceola, S., Gajula, P., Gast, P., Steinhoff, H.J., and Huber, M. (2006).** Distance between a native cofactor and a spin label in the reaction centre of *Rhodobacter sphaeroides* by a two-frequency pulsed electron paramagnetic resonance method and molecular dynamics simulations, *J. Magn. Reson.* 180(2), 178-185.
- Botzenhardt, J., Morbach, S., and Krämer, R. (2004).** Activity regulation of the betaine transporter BetP of *Corynebacterium glutamicum* in response to osmotic compensation, *Biochem. Biophys. Acta* 1667, 229-240.
- Bovell, C. R., Packer, L., and Hergerson, R. (1963).** Permeability of *Escherichia coli* to organic compounds and inorganic salts measured by light scattering, *Biochem. Biophys. Acta* 75, 257-266.
- Bradford, M.M. (1976).** A rapid and sensitive method for the quantitation of microgram quantities of protein utilizing the principle of protein-dye binding, *Anal. Biochem.* 72, 248-254.
- Bremer, E. and Krämer, R. (2000).** Coping with osmotic challenges: Osmoregulation through accumulation and release of compatible solutes in bacteria, in: *Bacterial Stress Responses* (Storz, G. and Hengge-Aronis, R., Herausgeber), ASM Press, Washington, D.C., USA, 77-97.
- Brown, J.R. (1975).** Structure of Bovine serum albumin, *Fed. Proc.* 34, 591.
- Burger, U. (2002).** Structure- und Funktionsanalysen am osmotisch regulierten Transporter BetP aus *Corynebacterium glutamicum*, dissertation, University of Cologne.
- Burr, M. and Koshland, D.E. Jr. (1964).** Use of "reporter groups" in structure-function studies of proteins, *Proc. Natl. Acad. Sci. USA* 52, 1017-1024.
- Cayley, S., Lewis, B.A., Guttman, H.J., and Record, M.T. Jr. (1991).** Characterization of the cytoplasm of *Escherichia coli* K-12 as a function of external osmolarity. Implications for protein-DNA interactions *in vivo*, *J. Mol. Biol.* 222(2), 281-300.

- Chang, G., Spencer, R.H., Lee, A.T., Barclay, M.T., and Rees, D.C. (1998).** Structure of the MscL homolog from *Mycobacterium tuberculosis*: a gated mechanosensitive ion channel, *Science* 282(5397), 2220-2226.
- Cairney, J., Booth, I.R., and Higgins, C.F. (1985a).** *Salmonella typhimurium proP* gene encodes a transport system for the osmoprotectant betaine, *J. Bacteriol.* 164(3), 1218-1223.
- Carpita, N. C. (1985).** Tensile strength of cell walls of living cells, *Plant Physiol.* 79, 485-488.
- Chater, K. F. and H. Nikaido (1999).** Cell regulation. Maintaining integrity and efficiency in microbial cells, *Curr. Opin. Microbiol.* 2,121-125.
- Chung, C. T., Niemela, S. L., and Mill, R. H. (1989).** One-step preparation of competent *Escherichia coli*: Transformation and storage of bacterial cells in the same solution, *Proc. Natl. Acad. Sci. USA* 86, 2172-2175.
- Cosgrove, D. J. (2000).** Der Wasserhaushalt der pflanzlichen Zellen, in *Physiologie der Pflanzen* (Taiz, L. and Zeiger, E., Herausgeber), Spektrum, Heidelberg, 60-100.
- Csonka, L. N. (1989).** Physiological and genetic responses of bacteria to osmotic stress. *Microbiol. Rev.* 53, 121-147.
- Csonka, L. N. and Epstein, W. (1996).** Osmoregulation, in *Escherichia coli and Salmonella, cellular and molecular biology* (Neidhardt, F.C., Herausgeber), ASM PRESS, Washington D.C..
- Culham, E. E., Lasby, B., Marangoni, A. G., Milner, L. J., Steer, A. B., van Nues, R. W., and Wood. J. M. (1993).** Isolation and sequencing of *Escherichia coli* gene *proP* reveals unusual structural features of the osmoregulatory proline/betaine transporter ProP, *J. Mol. Biol.* 229, 268-276.
- Culham, D.E., Tripet, B., Racher, K.I., Voegele, R.T., Hodges, R.S., and Wood, J.M. (2000).** The role of the carboxyl terminal alpha-helical coiled-coil domain in osmosensing by transporter ProP of *Escherichia coli*, *J. Mol. Recognit.* 13(5), 309-322.
- Culham, D.E., Henderson, J., Crane, R.A., and Wood, J.M. (2003).** Osmosensor ProP of *Escherichia coli* responds to the concentration, chemistry, and molecular size of osmolytes in the proteoliposome lumen, *Biochemistry* 42(2), 410-420.
- Daffé, M. and Draper, P. (1998).** The envelope layers of mycobacteria with reference to their pathogenicity, *Adv. Microb. Physiol.* 39, 131-203.
- Daffé, M. (2005).** The cell envelope of *Corynebacteria*. *Handbook of Corynebacterium glutamicum*, 121-148. (Eggeling L., Bott, M., Editors) CRC press, Boca Raton, USA.
- Desmond, C., Fitzgerald, G. F., Stanton, C., and Ross R. P. (2004).** Improved stress tolerance of GroESL-overproducing *Lactococcus lactis* and probiotic *Lactobacillus paracasei* NFBC 338, *Appl. Environ. Microbiol.* 70(10), 5929-5936.
- Dinnbier, U., Limpinsel, E., Schmidt, R., and Bakker, E. P. (1988).** Transient accumulation of potassium glutamate and its replacement by trehalose during adaptation of growing cells of *Escherichia coli* K-12 to elevated sodium chloride concentrations, *Arch. Microbiol.* 150, 348-357.

- Eaton, G.R. (1993).** A new EPR methodology for the study of biological systems. *Biophys. J.* 64(5), 1373-1374.
- Ebbighausen, H., Weil, B., and Krämer, R. (1991).** Na(+)-dependent succinate uptake in *Corynebacterium glutamicum*, *FEMS Microbiol. Lett.* 61(1), 61-65.
- Eichler, K., Bourgis, F., Buchet, A., Kleber, H. P., and Mandrand-Berthelot, M. A. (1994).** Molecular characterization of the *cai* operon necessary for carnitine metabolism in *Escherichia coli*, *Mol. Microbiol.* 13, 775-786.
- Farahbakhsh, Z. T., Huang, Q. L., Ding, L. L., Altenbach, C., Steinhoff, H. J., Horwitz, J., and Hubbell, W. L. (1995).** Interaction of alphacrystallin with spin-labelled peptides, *Biochemistry* 34, 509–516.
- Farwick, M., Siewe, R. M., and Krämer, R. (1995).** Glycine betaine uptake after hyperosmotic shift in *Corynebacterium glutamicum*, *J. Bacteriol.* 177, 4690-4695.
- Freed, J. H. (1976).** Theory of slow tumbling ESR spectra for nitroxides. In *Spin Labelling: Theory and Applications*. L. J. Berliner, editor. Academic Press, New York, 53–132.
- Frings, E., Kunte, H.J., and Galinski, E.A. (1993).** Compatible solutes in representatives of the genera *Brevibacterium* and *Corynebacterium* - occurrence of tetrahydropyrimidines and glutamine, *FEMS Microbiol. Lett.* 109, 25-32.
- Funke G., Larsson P. A. and Collins, M. D. (1995).** Heterogeneity within human-derived centers for disease control and prevention (CDC). Coryneform group AWF-1-like bacteria and description of *Corynebacterium aureus* sp. nov., *Int. J. Syst. Bacteriol.* 45, 735-739.
- Galinski, E. A. and Trüper, H. G. (1994).** Microbial behaviour in salt-stressed ecosystems, *FEMS Microbiol. Rev.* 39, 73-78.
- Gordeliy, V.I., Labahn, J., Moukhametzianov, R., Efremov, R., Granzin, J., Schlesinger, R., Büldt, G., Savopol, T., Scheidig, A.J., Klare, J.P., and Engelhard, M. (2002).** Molecular basis of transmembrane signalling by sensory rhodopsin II-transducer complex, *Nature* 419(6906), 484-487.
- Grant, S. G. N., Jessee, J., Bloom, F. R., and Hanahan, D. (1990).** Differential plasmid rescue from transgenic mouse DNAs into *Escherichia coli* K12, *J. Bacteriol.* 166, 6005-6612.
- Gross, C. (1996).** Function and regulation of the heat shock proteins. In *Escherichia coli and Salmonella: Cellular and Molecular Biology*, Vol. 1. Neidhardt, F.C., Washington DC, American Society for Microbiology Press, 1382–1399.
- Guo, Z., Cascio, D., Hideg, K., Kálái, T., and Hubbell, W.L. (2007).** Structural determinants of nitroxide motion in spin-labelled proteins: tertiary contact and solvent-inaccessible sites in helix G of T4 lysozyme, *Protein Sci.* 16(6), 1069-1086.
- Haardt, M., Kempf, B., Faatz, E., and Bremer, E. (1995).** The osmoprotectant proline betaine is a major substrate for the binding-protein-dependent transport system ProU of *Escherichia coli* K-12, *Mol. Gen. Genet.* 246, 783-786.
- Hamill, O.P. and Martinac, B. (2001).** Molecular basis of mechanotransduction in living cells, *Physiol. Rev.* 81(2), 685-740.

- Hamilton, C. L. and McConnell, H. M. (1968).** Spin Labels, in: Structural Chemistry and Molecular Biology (Rich, A. and Davidson, N., editors), 115.
- Hanahan, D. (1985).** Techniques for transformation of *Escherichia coli*, in: *DNA cloning* (Glover, D. M., editor), IRL Press, Oxford, 109-136.
- Hecker, M., Schumann, W., and Volker, U. (1996).** Heat-shock and general stress response in *Bacillus subtilis*, *Mol. Microbiol.* 19, 417-428.
- Hecker, M. and Völker, U. (2001).** General stress response of *Bacillus subtilis* and other bacteria, *Adv. Microb. Physiol.* 44, 35-91.
- Hermann, T. (2003).** Industrial production of amino acids by coryneform bacteria. *J. Biotechnol.* 104, 155-172.
- Hillar, A., Culham, D.E., Vernikovska, Y.I., Wood, J.M., and Boggs, J.M. (2005).** Formation of an antiparallel, intermolecular coiled coil is associated with *in vivo* dimerization of osmosensor and osmoprotectant transporter ProP in *Escherichia coli*, *Biochemistry* 44(30), 10170-10180.
- Hirayama, K., Akashi, S., Furuya, M., and Fukuhara, K. I. (1990).** Rapid confirmation and revision of the primary structure of bovine serum albumin by ESIMS and FRIT-FAB LC/MS. *Biochem. Biophys. Res. Commun.* 173, 639-646.
- Hoischen, C. and Krämer, R. (1990).** Membrane alteration is necessary but not sufficient for effective glutamate secretion in *Corynebacterium glutamicum*, *J. Bacteriol.* 172, 3409-3416.
- Holloway, P.W. (1973).** A simple procedure for removal of Triton X-100 from protein samples, *Anal. Biochem.* 53, 304-308.
- Hubbell, W. L. and Altenbach, C. (1994).** Investigation of structure and dynamics in membrane proteins using site-directed spin labeling, *Nature Structural Biology* 4, 566–573.
- Hubbell, W.L., Mchaourab, H.S., Altenbach, C., and Lietzow, M.A. (1996).** Watching proteins move using site-directed spin labelling, *Structure.* 4(7), 779-783.
- Hubbell, W.L., Gross, A., Langen, R., and Lietzow, M.A. (1998).** Recent advances in site-directed spin labeling of proteins, *Curr. Opin. Struct. Biol.* 8(5), 649-656.
- Hubbell, W. L., Cafiso, D. S., and Altenbach, C. (2000).** Identifying conformational changes with site-directed spin labeling, *Nature Structural Biology* 7, 735–739.
- Hustedt, E.J. and Beth, A.H. (1999).** Nitroxide spin-spin interactions: applications to protein structure and dynamics, *Annu. Rev. Biophys. Biomol. Struct.* 28, 129-153.
- Inoue, H., Nojime, H., and Okayama, H. (1990).** High efficiency transformation of *E. coli* with plasmids, *Gene* 96, 23-28.
- Jayaraman, S., Song, Y., and Verkman, A.S. (2001).** Airway surface liquid osmolality measured using fluorophore-encapsulated liposomes, *J. Gen. Physiol.* 117(5), 423-430.
- Jeschke G. (2002).** Distance measurements in the nanometer range by pulse EPR, *Chemphyschem.* 3(11), 927-932.



- Jeschke, G., Wegener, C., Nietschke, M., Jung, H., and Steinhoff, H.J. (2004).** Interresidual distance determination by four-pulse double electron-electron resonance in an integral membrane protein: the Na<sup>+</sup>/proline transporter PutP of *Escherichia coli*, *Biophys. J.* 86(4), 2551-2557.
- Jeschke, G. (2006).** DeerAnalysis 2006 User's Manual, 1-30.
- Jeschke, G. and H. W. Spiess, H.W. (2006).** Distance Measurements in Solid-State NMR and EPR Spectroscopy, *Lect. Notes Phys.* 684, 21-63.
- Jeschke, G. and Polyhach, Y. (2007).** Distance measurements on spin-labelled biomacromolecules by pulsed electron paramagnetic resonance. *Phys. Chem. Chem. Phys.* 9(16), 1895-1910.
- Jurica, S. M., Mesecar, A., Heath, P. J., Shi, W., Nowak, T., and Stoddard, B. L. (1998).** The allosteric regulation of pyruvate kinase by fructose-1,6-bisphosphate, *Structure* 6, 195-210.
- Kappes, R. M., Kempf, B., and Bremer, E. (1996).** Three transport systems for the osmoprotectant glycine betaine operate in *Bacillus subtilis*: Characterization of OpuD, *J. Bacteriol* 178, 5071-5079.
- Kasahara, M. and Hinkle, P.C. (1977).** Reconstitution and purification of the D-glucose transporter from human erythrocytes, *J. Biol. Chem.* 252(20), 7384-7390.
- Kataoka, M., Hashimoto, K.-I., Yoshida, M., Nakamatsu, T., Horinouchi, S., and Kawasaki, H. (2006).** Gene expression of *Corynebacterium glutamicum* in response to the conditions inducing glutamate overproduction, *Lett. Appl. Microbiol.* 42, 471-476.
- Kawahara, Y., Takahashi-Fuke, K., Shimizu, E., Nakamatsu, T., and Nakamori, S. (1997).** Relationship between the glutamate production and the activity of 2-oxoglutarate dehydrogenase in *Brevibacterium lactofermentum*. *Biosci. Biotech. Biochem.* 61, 1109-1112.
- Kempf, B. and Bremer, E. (1998).** Uptake and synthesis of compatible solutes as microbial stress responses to high-osmolality environments, *Arch. Microbiol.* 170, 319-330.
- Kinoshita, S. Ukada, S., and Shimono, M. (1957).** Studies on the amino acid fermentation: I. Production of L-glutamic acid by various microorganisms, *J. Gen. Appl. Microbiol.* 3, 193-205.
- Kim, K.K., Yokota, H., and Kim, S.H. (1999).** Four-helical-bundle structure of the cytoplasmic domain of a serine chemotaxis receptor, *Nature* 400(6746), 787-792.
- Klug, C.S., Eaton, S.S., Eaton, G.R., Feix, J.B. (1998).** Ligand-induced conformational change in the ferric enterobactin receptor FepA as studied by site-directed spin labeling and time-domain ESR, *Biochemistry* 37(25), 9016-9023.
- Koch, A. (1983).** The surface stress theory of microbial morphogenesis, *Adv. Microbiol. Physiol* 24, 301-336.

- Kunte, H.J., Crane, R.A., Culham, D.E., Richmond, D., and Wood, J.M. (1999).** Protein ProQ influences osmotic activation of compatible solute transporter ProP in *Escherichia coli* K-12, *J. Bacteriol.* 181(5),1537-1543.
- Kyhse-Andersen, J. (1984).** Electroblotting of multiple gels: a simple apparatus without buffer tank for rapid transfer of proteins from polyacrylamide to nitrocellulose, *J. Biochem. Biophys. Methods* 10, 203-209.
- Laemmli, U. K. (1970).** Cleavage of structural proteins during the assembly of the head of bacteriophage T4, *Nature London* 227, 680-685.
- Le Maire, M., Champeil, P., and Moller, J.V. (2000).** Interaction of membrane proteins and lipids with solubilizing detergents, *Biochim. Biophys. Acta.* 1508(1-2), 86-111.
- Lee, C. J. (2000).** Biopharmaceutical formulation, *Curr. Opin. Biotechnol.* 11 (1), 81-84.
- Levina, N., Töttemeyer, S., Stokes, N. R., Louis, P., Jones, M. A., and Booth, I. R. (1999).** Protection of *Escherichia coli* cells against extreme turgor by activation of MscS and MscL mechanosensitive channels: identification of genes required for MscS activity, *Embo J.* 18, 1730-1737.
- Lichtinger, T., Burkovski, A., Niederweis, M., Krämer, R., and Benz, R. (1998).** Biochemical and biophysical characterization of the cell wall porin of *Corynebacterium glutamicum*: the channel is formed by a low molecular mass polypeptide, *Biochemistry* 37, 15024-15032.
- Likhtenstein, G. I. (1976).** Spin Labeling Methods in Molecular Biology, John Wiley, New York.
- Ley, O. (2001).** Bedeutung der Prolinbiosynthese bei der Osmoregulation von *Corynebacterium glutamicum*, diploma thesis, University of Cologne.
- Malmberg, N.J. and Falke, J.J. (2005).** Use of EPR power saturation to analyze the membrane-docking geometries of peripheral proteins: applications to C2 domains, *Annu. Rev. Biophys. Biomol. Struct.* 34, 71-90.
- Martinac B. (2001).** Mechanosensitive channels in prokaryotes, *Cell. Physiol. Biochem.* 11(2), 61-76.
- Marx, A., de Graaf, A.A., Wiechert, W., Eggeling, L., and Sahm, H. (1996).** Determination of the fluxes in the central metabolism of *Corynebacterium glutamicum* by nuclear magnetic resonance spectroscopy combined with metabolite balancing, *Biotechnol Bioeng.* 49(2), 111-129.
- McConnell, H.M. and McFarland, B.G. (1970).** Physics and chemistry of spin labels, *Quart. Rev. Biophys.* 3, 91.
- Mchaourab, H. S., Lietzow, M. A., Hideg, K., and Hubbell, W. L. (1996).** Motion of spin-labelled side chains in T4 lysozyme. Correlation with protein structure and dynamics, *Biochemistry* 35, 7692–7704.
- Mchaourab, H.S., Oh, K.J., Fang, C.J., and Hubbell, W.L. (1997).** Conformation of T4 lysozyme in solution. Hinge-bending motion and the substrate-induced conformational transition studied by site-directed spin labelling, *Biochemistry* 36(2), 307-316.

- Mchaourab, H. S. and Perozo, E. (2000).** Determination of protein folds and conformational dynamics using spin-labeling EPR spectroscopy, in: Distance Measurements in Biological Systems by EPR (L. Berliner, S. S. Eaton, and G. R. Eaton, editors), Kluwer, New York.
- McLaggen, D., Naprstek, J., Buurman, E. T., and Epstein, W. (1994).** Interdependence of K<sup>+</sup> and glutamate accumulation during osmotic adaptation of *Escherichia coli*, *J. Biol. Chem.* 269, 1911-1917.
- Minton, A.P. (2005).** Influence of macromolecular crowding upon the stability and state of association of proteins: predictions and observations, *J. Pharm. Sci.* 94(8), 1668-1675.
- Morbach, S. and Krämer, R. (2000).** Osmoregulation and osmosensing by uptake carriers for compatible solutes in bacteria, in: E. Bales, R. Krämer (Eds.), *Molecular Mechanisms Controlling Transmembrane Transport*, Springer, Heidelberg, 2000, 155-174.
- Morbach, S. and Krämer, R. (2002).** Bodyshaping under water stress: osmosensing and osmoregulation of solute transport in bacteria, *Chem. Bio. Chem.* 3, 384-397.
- Morbach, S. and Krämer, R. (2003)** Impact of transport processes in the osmotic response of *Corynebacterium glutamicum*, *J. Biotechn.* 104, 69-75.
- Morbach, S. and Krämer, R. (2004a).** Osmoregulation and osmosensing by uptake carriers for compatible solutes in bacteria, in: *Molecular mechanisms controlling transmembrane transport* (Boles, E. and Krämer, R., Herausgeber), Springer, Heidelberg.
- Morbach, S. and Krämer, R. (2004b).** BetP of *Corynebacterium glutamicum*, a transporter with three different functions: betaine transport, osmosensing and osmoregulation, *Bioch. Biophys. Acta* 1658, 31-36.
- Morein, S., Andersson, A., Rilfors, L., and Lindblom, G. (1996).** Wild-type *Escherichia coli* cells regulate the membrane lipid composition in a "window" between gel and non-lamellar structures, *J. Biol. Chem.* 271(12), 6801-6809.
- Möker, N., Brocker, M., Schaffner, S., Krämer, R., Morbach, S., and Bott, M. (2004).** Deletion of two genes encoding the MtrA-MtrB two-component system of *Corynebacterium glutamicum* has strong influence on cell morphology, antibiotics susceptibility and expression of genes involved in osmoprotection, *Mol. Microbiol.* 54, 420-438.
- Mullis, K., Faldoma, F., Scharf, S., Saiki, R., Horn, G., and Erlich, H. (1986).** Specific enzymatic amplification of DNA in vitro: the polymerase chain reaction, *Cold Spring Harbour Symp. Quant. Biol.* 51, 263-273.
- Munro, G. F., Hercules, K., Morgan, J., and Sauerbier, W. (1972).** Dependence of the putrescine content of *Escherichia coli* on the osmotic strength of the medium, *J. Biol. Chem.* 247, 1272-1280.
- Nicklisch, S. (2005).** ESR-spektroskopische Untersuchung der Funktion der C-terminalen Domäne des Glycinbetain-Transporters BetP aus *Corynebacterium glutamicum* bei der Aktivitätsregulation, diploma thesis, University of Cologne.
- Nikaido, H. (1994).** Prevention of drug access to bacterial targets: permeability barriers and active efflux, *Science* 264, 382-388.

- Nikaido, H. (2003).** Molecular basis of bacterial outer membrane permeability revisited. *Microbiol. Mol. Biol.* 67(4), 593-656.
- Nottebrock, D., Meyer, U., Krämer, R., and Morbach, S. (2003).** Molecular and biochemical characterization of mechanosensitive channels in *Corynebacterium glutamicum*, *FEMS Microbiol. Lett.* 218, 305-309.
- Olsen, F., Hunt, C. A., Szoka, F.C., Vail, W.J., and Papahadjopoulos (1979).** Preparation of Liposomes of defines size distribution by extrusion through polycarbonate membranes, *Biochim. Biophys. Act.* 557, 9-23.
- Oren, A. (2006).** The Prokaryotes, New York, Springer New York, 113-164.
- Oren A. (2008).** Microbial life at high salt concentrations: phylogenetic and metabolic diversity, *Saline Systems*, 4:2.
- Ott, V. (2005).** Funktion cytoplasmatischer Proteinschleifen und der C-terminalen Domäne bei der Aktivitätsregulation des Glycinbetain-Transporters BetP aus *Corynebacterium glutamicum*, diploma thesis, University of Cologne.
- Ott, V. (2008).** Der Regulationsmechanismus des Osmosensors BetP aus *Corynebacterium glutamicum*, dissertation, University of Cologne.
- Pannier, M., Veit, S., Godt, A., Jeschke, G., and Spiess, H.W. (2000).** Dead-time free measurement of dipole-dipole interactions between electron spins, *J. Magn. Reson.* 142(2), 331-340.
- Papahadjopoulos, D. and Vail, W.J. (1978).** Incorporation of macromolecules within large unilamellar vesicles (LUV), *Ann. NY Acad. Sci.* 308, 259-267.
- Patzlaff, J.S., van der Heide, T., and Poolman, B. (2003).** The ATP/substrate stoichiometry of the ATP-binding cassette (ABC) transporter OpuA, *J. Biol. Chem.* 278(32), 29546-29551.
- Perozo, E., Cortes, D. M., and Cuello, L. G. (1998).** Three-dimensional architecture of a K1 channel: implications for the mechanism of ion channel gating, *Nat. Struct. Biol.* 5, 459-469.
- Peter, H., Burkovski, A., and Krämer, R. (1996).** Isolation, characterization and expression of the *Corynebacterium glutamicum betP* gene, encoding the transport system for the compatible solute glycine betaine, *J. Bacteriol.* 178, 5229-5234.
- Peter, H., Bader, A., Burkovski, A., Lambert, C., and Krämer, R. (1997).** Isolation of the uptake *putP* gene of *Corynebacterium glutamicum* and characterization of a low affinity uptake system for compatible solutes, *Arch. Microbiol.* 168, 143-151.
- Peter, H., Burkovski, A., and Krämer, R. (1998a).** Osmosensing by N- and C- terminal extensions of the glycine betaine Uptake system BetP of *Corynebacterium glutamicum*, *J. Biol. Chem.* 273, 2567-2574.
- Peter, H., Weil, B., Burkovski, A., Krämer, R., and Morbach, S. (1998b).** *Corynebacterium glutamicum* is equipped with four secondary carriers for compatible solutes: identification, sequencing and characterization of the proline/ectoine uptake

system, ProP, and the ectoine/proline/glycine betaine Carrier, EctP, *J. Bacteriol.* 180, 6005-6012.

**Philippot, J., Mutaftchiev, S., and Liautard, J.P. (1983).** A very mild method allowing the encapsulation of very high amounts of macromolecules into very large (1000nm) unilamellar liposomes, *Biochim. Biophys. Acta* 734, 137-143.

**Pick, U. (1981).** Liposomes with a large trapping capacity prepared by freezing and thawing of sonicated phospholipid mixtures, *Arch. Biochem. Biophys.* 212(1), 186-194.

**Poolman, B. and Glaasker, E. (1998).** Regulation of compatible solute accumulation in bacteria, *Mol. Microbiol.* 29, 397-407.

**Puech, V., Chami, M., Lemassu, A., Lanéelle, M.-A., Schiffler, B., Gounon, P., Bayan, N., Benz, R., and Daffé, M. (2001).** Structure of the cell envelope of corynebacteria: importance of the non-covalently bound lipids in the formation of the cell wall permeability barrier and fracture plane, *Microbiol.* 147, 1365-1382.

**Rabenstein, M. D. and Shin, Y. K. (1995).** Determination of the distance between two spin labels attached to a macromolecule. *National Academy of Sciences of the United States of America* 92, 8239–8243.

**Racher, K.I., Culham, D.E., and Wood, J.M. (2001).** Requirements for osmosensing and osmotic activation of transporter ProP from *Escherichia coli*, *Biochemistry* 40(24), 7324-7333.

**Racusen D. (1973).** Stoichiometry of the amido black reaction with proteins, *Anal Biochem.* 52(1), 96-101.

**Reed, R.G., Putnam, F.W., and Peters, T. Jr. (1980).** Sequence of residues 400-403 of bovine serum albumin, *Biochem. J.* 191, 867-868.

**Ressl, S., Van Scheltinga, T., Vornrhein, C., Ott, V., and Ziegler, C. (2008).** Molecular basis of regulation and Na<sup>+</sup>-coupled transport in the glycine-betaine symporter BetP, submitted.

**Rigaud, J.L., Paternostre, M.T., and Bluzat, A. (1988b).** Mechanisms of membrane protein insertion into liposomes during reconstitution procedures involving the use of detergents. 2. Incorporation of the light-driven proton pump bacteriorhodopsin, *Biochemistry* 27(8), 2677-2688.

**Rigaud, J. L., Pitard, B., and Levy, D. (1995).** Reconstitution of membrane proteins into liposomes: application to energy-transducing membrane proteins, *Biochem. Biophys. Acta* 1231, 223-246.

**Rigaud, J.L., Mosser, G., Lacapere, J.J., Olofsson, A., Levy, D., and Ranck, J.L. (1997).** Bio-Beads: an efficient strategy for two-dimensional crystallization of membrane proteins, *J. Struct. Biol.* 118(3), 226-235.

**Rigaud, J.-L., D. Levy, G. Mosser, and O. Lambert. (1998).** Detergent removal by non-polar polystyrene beads, *Eur. Biophys. J.* 27, 305-319.

**Rink, T., Pfeiffer, M., Oesterhelt, D., Gerwert, K., and Steinhoff, H.J. (2000).** Unraveling photoexcited conformational changes of bacteriorhodopsin by time resolved electron paramagnetic resonance spectroscopy, *Biophys. J.* 78(3), 1519-1530.

- Rönsch, H., Krämer, R., and Morbach, S. (2003).** Impact of osmotic stress on volume regulation, cytoplasmic solute composition and lysine production in *Corynebacterium glutamicum* MH20-22B, *J. Biotechnol.* 104, 87-97.
- Rübenhagen, R., Rönsch, H., Jungs, H., Krämer, R., and Morbach, S. (2000).** Osmosensor and osmoregulator properties of the betaine carrier BetP from *Corynebacterium glutamicum* in proteoliposomes, *J. Biol.Chem* 275, 735-741.
- Rübenhagen, R., Morbach, S., and Krämer, R. (2001).** The osmoreactive betaine carrier BetP from *Corynebacterium glutamicum* is a sensor for cytoplasmic K<sup>+</sup>, *EMBO J.* 20, 5412-5420.
- Rübenhagen, R. (2001).** Der Glycinbetain-Transporter BetP aus *Corynebacterium glutamicum* als Osmosensor, dissertation, University of Cologne.
- Ruffert, S., Lambert, C., Peter, H., Wendisch, V. F., and Krämer, R. (1997).** Efflux of compatible solutes in *Corynebacterium glutamicum* mediated by osmoregulated channel activity, *Eur. J. Biochem.* 247, 572-580.
- Ruffert, S., Berrier, C., Krämer, R., and Ghazi, A. (1999).** Identification of mechanosensitive ion channels in the cytoplasmic membrane of *Corynebacterium glutamicum*, *J. Bacteriol.* 181, 1673-1679.
- Saier, M. H. Jr. (2000).** Families of transmembrane transporters selective for amino acids and their derivatives, *Microbiology* 146, 1775-1795.
- Sambrook, J., Fritsch, E. F., and Maniatis, T. (1989).** Molecular cloning: A laboratory manual (2<sup>nd</sup> ed.), Cold spring harbour laboratory press, New York, USA.
- Sanger, F., Nicklen, S., and Coulson, A. R. (1977).** DNA sequencing with chain terminating inhibitors, *Proc. Natl. Acad. Sci. USA* 74, 5463-5467.
- Schaffner, W. and Weissmann, C. (1973).** A rapid, sensitive and specific method for the determination of protein in dilute solution, *Anal. Biochem.* 56, 502-514.
- Schiller, D. (2004).** Osmosensorische Eigenschaften des Glycin-Betain-Transporters BetP aus *Corynebacterium glutamicum*, dissertation, University of Cologne.
- Schiller, D., Krämer, R., and Morbach, S. (2004a).** Cation specificity of osmosensing by the betaine carrier BetP of *Corynebacterium glutamicum*, *FEBS Letters* 563, 108-112.
- Schiller, D., Rübenhagen, R., Krämer, R., and Morbach, S. (2004b).** The C-terminal domain of the betaine carrier BetP of *Corynebacterium glutamicum* is directly involved in Sensing K<sup>+</sup> as an osmotic stimulus, *Biochemistry* 43, 5583-5591.
- Schiller, D., Ott, V., Krämer, R., and Morbach, S. (2006).** Influence of membrane composition on osmosensing process of the betaine carrier BetP from *Corynebacterium glutamicum*, *J. Biol. Chem.* 281, 7737-7746.
- Schlösser, A., Meldorf, M., Stumpe, S., Bakker, E.P., and Epstein, W. (1995).** TrkH and its homolog, TrkG, determine the specificity and kinetics of cation transport by the Trk system of *Escherichia coli*, *J. Bacteriol.* 177(7),1908-1910.
- Skerra, A. (1994).** Use of the tetracycline promoter for the tightly regulated production of a murine antibody fragment in *Escherichia coli*, *Gene* 151, 131-135.

- Sleator, R. D., Gahan, C. G., Abee, T., and Hill, C. (1999).** Identification and disruption of BetL, a secondary glycine betaine transport system linked to the salt tolerance of *Listeria monocytogenes* LO28, *Appl. Environ. Microbiol.* 65, 8974-8982.
- Stackebrandt, E., Rainey, F. A., and Ward-Rainey, N. L. (1997).** Proposal for a new hierarchical classification system, *Actinobacteria* classis nov. *Int. J. Syst. Bacteriol.* 47, 784-791.
- Steger, R., Weinand, M., Krämer, R., and Morbach, S. (2004).** LcoP, an osmoregulated betaine/ectoine uptake system from *C. glutamicum*, *FEBS Letters* 573, 155-160.
- Steinhoff HJ. (1990).** Residual motion of hemoglobin-bound spin labels and protein dynamics: viscosity dependence of the rotational correlation times, *Eur. Biophys. J.* 18(1), 57-62.
- Steinhoff, H. J., Dombrowsky, O., Karin, C., and Schneiderhan, C. (1991).** Two dimensional diffusions of small molecules on protein surfaces: an EPR study of the restricted translational diffusion of protein bound spin labels, *European Biophysical Journal* 20, 293–303.
- Steinhoff, H. J., Mollaaghababa, R., Altenbach, C., Hideg, K., Krebs, M., Khorana, H. G., and Hubbell, W. L. (1994).** Time-resolved detection of structural changes during the photocycle of spin-labelled bacteriorhodopsin, *Science* 266, 105–107.
- Steinhoff, H.J. and Hubbell, W.L. (1996).** Calculation of electron paramagnetic resonance spectra from Brownian dynamics trajectories: application to nitroxide side chains in proteins, *Biophys J.* 71(4), 2201-2212.
- Steinhoff, H.J., Pfeiffer, M., Rink, T., Burlon, O., Kurz, M., Riesle, J., Heuberger, E., Gerwert, K., and Oesterhelt, D. (1999).** Azide reduces the hydrophobic barrier of the bacteriorhodopsin proton channel, *Biophys. J.* 76(5), 2702-2710.
- Steinhoff, H.J. (2002).** Methods for study of protein dynamics and protein-protein interaction in protein-ubiquitination by electron paramagnetic resonance spectroscopy, *Front. Biosci.* 7, c97-110.
- Steinhoff, H.J. (2005).** Intra- und intermolekulare Abstandsmessungen mittels ESR-Spektroskopie, *Biospektrum* 2/2005, 176.
- Sukharev, S. I., Martinac, B., Arshavsky, V. Y., and Kung, C. (1993).** Two types of mechanosensitive channels in the *Escherichia coli* cell envelope: solubilization and functional reconstitution, *Biophys. J.* 65, 177-183.
- Sukharev, S. I., Blount, P., Martinac, B., Blattner, F. R., and Kung, C. (1994).** A large mechanosensitive channel in *Escherichia coli* is encoded by *mscL* alone, *Nature* 368, 265-268.
- Sukharev, S. I. (1999).** Mechanosensitive channels in bacteria as membrane tension reporters, *The FASEB Journal* 13, S55-61.
- Tiebel, B., Radzwill, N., Aung-Hilbrich, L. M., Helbl, V., Steinhoff, H. J., and Hillen, W. (1999).** Domain motions accompanying Tet Repressor induction defined by changes of interspin distances at selectively labelled sites, *Journal of Molecular Biology* 290, 229–240.

- Timofeev, V. P. and Tsetlin, V. I. (1983).** Analysis of mobility of protein side chains by a spin label technique, *Biophys. Struct. Mech.* 10(1-2), 93-108.
- Timasheff, S. N. (1991).** A physicochemical basis for the selection of osmolytes of Cholin oxidase from *Cylindrocarpus didymus* M-1, *Agric. Biol. Chem.* 43, 815-820.
- Timasheff, S.N. (1998).** Control of protein stability and reactions by weakly interacting cosolvents: the simplicity of the complicated, *Adv. Protein. Chem.* 51, 355-432.
- Todd, A.P., Cong, J., Levinthal, F., Levinthal, C., and Hubbell, W.L. (1989).** Site-directed mutagenesis of colicin E1 provides specific attachment sites for spin labels whose spectra are sensitive to local conformation, *Proteins* 6(3), 294-305.
- Tsatskis, Y., Khambati, J., Dobson, M., Bogdanov, M., Dowhan, W., and Wood, J.M. (2005).** The osmotic activation of transporter ProP is tuned by both its C-terminal coiled-coil and osmotically induced changes in phospholipid composition, *J. Biol. Chem.* 280(50), 41387-41394.
- Udaka, S. (1960).** Screening method for microorganisms accumulating metabolites and its use in the isolation of *Micrococcus glutamicus*, *J. Bacteriol.* 79, 754-755.
- Van der Heide, T. and Poolman, B. (2000).** Osmoregulated ABC-transport system of *Lactococcus lactis* senses water stress via changes in the physical state of the membrane, *Proc. Natl. Acad. Sci. USA* 97(13), 7102-7106.
- Van der Heide, T., Stuart, M.C., and Poolman, B. (2001).** On the osmotic signal and osmosensing mechanism of an ABC transport system for glycine betaine, *EMBO J.* 20(24), 7022-7032.
- Varela, C.A., Baez, M.E., and Agosin, E. (2004).** Osmotic stress response: quantification of cell maintenance and metabolic fluxes in a lysine-overproducing strain of *Corynebacterium glutamicum*, *Appl. Environ. Microbiol.* 70(7), 4222-4229.
- Vinothkumar, K.R., Raunser, S., Jung, H., and Kühlbrandt, W. (2006).** Oligomeric structure of the carnitine transporter CaiT from *Escherichia coli*, *J. Biol. Chem.* 281(8), 4795-4801.
- Von Blohn, C., Kempf, B., Kappes, R.M., and Bremer, E. (1997).** Osmostress response in *Bacillus subtilis*: characterization of a proline uptake system (OpuE) regulated by high osmolarity and the alternative transcription factor sigma B, *Mol. Microbiol.* 25(1), 175-187.
- Wegener, A.-A., Chizov, I., Engelhard, M., and Steinhoff, H. J. (2000).** Time-resolved detection of transient movement of helix F in spinlabelled Pharaonis sensory rhodopsin II, *Journal of Molecular Biology* 301, 881-891.
- Weinand, M., Krämer, R., and Morbach, S. (2007).** Characterization of compatible solute transporter multiplicity in *Corynebacterium glutamicum*, *Appl. Microbiol. Biotechnol.* 76(3), 701-708.
- Whatmore, A.M. and Reed, R.H. (1990).** Determination of turgor pressure in *Bacillus subtilis*: a possible role for K<sup>+</sup> in turgor regulation, *J. Gen. Microbiol.* 136(12), 2521-2526.
- Whatmore, A. M., Chudek, J. A., and Reed, R. H. (1990).** The effects of osmotic upshock on the intracellular solute pools of *Bacillus subtilis*, *J. Gen. Microbiol.* 136, 2527-2536.



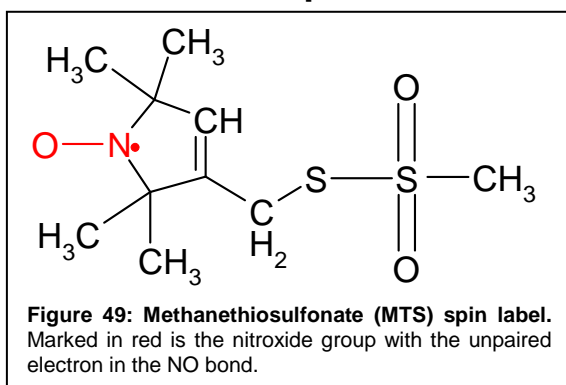
- 
- White G.F., Racher, K.I., Lipski, A., Hallett, F.R., and Wood, J.M. (2000).** Physical properties of liposomes and proteoliposomes prepared from *Escherichia coli* polar lipids, *Biochim. Biophys. Acta* 1468, 175–186.
- Wolf, A., Krämer, R., and Morbach, S. (2003).** Three pathways for trehalose metabolism in *Corynebacterium glutamicum* ATCC13032 and their significance in response to osmotic stress, *Mol. Microbiol.* 49, 1119-1134.
- Wood, J. M. (1999).** Osmosensing by bacteria: signals and membrane-based sensors, *Microbiol. Mol. Biol. Rev.* 63, 230-262.
- Wood, J.M., Bremer, E., Csonka, L.N., Kraemer, R., Poolman, B., van der Heide, T., and Smith, L.T. (2001).** Osmosensing and osmoregulatory compatible solute accumulation by bacteria, *Comp. Biochem. Physiol. A. Mol. Integr. Physiol.* 130(3), 437-460.
- Wood, J. M. (2006).** Osmosensing by bacteria, *Sci. STK* 17, 43-47.
- Wood, J. M. (2007).** Bacterial Osmosensing Transporters, *Methods Enzymol.* 478, 77-107.
- Zavoisky, E. K. (1944).** Paramagnetic absorption of a solution in parallel fields, *J. Phys. USSR* 8, 377-380.
- Zhang, D., Yasuda, T., Yu, Y., and Okada, S. (1994).** Physicochemical damage to liposomal membrane induced by iron- or copper-mediated lipid peroxidation, *Acta Med. Okayama* 48(3), 131-136.
- Ziegler, C., Morbach, S., Schiller, D., Krämer, R., Tziatzios, C., Schubert, D., and Kühlbrandt, W. (2004).** Projection structure and oligomeric state of the osmoregulated sodium/glycine betaine symporter BetP of *Corynebacterium glutamicum*, *J. Mol. Biol.* 337, 1137-1147.
- Zimmermann, J., Voss, H., Schwager, C. Stegemann, J., Erfle, H., Stucky, K., Kristensen, T., and Ansorge, W. (1990).** A simplified protocol for fast plasmid DNA sequencing, *Nucleic Acids Res.* 18, 105-109.
- Zuidam, N. J. (2003).** Stability, storage, and sterilization of liposomes, in: *Liposomes* (Torchilin, V. P., Weissig, V., editors), Oxford University Press, New York, 149-165.

## 7. Appendix

### 7.1. EPR theory, in short

In general, EPR is - like the well known optical UV- and IR-spectroscopy - a form of resonance absorption spectroscopy. Thereby, an electromagnetic radiation is sent through a sample and a portion of this radiation, at certain (resonance) frequencies (wavelengths), is absorbed in the sample. In general, the main difference between EPR and e.g. the optical spectroscopy is that absorption of microwave energy occurs in the presence of an external magnetic field (except for the so-called zero field splitting). For this purpose, the respective sample has to contain magnetic dipoles or magnetic moments that may lead to a magnetic resonance in an external magnetic field. But a net magnetic moment only occurs, if an unpaired electron with its magnetic and angular moment (together circumscribed as "electron spin"; in classical mechanics = self rotation, e.g. rotation of the electron around its own centre of mass) is present in the sample. However, in biological systems these so called paramagnetic electrons only occur in transition elements with incomplete sub-shells or in free radicals and radical ions with an unpaired valence electron. Thus, a macromolecule under study, if it does not contain paramagnetic species, has to be marked with a unique paramagnetic spin probe to be amenable for EPR spectroscopy.

#### 7.1.1. Nitroxide spin label

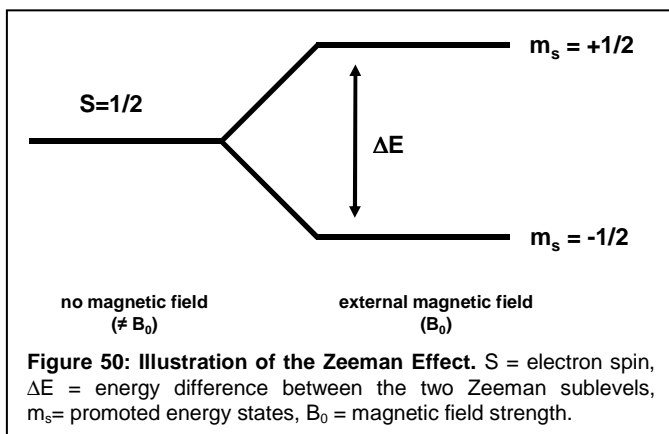


In the absence of paramagnetic species in the macromolecule, a stable free radical (spin label) has to be covalently linked to the macromolecule under study. These spin labels comprise, in general, two functional parts: (1) an EPR active and stable free radical and (2) a marker group that binds to a specific target in the biological object

(Figure 49). The nitroxide spin label used in this work (MTS=(1-oxyl-2,2,5,5-tetramethylpyrroline-3-methyl)-methanethiosulfonate) has been proven to meet these claims best: (1) it possesses an unpaired electron (located on the N-O bond) which is highly stable due to the sterical hindering by four surrounding methyl groups (Figure 49), (2) it exhibits highly reactive and selective SH-groups, allowing the labelling of specific positions by a covalent attachment to cysteine residues in the macromolecule under study, (3) it is neither hydrophobic nor hydrophilic, and (4) chemically inert to substances

in neutral and alkali solutions as well as unsusceptible to oxygen (Hamilton *et al.*, 1968; McConnell *et al.*, 1970).

### 7.1.2. Zeeman Effect



If such a paramagnetic probe is placed into an external magnetic field B, the energy levels accessible to the unpaired electronic spin are split by that field. Since an electron has a spin of  $S=1/2$  (fermions), they can enter two possible energy levels: a low energy state ( $m_s=-1/2$ ) and a high energy state ( $m_s=+1/2$ ).

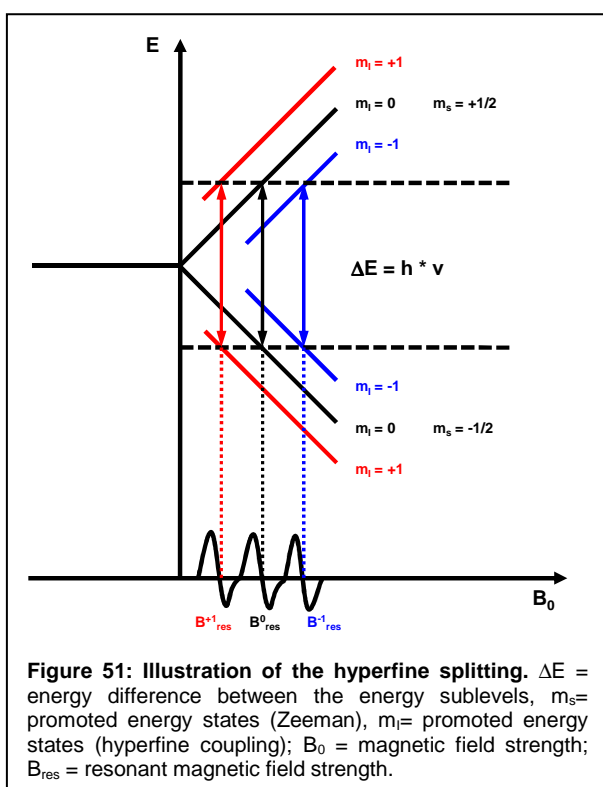
This so called Zeeman-effect was discovered in 1896 (Pieter Zeeman; Figure 50) and is exploited in EPR spectroscopy, where the spin labelled sample is placed inside an inhomogeneous magnetic field and exposed to a constant frequency microwave radiation (e.g. 9.7GHz X-band). The distance between the two (Zeeman-) energy sublevels is proportional to the magnetic field strength:

$$(8) \Delta E = h \cdot \nu = g \cdot \mu_B \cdot B_0$$

With  $h$ =Planck constant,  $\nu$ =frequency of microwave radiation,  $B_0$ =magnetic field strength,  $\mu_B$ =Bohr magneton,  $g$ =g-factor or „Landé“-factor.

If the energy of the applied microwave radiation is equal (equation (8)) to the energy difference necessary to promote an electron from the low-energy state ( $m_s=-1/2$ ) to the high-energy state ( $m_s=+1/2$ ), a resonant absorption of a portion of the microwave energy occurs resulting in the appearance of an EPR line. To increase the sensitivity, EPR spectra are recorded as the rate of change of microwave absorption as function of external magnetic field. In addition, a field modulation is applied with a modulation frequency much lower than the microwave frequency and a modulation amplitude much lower than the signal amplitude. The consequence of the field modulation is the first derivative lineshape of the detected absorption, the typical EPR spectrum (Figure 13, lower left, Introduction).

### 7.1.3. Hyperfine coupling and resulting EPR spectra



By additional interactions of the magnetic moments the electron spin  $S$  and nearby nuclear spins  $I$ , the Zeeman energy levels can further be split into  $(2I+1)$  allowed energy levels, a so called hyperfine splitting (HFS, Figure 51). This phenomenon is called hyperfine splitting (HFS) if the interaction takes place with the associated atom of the radical or superhyperfine splitting (SHFS) if it takes place with neighbouring atoms. The EPR spectrum of nitroxide radical at X-band frequencies ( $\sim 9-10$  GHz) is dominated by the hyperfine coupling to the  $^{14}\text{N}$  nucleus of the N-O group. Since  $^{14}\text{N}$  has a nuclear spin of  $I=1$ , the hyperfine interactions lead

to a triplet splitting of the resonance line. The selection rule of magnetic dipole moments ( $\Delta m_s=1, \Delta m_l=0$ ) allows three resonant EPR transitions (Figure 51) at magnetic field strengths determined by:

$$(9) B_{res} = B_0 - A * m_l,$$

where  $B_{res}$  is resonant magnetic field,  $B_0$  is resonant magnetic field strength in the absence of hyperfine coupling,  $m_l$  correspond to nuclear magnetic moment, and  $A$  is the hyperfine coupling constant between the electron spin and the nucleus spin. The hyperfine coupling constant  $A$  is dependent on the electron density of the surrounding medium, which in turn influence the local polarity of the nitroxide spin label. Thus, information about the polarity of the immediate environment of the spin label can be derived or even whole polarity profiles (Steinhoff *et al.*, 1999; Steinhoff *et al.*, 2000).

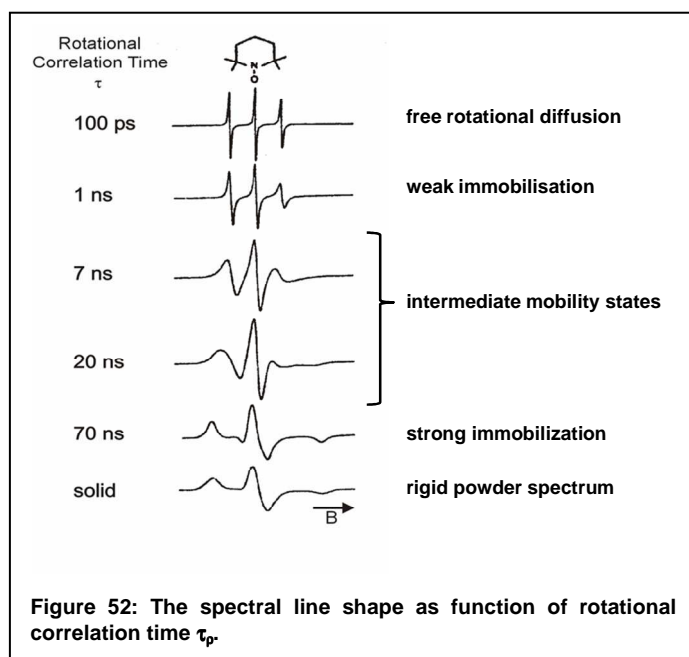
However, to describe an ESR-spectrum properly, the so-called Spin-Hamilton-Operator (SHO)  $\hat{H}$  is used:

$$(10) \hat{H} = \mu_B * B_0 * g * S + S * A * I$$

Where  $\mu_B$  is the Bohr magneton,  $B_0$  is the (external) magnetic field strength,  $g$  is the  $g$ -factor,  $S$  and  $I$  are the electron and nuclear spins, respectively, and  $A$  is the hyperfine coupling constant.

Here, the first term describes the interactions of the electron with the magnetic field and the second term describes the interactions between the electron and nucleus. In general both, the  $g$ -value and the hyperfine coupling are anisotropic and depend on the orientation of spin label relative to the external magnetic field. Hyperfine coupling is maximal along the direction of the  $\pi$ -orbital of the nitrogen ( $A_{zz} \sim 34\text{G}$ ) and minimal in the plane perpendicular to that direction ( $A_{xx} \sim A_{yy} \sim 6\text{G}$ ). The maximum of the  $g$ -value ( $g_{xx} \sim 2.0090$ ) is along the N-O bond, the minimum value is along the direction of the  $\pi$ -orbital ( $g_{zz} \sim 2.0025$ ) and the intermediate value of  $g$  is along the molecular  $y$ -axis ( $g_{yy} \sim 2.0060$ ) (Berliner *et al.*, 1976; Hustedt and Beth, 1999).

#### 7.1.4. Spectral line shape and spin label mobility



If the molecule rotates fast (rotational correlation time  $\tau_R < 100\text{ps} = \tau_1 = \text{fast rotation limit}$ ), an isotropic spectrum with three sharp and distinct lines can be observed (Figure 52, top spectrum). The splitting corresponds to the isotropic hyperfine splitting  $(34+6+6)/3 \sim 15\text{G}$ . If the spin label molecule rotates with a rate that is smaller than the line width ( $\tau_R > 1\mu\text{s} = \tau_2 = \text{rigid rotation limit}$ ), the spectrum is static. It corresponds

to a superposition of the spectra of all possible orientations of the spin label molecule with respect to the external magnetic field, i.e. to a powder pattern (Figure 52, bottom spectrum). For example, if the spin label is in a solution with a low viscosity, a free spin label rotation and thus a sharp EPR spectrum will be observed. On the contrary, if the spin label is buried inside a protein or in a highly viscous solution, it will show a powder EPR spectrum (Figure 52). In the intermediate regime, the hyperfine lines are broadened and the rotational correlation time  $\tau_R$  can be determined by a spectral simulation. For instance, depending on its rotameric state as well as on the nearby surrounding (e.g. side chains of the protein), the spin label may rotate with different rates around different axis and as a result different EPR spectra will be observed (Figure 53). For the isotropic motion there

are more simple ways of determining the rotational correlation times. In the fast tumbling regime ( $\tau_R < \text{a few ns}$ ), the rotational correlation time in [sec/G] can be determined from the relative intensities of the three EPR lines and the peak-to-peak line width  $\Delta B_0$  of the central line:

$$(11) \begin{aligned} \tau_P^I &= 6.8 * 10^{-10} * \Delta B_0 * (\sqrt{h_0/h_{-1}} - \sqrt{h_0/h_1}), \\ \tau_P^{II} &= 6.7 * 10^{-10} * \Delta B_0 * (\sqrt{h_0/h_{-1}} + \sqrt{h_0/h_1} - 2), \\ \tau_P^{III} &= 6.6 * 10^{-10} * \Delta B_0 * (\sqrt{h_1/h_{-1}} - 1), \end{aligned}$$

where  $\Delta B_0$  is the line width of the central line (peak-to-peak distance),  $h_0$  is the amplitude

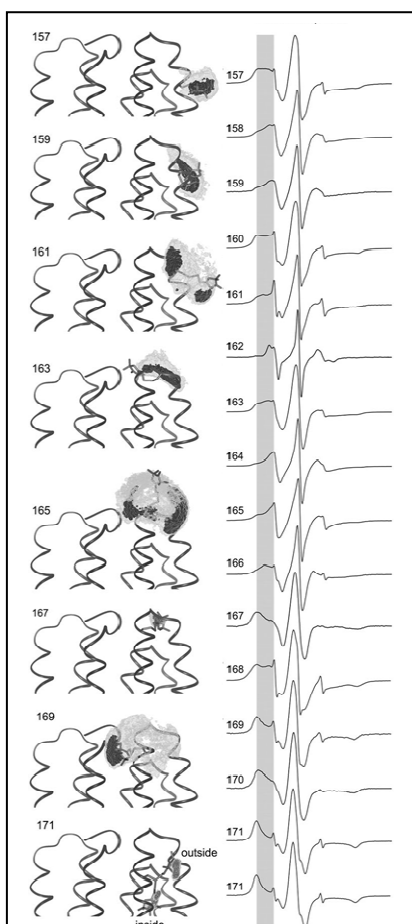


**Figure 53: cw-EPR spectra of consecutive spin label positions within bacteriorhodopsin (Beier et al., 2006).** The spin label and its accessible space for each odd position are shown on the left. Respective EPR spectra are shown on the right.

of the central line,  $h_{-1}$  the amplitude of the high field line and  $h_1$  the amplitude of the low field line (Figure 52, top spectrum). If the rotational diffusion is isotropic, the three values ( $\tau_P^I$ ,  $\tau_P^{II}$  and  $\tau_P^{III}$ ) are equal. If there are slight variations, an estimate of the rotational correlation time can be obtained from the average of the three values (a difference indicates that some anisotropy of the spin label motion is present in the sample under study).

According to the Stokes-Einstein Relation correlation time is defined as:

$$(12) \tau = (4 * \Pi * \eta * r^3) / (3 * \kappa_B * T),$$

where  $r$  is the average particle radius,  $\eta$  is the viscosity of the medium,  $T$  is the absolute temperature in  $\text{K}$  and  $\kappa_B$  is the Boltzmann constant.

Thus, the viscosity of the medium (in the local environment of the spin label) can be determined using equations (11) and (12) (Timofeev and Tsetlin, 1983; Berliner, 1976).

### 7.1.5. Distance measurements

To conduct EPR distance measurements, molecular systems with at least two paramagnetic centres are needed. Thereby, both unpaired electrons can be introduced in one single protein (Likhtenstein, 1976) to determine intramolecular interspin distances or the additional spin labels might be attached to interaction partners like receptors, nucleic acids or enzymes (Tiebel *et al.*, 1999; Wegener *et al.*, 2000).

Beside the hyperfine coupling constant  $A$  and the  $g$ -factor, in double or multiple labelled macromolecules further dipole-dipole interactions may occur according to W. Pauli and W. Heisenberg, e.g. the so called J-coupling  $J$  (indirect dipole-dipole coupling) and the exchange interaction  $D$ . The anisotropic dipolar exchange interaction  $D$  causes a so called zero-field-splitting, e.g. the abolition of spin degeneracy ( $\neq$  Boltzmann distribution) in the absence of an external magnetic field. If two or more unpaired electrons in a sample are in close vicinity and if a high dynamical flexibility of the spin label favours rapid electron collisions, the resulting wave function overlap of both fermions (electrons) additionally leads to J-coupling. Both quantum mechanical effects influence the EPR spectrum of a given sample by a broadening of the HFS lines.

#### 7.1.5.1. DEER approach used in this thesis

In short, intra- or intermolecular distance measurements with EPR spectroscopy rely on the dipole-dipole coupling between electrons spins which is inversely proportional to the cube of the distance (Jeschke and Spiess, 2006). A set of techniques and proper analysis tools are available to specify the respective inter-spin-vector lengths and its orientation with respect to both nitroxide labels. The overlapping estimations of each method thus permit a full and detailed identification of spin-spin spacing up to 60Å (in very favourable cases up to 80Å).

For distances shorter than 20Å, the dipolar coupling between two spin labels leads to pronounced spectral broadening of the usual cw-EPR spectrum. However, for distances shorter than 8Å the partial overlap of the  $\Pi$ -orbital of each spin label lead to strong (Heisenberg) exchange interactions ( $D$ , see above) that influence the respective cw-spectrum with a superimposing spectral broadening. To discriminate exchange effect from dipole-dipole interaction, the so called half-field EPR transitions have to be observed. Thereby, the amplitude of the respective half-field line is proportional to the sixth power of the inversed distance if dipolar coupling is present (Steinhoff, 2005). For inter-spin distances above 20-25Å the spectral broadening due to dipolar coupling is much smaller than that caused by other interfering effects (e.g. matrix proton modulation, nuclear modulation,  $g$  anisotropy). In this case pulsed EPR techniques have to be applied. The most widely used pulsed method is the so called Double-Electron-Electron-Resonance

(DEER) experiment. This technique was used in this work to determine intra- and/or intermolecular spin-spin distances in BetP variants reconstituted into proteoliposomes (for details see Pannier *et al.*, 2000; Jeschke, 2002; Jeschke and Polyhach, 2007).

For each four-pulse DEER measurement we determined the respective spin echo signal  $V(t)$  as a function of the dipolar evolution time  $t$ . According to Jeschke and Polyhach (2007),  $V(t)$  is defined as:

$$(13) V(t) = F(t) * B(t)$$

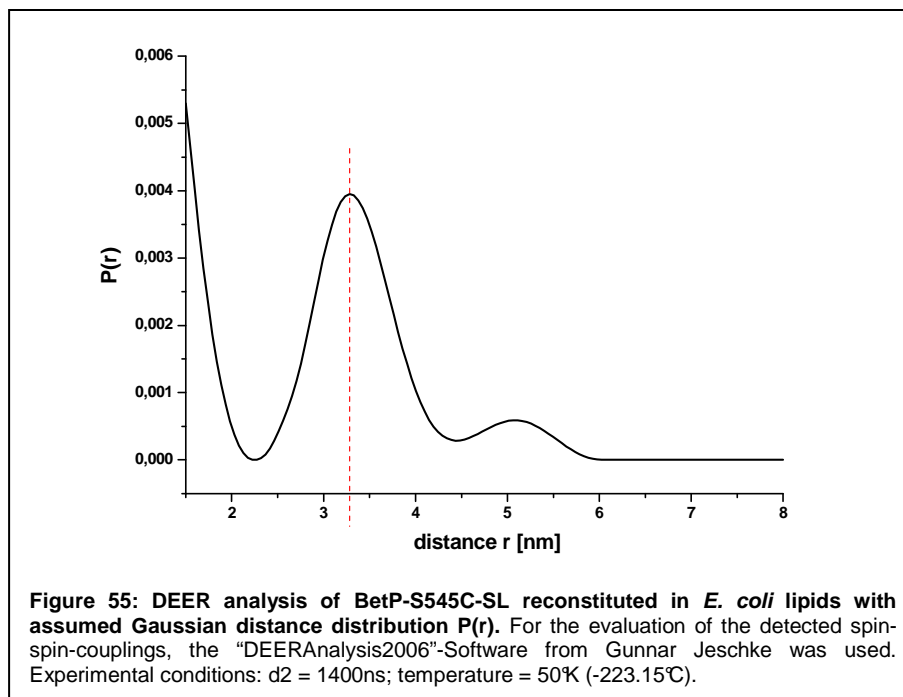
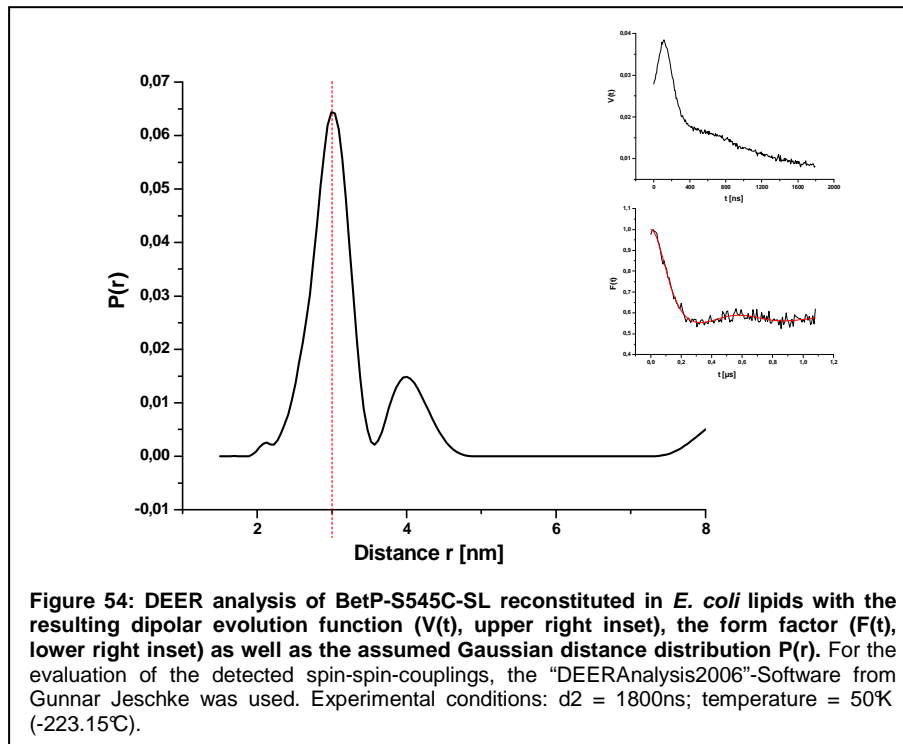
With  $F(t)$  = form factor (interactions of intramolecular spins) and  $B(t)$  = background factor (interactions with neighbouring spins).

Thereby the spin echo signal  $V(t)$  was recorded and subsequently divided by the manually fitted background factor  $B(t)$  (DEERAnalysis2006, Jeschke 2006) to obtain the form factor  $F(t)$ . As already mentioned above,  $F(t)$  is inversely proportional to the cube of the mean distance between two electron spins, which then can be plotted in a Gaussian distance distribution with a mean distance value  $r$  and a dedicated standard deviation  $\sigma$  (Table 8).

To prevent the averaging of possible dipolar interactions due to spin label movements and/or overall reorientation of the tagged molecule, the respective degree of freedom was restricted by cooling the sample far below the glass transition temperature ( $T < 200\text{K}$ ; experimental condition: 50K) and/or by increasing the viscosity of the solvent with glycerol or ethylene glycol.



## 7.2. Additional results from the DEER analysis with BetP-S545C-SL in *E. coli* lipids



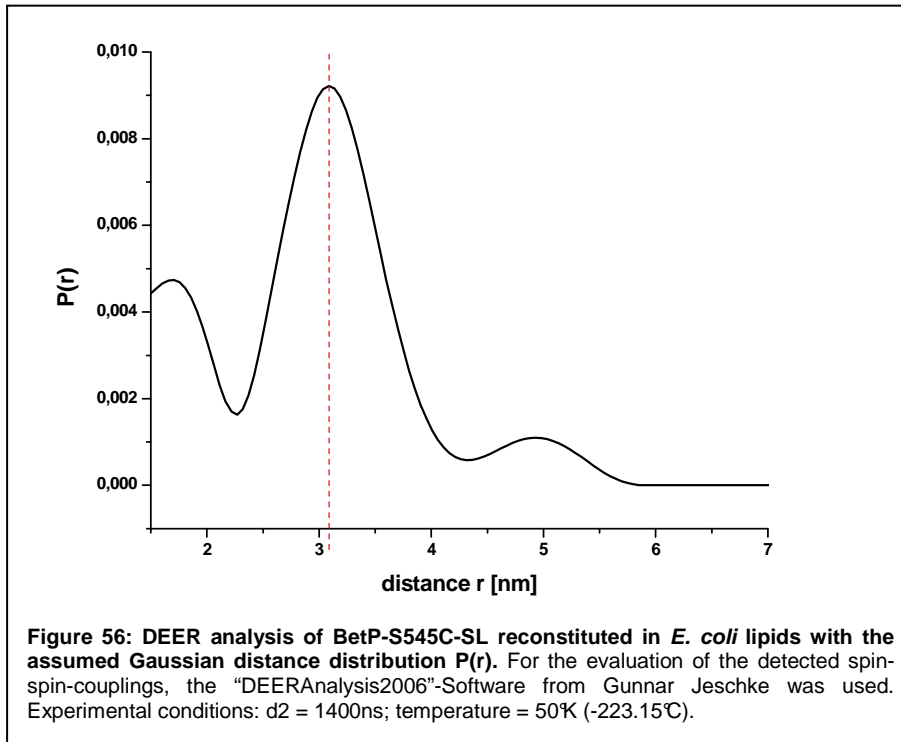
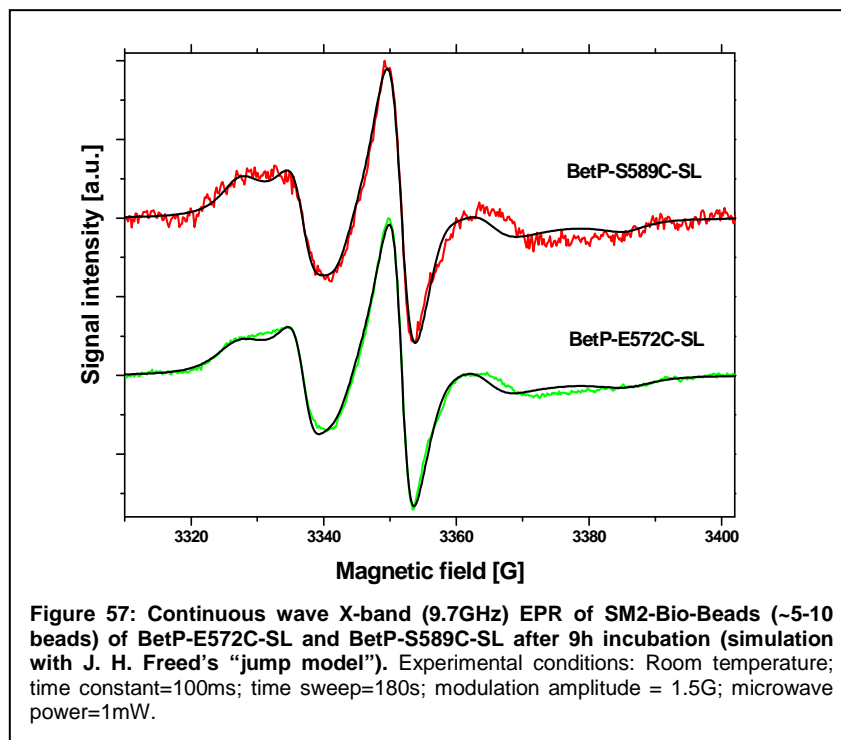


**Table 9:  $d_2$ -times with the respective dipolar frequencies  $\nu$  and maximal detectable distances  $r$  via DEER EPR spectroscopy with the Bruker Elexys E580 spectrometer.**

$d_2$ [ns]	$\nu$ [MHz]	Maximal distance [nm]
800	1.3	3.5
900	1.1	3.6
1000	1.0	3.7
1200	0.8	4.0
1400	0.7	4.2
1600	0.6	4.4
1800	0.6	4.5
2000	0.5	4.7
2400	0.4	5.0
2800	0.4	5.3
3200	0.3	5.5
3600	0.3	5.7
4000	0.3	5.9
5000	0.2	6.4
6000	0.2	6.8

### 7.3. Additional results from cw X-band EPR studies on Bio-Bead absorption of BetP



## Danksagung

Herrn Prof. Dr. Reinhard Krämer danke ich für das mir anvertraute, herausfordernde Arbeitsthema, die intensive Betreuung durch „Rat und Tat“ sowie das Interesse am Fortschritt der Arbeit. Zudem danke ich Herrn Prof. Dr. Günter Schwarz für die freundliche Übernahme des Koreferates.

Ein ganz besonderer Dank geht an PD Dr. Susanne Morbach, die mir bis in die letzten Züge meiner Arbeit mit effizienten Ratschlägen und einer großen Portion an Zuversicht und Vertrauen den Weg zum erfolgreichen Abschluss der Arbeit ebnete.

Susanne Ressler möchte ich für ihre aussergewöhnliche Hilfsbereitschaft bei meiner stets erfolglosen Suche nach Spezial-„paper“ sowie die überaus „lockeren“ Diskussionsrunden bei Kaffee und Kuchen bedanken. Mein Dank gilt auch Herrn Prof. Dr. H.-J. Steinhoff, Dorith Wunnicke und Dr. Johann Klare für eine spontane, aber sehr produktive und lehrreiche Kooperation bzw. Kooperations-Übernahme im letzten Jahr meiner Doktorarbeit. Vitali Zielke danke ich für seinen selbstlosen und absolut zuverlässigen Einsatz bei der Auswertung und Interpretation jeglicher Art von EPR-Daten.

Der gesamten Osmogruppe, aber auch allen anderen „Welten“, danke ich für die überaus geselligen und unterhaltsamen Zwischenpausen sowie die „feucht-fröhliche“ Atmosphäre während meiner Diplom- und Doktorarbeit. Phil und Jensi danke ich für das aufheiternde „Zocken“, die vielen „Männergespräche“ in Zeiten der Not sowie das „Posen“ am Nachmittag. Ninaaargh danke ich für ihre ausgeflippte „Flummy“-Art im Laboralltag, ihre Hege und Pflege in Boston und für ihre schönen Liegestütze. Ein besonderer Dank gilt auch Ute, Eva und Gabi, die als ultimative „Laborfeen“ so manch ausweglose Situation mit unbezahlbaren Tipps und Handreichungen zu meistern vermochten.

Meiner liebsten Kollegin und „Labor-Ehefrau“ Veralein danke ich für das Ertragen meiner Ordnungsliebe, das Verbrauchen meiner „gehamsterten“ Puffer ;) sowie ganz besonders für die rücksichtvolle und wohl wollende Art während meiner gesamten Laborzeit im Schatten von BetP.

Very sincere thanks goes out to my „EPR-mentor“ and supervisor Dr. Igor V. Borovykh for his self-sacrificing and highly encouraging help and assistance to save the day during all our measurements and also after work. In addition, I send my special thanks to Crissi, Tavi and Maria for the „days of my life“ in rumania and for the infinite „happy-ups“ during the writing of this thesis - mulțumesc!

Ich danke meinen Eltern und meiner Schwester für die seelische und auch finanzielle Unterstützung während meines gesamten Studiums und der Doktorarbeit. Ganz besonders bedanke ich mich bei meinen Freunden Günni, Nicole, Eva, Jusch, das Ötzi-Tunteo-Glatze-Team und Martina für ihr unentwegt aufbauendes Mitgefühl sowie den unermüdlichen Glauben an mich und mein Leistungsvermögen.

## Erklärung

Ich versichere, dass ich die von mir vorgelegte Dissertation selbständig angefertigt, die benutzten Quellen und Hilfsmittel vollständig angegeben und die Stellen der Arbeit - einschließlich Tabellen, Karten und Abbildungen -, die anderen Werken im Wortlaut oder dem Sinn nach entnommen sind, in jedem Einzelfall als Entlehnung kenntlich gemacht habe; dass diese Dissertation noch keiner anderen Fakultät oder Universität zur Prüfung vorgelegen hat; dass sie noch nicht veröffentlicht worden ist sowie, dass ich eine solche Veröffentlichung vor Abschluss des Promotionsverfahrens nicht vornehmen werde. Die Bestimmungen dieser Promotionsordnung sind mir bekannt. Die von mir vorgelegte Dissertation ist von Prof. Dr. R. Krämer am Institut für Biochemie der Mathematisch-Naturwissenschaftlichen Fakultät der Universität zu Köln betreut worden.

Ich versichere, dass ich alle Angaben wahrheitsgemäß nach bestem Wissen und Gewissen gemacht habe und verpflichte mich, jedmögliche, die obigen Angaben betreffende Veränderung dem Dekanat unverzüglich mitzuteilen.

Datum: Köln, Oktober 2008

Unterschrift: \_\_\_\_\_

(Sascha Nicklisch)

# Lebenslauf

## Persönliche Daten

Name	<u>Sascha</u> -Carsten-Thomas Nicklisch
Adresse	Esserstr.40, 51105 Köln-Humboldt/Gremberg
Telefonnummer	0221/ 16920265
Geburtsdatum	02.09.1978
Geburtsort	Köln
Familienstand	ledig

## Schulischer und beruflicher Werdegang

08.1985 – 06.1989	Gemeinschaftsgrundschule in Köln-Holweide
08.08.1989 – 12.06.1998	Herder-Gymnasium in Köln-Buchheim (Abschluss: Abitur)
03.08.1998 – 31.08.1999	Zivildienst; St. Vinzenz Haus, Köln (Brück)
09.1999 – 07.2005	Biologie-Studium an der Universität zu Köln (Abschluss: Diplom)
10.2005-12.2008	Promotion am Institut für Biochemie der Universität zu Köln; Arbeitsgruppe: Prof. Dr. R. Krämer